CHALMERS
UNIVERSITY OF TECHNOLOGY

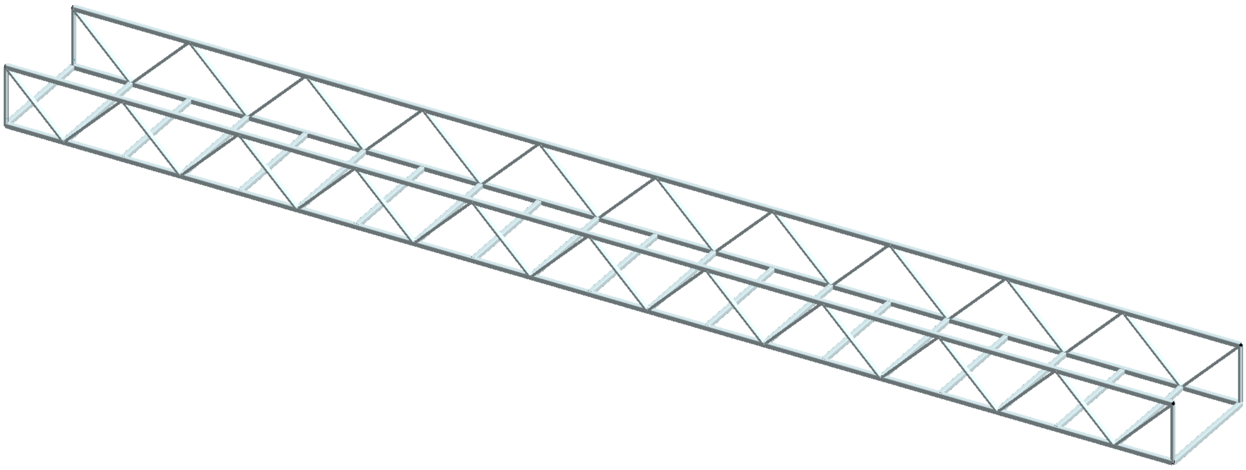

Sustainability and cost-effectiveness of steel truss pedestrian bridges

A case study focusing on truss optimisation, deck systems and materials

Master's thesis in the Master's Programme Structural Engineering and Building Technology

JOSEFIN TJERNLUND

Department of Architecture and Civil Engineering
Division of Structural Engineering
Lightweight Structures
CHALMERS UNIVERSITY OF TECHNOLOGY
Master's Thesis ACEX30-19-16
Gothenburg, Sweden 2019

MASTER’S THESIS ACEX30-19-16

Sustainability and cost-effectiveness of steel truss pedestrian bridges

A case study focusing on truss optimisation, deck systems and materials

Master’s Thesis in the Master’s Programme Structural Engineering and Building Technology

JOSEFIN TJERNLUND

Department of Architecture and Civil Engineering
Division of Structural Engineering
Lightweight Structures
CHALMERS UNIVERSITY OF TECHNOLOGY

Göteborg, Sweden 2019

Sustainability and cost-effectiveness of steel truss pedestrian bridges
A case study focusing on truss optimisation, deck systems and materials

Master's Thesis in the Master's Programme Structural Engineering and Building Technology

JOSEFIN TJERNLUND

Examensarbete ACEX30-19-16
Institutionen för arkitektur och samhällsbyggnadsteknik
Chalmers tekniska högskola, 2019

Department of Architecture and Civil Engineering
Division of Structural Engineering
Lightweight Structures
Chalmers University of Technology
SE-412 96 Göteborg
Sweden
Telephone: + 46 (0)31-772 1000

Cover:
Configuration of two trusses acting as primary beams with transverse beams in between, see Chapter 4 for different designs.

Chalmers Reproservice
Göteborg, Sweden, 2019

Sustainability and cost-effectiveness of steel truss pedestrian bridges

A case study focusing on truss optimisation, deck systems and materials

Master's thesis in the Master's Programme Structural Engineering and Building Technology

JOSEFIN TJERNLUND

Department of Architecture and Civil Engineering
Division of Structural Engineering
Lightweight Structures
Chalmers University of Technology

ABSTRACT

The interest to design more durable steel bridges has increased in the last few decades. This is mainly to minimize extra costs associated with steel corrosion that requires cumbersome preventive measures, such as painting and airtightness of welded closed-sections, and extensive repair and maintenance work. For the case of pedestrian bridges, it is fairly common to utilize steel trusses made with standard hollow profiles in carbon steel as primary load-bearing elements of the structure, thus posing a high risk for corrosion. Such risks, and consequently extra costs, could be significantly reduced by implementing stainless steel instead of carbon steel. Moreover, the deck could also be replaced by more lightweight and durable materials such as fiber reinforced polymer (FRP) deck systems. Both stainless steel and FRP would lower the amount of reparation work which decreases the future costs over the service life of a bridge. The initial cost could, however, be higher than for the conventional alternatives.

This dilemma is investigated through a case study comparing five different truss bridge solutions made in either carbon steel, stainless steel or FRP, showing the effect on material-, cost- and environmental parameters when optimising the bridge designs. The aim is to compare and evaluate the outcome when using these new approaches, with the main objective to show differences gathered from the case study.

The results show that the initial costs increase as the corrosion steel is replaced with stainless steel. This upgrade of material cost more than twice as much, while FRP as a substitute to the steel deck has similar investment price. But for the total cost over a 50-year long service life, these implementations are more cost efficient for this specific bridge. The overall cause for this outcome is mainly the expensive corrosion paint that's required to be added to the carbon steel periodically. However, the carbon dioxide emissions are increased when looking at the production of stainless steel, but decreased for FRP due to the much lower weight compared to an ordinary steel deck. Also the investigated truss optimisation were shown to contribute to the material efficiency of the bridge with a truss configuration of different profiles between chords and diagonals. It is also shown that together with the new materials and design concepts, it is possible to achieve lighter, more durable and less costly pedestrian bridges.

Key words: pedestrian bridge, steel, truss, deck system, optimisation, stainless steel, FRP, life cycle cost analysis, life cycle assessment

Hållbarhet och kostnadseffektivitet för stålfackverksbroar för gångtrafik

En fallstudie med fokus på fackverksoptimering, däcksystem och material

Examensarbete inom masterprogrammet Structural Engineering and Building Technology

JOSEFIN TJERNLUND

Institutionen för arkitektur och samhällsbyggnadsteknik
Avdelningen för Konstruktionsteknik
Lättviktskonstruktioner
Chalmers tekniska högskola

SAMMANFATTNING

Intresset för att bygga mer hållbara broar har ökat de senaste årtiondena. Huvudsakligen för att minimera de extra kostnaderna kopplade till kolstål som kräver besvärliga förebyggande åtgärder, så som målning och lutftätning av svetsade slutna tvärsnitt, samt dyra reparations och underhållsarbeten. För fallet med gång- och cykeltrafik är det vanligt att utnyttja stålfackverk beståendes av standardhålprofiler i kolstål som konstruktionens huvudbärverk, trots den höga risken för korrosion. Sådana risker, och följaktiga kostnader, kan minskas markant genom implementering av rostfritt stål istället för kolstål. Dessutom kan däcket också bytas mot mer lättvikts- och hållbara material som till exempel däcksystem av fiberarmerad polyester (FRP). Både rostfritt stål och FRP skulle minska mängden reparationer och därmed också de framtida kostnaderna över brons livslängd. Däremot skulle investeringskostnaderna kunna bli högre än för de konventionella alternativen.

Detta dilemma är undersökt genom en fallstudie som jämför fem olika fackverksbroar av antingen kolstål, rostfritt stål eller FRP, och visar den tillhörande påverkan på material-, kostnads- och miljöparametrar vid optimering av brodesignen. Syftet är att jämföra och utvärdera resultatet vid användningen av dessa olika material och konstruktionssätt, med huvudmål att visa konkreta skillnader från fallstudien.

Resultatet visar att investeringskostnaderna ökar i takt med att kolstålet byts ut mot rostfritt stål. Uppgraderingen av material kostar mer än dubbelt så mycket, samtidigt som FRP som ett substitut till ståldäcket har likvärdig investeringspris. Men sett till den totala kostnaden över en livslängd på 50 år är dessa implementeringar mer kostnadseffektiva för denna typ av bro. Den huvudsakliga anledningen till detta resultat är den kostsamma rostfria färgen som behöver adderas på kolstålet med ett jämnt intervall. Dock ökar mängden utsläpp av koldioxid sett till materialtillverkningen av rostfritt stål, men minskar vid användning av FRP på grund av materialets mycket lägre vikt jämfört med ett vanligt ståldäck. Det visar sig även att optimeringen av fackverken bidrar till en tydlig materialeffektivisering av bron, med olika profiler för ram och diagonaler. Resultatet indikerar även att tillsammans med nya material och koncept är det möjligt att uppnå lättare, mer hållbara och mindre kostsamma gångbroar.

Nyckelord: gångbro, stål, fackverk, däcksystem, optimering, rostfritt stål, FRP, livscykelkostanalys, livscykelanalys

Contents

Preface

This master's thesis was carried out during autumn and spring 2018/2019 at the Division of Structural Engineering, department of Architecture and Civil Engineering at Chalmers University of Technology, Gothenburg, Sweden. The thesis was made in collaboration with WSP Bridge Department in Gothenburg and evaluates the sustainability and cost-effectives in terms of material efficiency and carbon dioxide emissions for a specific steel truss pedestrian bridge.

I would like to give the greatest thank you to Dr. Mohsen Heshmati, my supervisor, who's been supporting me and spending a lot of time and dedication to form this thesis. His positivity and way of making this subject feel important have made the work inspiring and fun. Also, thank you Associate Professor Mohammad Al-Emrani, my examiner, for valuable inputs and feedback during the work. Finally, an overall thank you to my colleagues at WSP for taking care of me during my last course at Chalmers.

Gothenburg, April 2019

Josefin Tjernlund

Notations

Roman upper case letters

$\boldsymbol{D}$ Rigidity matrix

$\boldsymbol{D_b}$ Bending stiffness matrix

$\boldsymbol{D_m}$ Membrane stiffness matrix

$\boldsymbol{D_s}$ Shear stiffness matrix

E Young’s modulus

G Shear modulus

$S_{j.ini}$ Initial rotational stiffness

Roman lower case letters

g Selfweight

f_u Ultimate tensile strength

f_y Yield strength

Greek lower case letters

$\propto$ Thermal expansion coefficient

α_{LT} Imperfection factor

β Factor for initial rotational stiffness

c Specific heat capacity

γ_{M0} , γ_{M1} , γ_{M2} Partial factors

λ Thermal conductivity

λ_0 Limit slenderness

v Poisson’s ratio

ρ Density

χ_{LT} Factor for buckling force

ψ Factor for thermal actions

Abbreviations

FRP	Fiber reinforced polymer
OSD	Orthotropic steel deck
TRP	Trapezoidal sheet
ULS	Ultimate limit state
VKR	Hot-rolled hollow sections

1 Introduction

As introduction the scope of the Master's Thesis is explained starting with the background for the project, followed by the aim and objective. Also the method used and limitations for the project are described. Finally the outline of the thesis is presented.

1.1 Background

Truss bridges are one of the oldest types of modern bridges but were developed later than the beam-, cantilever-, suspension- and arch bridge which together with the truss are the five basic bridge types. The characteristic of the truss is its material efficiency and economical construction. Since it can be manufactured off-site without interfering with traffic it has been a common solution when designing pedestrian bridges since the 1930s (DeCelle *et al.*, 2013).

The era of truss bridges started in timber because of its abundance and lightweight, but have been replaced with carbon steel to get more strength out of the material. In addition, the increased knowledge about performance and reliability aspects of different steel materials have made it a common solution. The work efficiency with big amount of standard profiles for steel products is also a driving cause. However, similar to timber products the durability issues are a disadvantage of carbon steel material. Corrosion can cause severe damage to steel bridges which requires expensive protective measures such as painting. Another issue is to avoid moisture ingression through the continuous welds that connect structural elements and makes them closed cross sections, to eliminate corrosion on more hidden places. These welds require extensive welding work and quality control which significantly increases the production costs. Furthermore, additional costs associated with the continuous monitoring and repair work can make such bridges expensive to maintain.

To overcome these difficulties more durable materials have gained increased popularity in the bridge sector during the past few decades. Among these are stainless steel and fibre-reinforced polymer, which provides enhanced properties like corrosion resistance, more light weight and higher strength in comparison to carbon steel. However, these materials are still considerably more expensive than the conventional carbon steel products. Therefore, it is extremely beneficial to further optimise the material utilisation by using innovative approaches in the bridge designs. In Sweden today, about 15 % of all road bridges are made of carbon steel, with a span over two meter as the definition of a bridge (SBI, 2008).

1.2 Aim

The main purpose of this master's thesis is to further optimize the conventional steel truss footbridge by making use of innovative approaches and products, such as use of stainless steel and deck systems of fibre-reinforced polymer. The intention of the truss optimization is to reduce the amount of material and get a more lightweight steel truss resulting in a more economically advantageous bridge.

1.3 Objective

The following questions will compile the objective of this thesis.

- Will optimised steel trusses save enough material to see a profit when comparing to the work needed for strengthening of connections in the truss?

- After optimisation of profiles in the truss, will the less amount of material give enough economic profit to see the opportunity to further develop new innovative bridge designs? Primary new deck systems with more expensive initial material costs.

- Will a pedestrian truss bridge made of stainless steel be more economical than the same design made of carbon steel, seen in its whole life cycle? And will it release less carbon emission in comparison, seen in its whole life cycle?

- Will implementation of FRP deck be beneficial economically and environmentally, seen in its whole life cycle?

1.4 Method

In order to obtain enough background knowledge about why to investigate more lightweight steel truss bridges, the first part of the thesis consist of a literature study. Brief information about trusses in general are collected as well as knowledge about materials used later in the design work.

As a following step old calculation sheets for designing bridges of similar type are processed to chart the dimensioning of a steel truss pedestrian bridge, for a truss made of hot-rolled hollow sections in carbon steel. This knowledge gives the fundamental parts to consider later on in the case study.

The work will then continue with a case study to show the effects for different parameters when optimising the configuration of the truss, such as weight, welding length and amount of corrosion paint needed. This will be done in StruSoft's software for finite element analysis FEM-Design. A following study for total life cycle cost and life cycle assessments will end the research showing the economic and environmental aspects in each design. The results will be compared to make conclusions whether the innovative designs are as good in practise as in theory.

1.5 Limitations

The following limitations will be applied in the thesis.

- Only the superstructure of the bridge is considered, i.e. the structure reaching between the two supports. The substructure underneath is neglected as well as bearing and other bridge details.

- The geometry of the bridge is limited in both length, width and height.

- Deign of joints are not included in dimensioning of the truss. The critical initial rotational stiffness won't be considered even though the theory behind are treated in the literature study.

- Horizontal acceleration in the bridge won't be calculated since only the vertical movement of the bridge is seen as critical.

1.6 Outline

In Chapter 2 the theory used within this thesis are presented. It covers the basic about truss- and deck systems and mechanical properties of carbon steel and its material substitutes. Also dimensioning of bridges are covered as well as an overview of acting loads on a bridge.

Chapter 3 describes the work when designing a deck system with linear finite elements. Stiffness matrixes are also defined which later are the input in FEM analyses. The theory behind the fundamental initial rotational stiffness in truss joints are also treated.

Chapter 4 covers the case study over five different bridge designs, presenting the different amount of steel needed and other important parameters for evaluation of the concepts. Sketches over joints are also shown.

In Chapter 5 the life cycle cost for the bridges in the previous case study are calculated and presented.

Chapter 6 further evaluates the bridge designs of environmental impact in a life cycle assessment, showing the carbon dioxide emissions.

In Chapter 7 the case study is discussed including all parts from optimisation to life cycle assessment. Also the future use of a FRP deck are discusses. Finally, a summary of advantages and disadvantage for each bridge design is produced.

Chapter 8 covers conclusions regarding aim and objective of the thesis.

In Chapter 9 a reference list is presented over literature used within the thesis. Appendices containing supplementary information are attached in the end.

2 Theory

The theory presented in this chapter includes basic information about truss bridges in general, and pedestrian truss bridges in particular. Initially a brief introduction to steel trusses and deck systems are presented, i.e. the two main components of the bridge type studied. After that the choice of material is handled with discussion about mechanical properties. Here carbon steel, stainless steel and fibre-reinforced polymer will be looked further into. Furthermore, a brief section about dimensioning of pedestrian bridges will follow as well as a review of acting loads on a pedestrian bridge.

2.1 Steel truss bridges

The steel truss bridge became commonly used in the early 18th century and was unique in the design with strong triangular structures (Duan, 2017). For long spans and heavy weights the loads on the primary beams got high, and a truss system became an efficient way to decrease the weight of the primary beams itself (SBI, 2008).

2.1.1 Different truss systems

A truss is a simple skeletal structure with vertical or diagonal bar members connecting a top and bottom chord, see Figure 2.1 (Allen and Zalewski, 2010). The bars work axially, only subjected to tension or compression, and distributes the load to the chords which takes care of axial forces and resisting bending moment. The connections between the steel bars can either be done with welds, bolts or rivets (Duan, 2017).

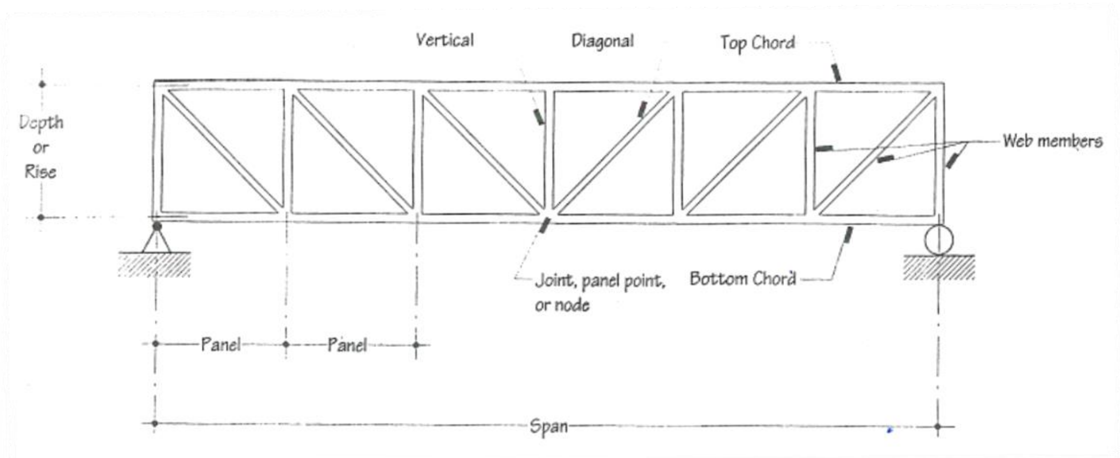

Figure 2.1 Terms and components in a truss (Allen and Zalewski, 2010).

The efficiency of axially acting members in the truss makes it possible for long spans in bridge design (Allen and Zalewski, 2010). It spans longer than beams and frames, but shorter than cable structures and arches. In Sweden steel truss bridges has been used for road traffic for spans up to 100 meters, but is no longer an applied bridge design because of a high production cost (Trafikverket, 2008). However, this has to be weighed against the efficient material use in the structural elements followed by a reduced dead weight of the superstructure (Allen and Zalewski, 2010). For pedestrian bridges though, the lack of truss constructions doesn't apply because of its easy way of being lifted into place with cranes. This quick installation decreases the onsite costs (DeCelle, Efron, Ramos Jr and Tully, 2013).

Another advantage with a truss bridge over other types is its capability to manage many different load distribution patterns without changing its shape (Allen and Zalewski, 2010). Therefore, that type of system is often used in deck structures in suspension bridges, for example Älvsborgsbron in Gothenburg, to easily distribute loads between the cables when the load patterns shift to prevent the cables to change its shape. Also in arches the resistance to changed shape and buckling increases with a truss system.

A typical truss bridge design consists of two parallel vertical trusses acting as primary beams with a horizontal deck in between, transferring the loads to the trusses, see Figure 2.2.

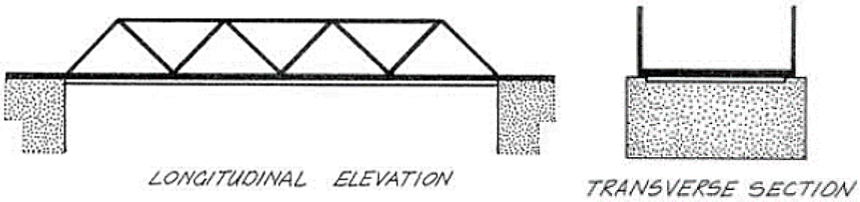

Figure 2.2 Longitudinal and transverse sections for a truss bridge (Comp, Jackson and Jones, 1976).

When designing a truss bridge there are several ways to do it. The three common ways are the through truss, the pony truss and the deck truss, see Figure 2.3 (Allen and Zalewski, 2010). The through truss bridge allows pedestrians to pass between the two deep trusses, braced together between the two top chords. The pony truss bridge is similar except the removal of the top lateral bracing. For the deck truss bridge the trusses are placed entirely below the deck.

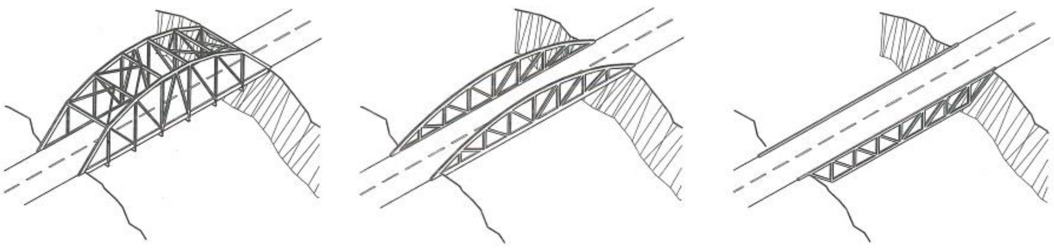

Figure 2.3 Three ways of designing a truss bridge. Starting from the left: Through truss, pony truss and deck truss (Allen and Zalewski, 2010).

After deciding how to use the truss in a bridge, there are several standard truss forms to choose among, see the most common ones in Figure 2.4 (Allen and Zalewski, 2010).

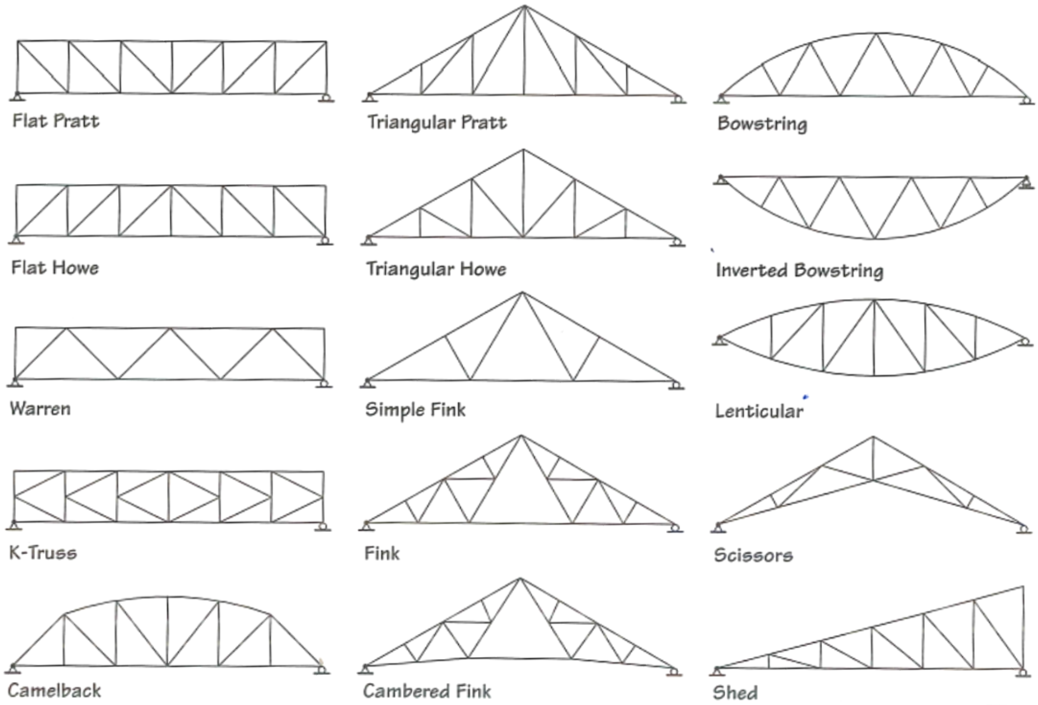

Figure 2.4 Different commonly used truss forms for design of a structure (Allen and Zalewski, 2010).

All of the truss forms are structured with triangular elements and appropriate for different systems with its specific advantages and disadvantages (Allen and Zalewski, 2010). The Pratt truss has vertical members in compression and diagonal members in tension, which can be found suitable for a steel truss since tensioned bars won’t be subjected to bending and the webs can be remained slender. The Howe truss is the Pratt’s opposite with compressive diagonals and tensioned verticals, and consequently preferred for a heavy timber truss. A Warren truss has its peculiar appearance with web elements of same size, shape and equal joints. This makes the truss design the most simple to fabricate, the easiest to maintain and is by that also the most common one in bridge design (Duan, 2017).

2.1.2 Different deck systems

Between the two trusses in the bridge, a deck is placed and designed to transfer the loads acting on the structure to the primary load bearing system. The most commonly used deck design in bridge applications are the orthotropic steel deck, OSD, which consist of a top plate stiffened in two perpendicular directions. The stiffeners in the longitudinal direction, also named ribs, can either be open or closed and are supported on the transverse stiffeners, also called floor beams, see Figure 2.5 (Kolstein, 2007). This whole deck system rests on the main girders, which in a truss bridge is the vertical trusses. The orthotropic deck name refers to two anisotropic stiffeners with different properties in different directions together working orthogonal, i.e. orthogonal-anisotropic system which is shortened to orthotropic deck system (US Department of Transportation, 2012).

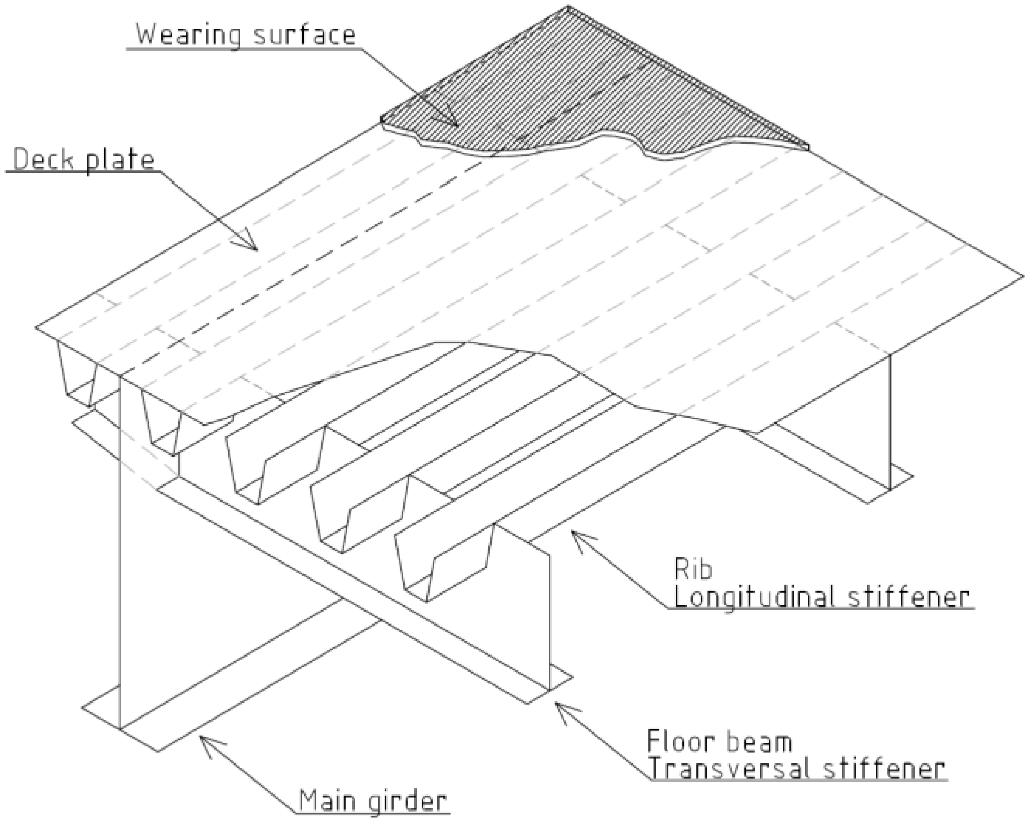

Figure 2.5 *Components in an orthotropic steel deck with the load being transferred through the different stiffeners to the main girder (Karlsson and Wesley, 2015).*

The concept with an OSD is the components acting as one structural unit, with the main girder, floor beams and ribs utilising the deck plate as a top flange (US Department of Transportation, 2012). This is a very effective use of material with the load path starting from the deck plate to the ribs, transferring the load to the floor beam who finally transport the load to the main girders, see Figure 2.6.

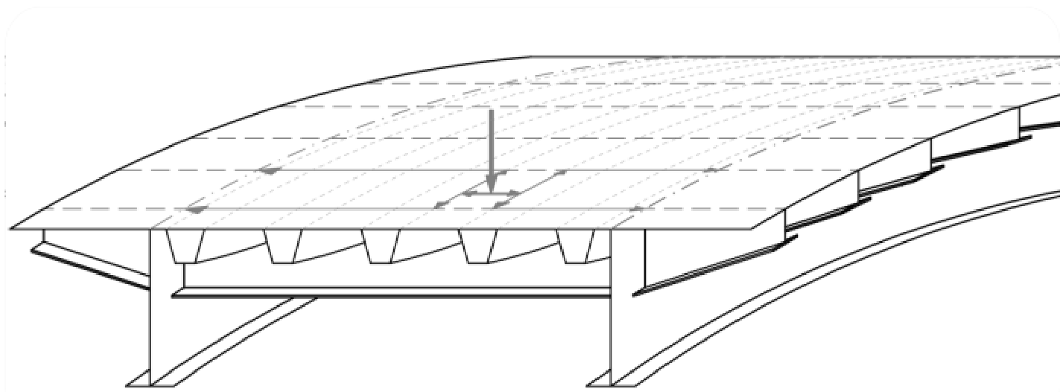

Figure 2.6 *Load distribution through an OSD bridge from deck plate to main girder (Karlsson and Wesley, 2015).*

The two different types of OSD bridges are plate girder bridges and box girder bridges (US Department of Transportation, 2012). The difference is that box girders provide a bottom lateral bracing system, which the plate girder doesn't, see Figure 2.7. This bracing system gives the deck more torsional stiffness.

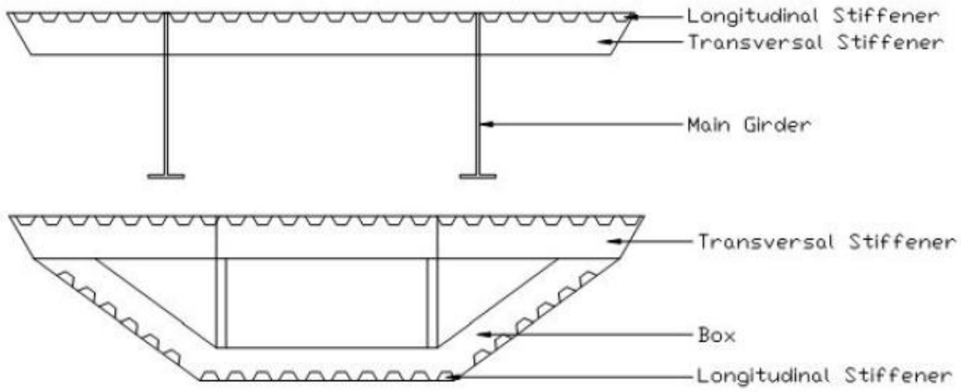

Figure 2.7 *A plate girder in the top of picture and a single-cell box girder in the bottom (Håkansson and Wallerman, 2015).*

Starting from the top in the deck system, the wearing surface's main purpose is to distribute traffic loads, protect the plate from corrosion and provide a smooth surface, and is normally made of concrete, bitumen or polymer material (US Department of Transportation, 2012). Because of the material efficiency in OSD bridges, the thickness of the coating is directly influencing the self-weight of the system.

The deck plate is the base to the wearing surface with the function to transfer the loads to the ribs. For the whole OSD bridge, the thin plate acts like the top flange with better stress-performance for increased thickness.

Giving supports to the deck plate is the functionality of the ribs. But also to increase the flexural rigidity of the cross section and transfer loads to the floor beam. Usually the ribs are continuous over the length of the deck and cut where they meet the floor beam. The shape of the ribs varies between either closed or open, with the trapezoidal as the most common one, see Figure 2.8 (Kolstein, 2007).

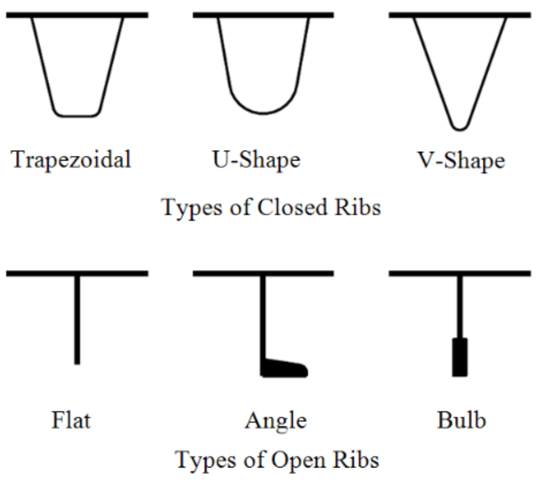

Figure 2.8 *The most common types of closed and open ribs used for OSD in bridges (US Department of Transportation, 2012).*

The advantage with closed ribs is the higher torsional and flexural stiffness (US Department of Transportation, 2012). To compensate for this when using open ribs, the spacing between ribs, and also between floor beams, needs to be decreased. This require more material and also more welding, se Figure 2.9. But the advantages with open ribs are the easier production methods, inspections and maintenance.

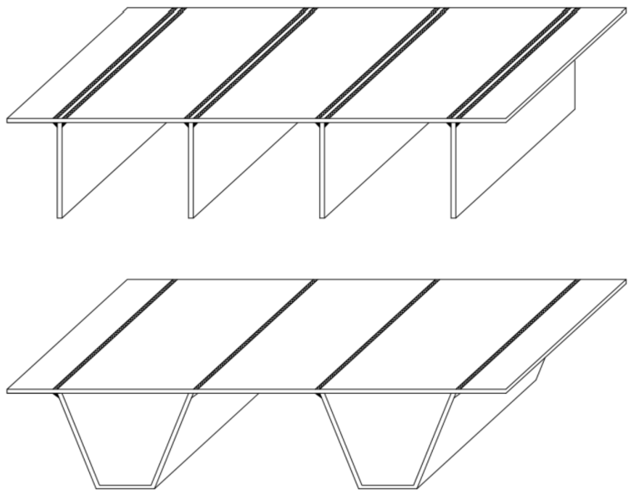

Figure 2.9 Needed welds for open and closed ribs respectively. It's twice as many for open than for closed (Karlsson and Wesley, 2015).

Finally the floor beams transfer the load from the ribs to the main girder and provides support to the ribs. Normally it has the geometry of an inverted T-section which are welded to the deck plate (AISC, 1963).

2.2 Materials

Through history, most bridges are made of wood, masonry, steel or concrete but are in general dependent on materials with enough capacities and properties for the acting loads (Allen and Zalewski, 2010). Nowadays new stronger materials based on fibres of glass, carbon or aramid are advancing on the market. The materials in focus in this chapter will be conventional carbon steel and its two substitutes stainless steel and FRP.

2.2.1 Carbon Steel

Carbon steel is the formal name for regular steel and is the most commonly used steel product for construction. It's an ally of iron and carbon, which should have the maximum amount of 2% carbon, and were developed with the industrialization and growth of the rail network (SBI, 2008). The Ironbridge in England was the first bigger iron construction built in the middle of the 18th century. For Sweden it took another century before steel bridges appeared. Two early ones are Jernbron in Uppsala and a bridge over Göta River to Vargön. Nowadays pure steel bridges are unusual, instead composite steel and concrete bridges are dominating the market.

2.2.1.1 Material

Steel are made of small crystals, strong in both tension and compression and for that reason often used as structural frames in bridges. As previously mentioned, if the amount of carbon is below 2 weight-%, steel is produced. With increased amount of carbon, the strength increase as well but the toughness decreases (SBI, 2008). For cast iron the carbon amount is between 2 and 4 weight-%.

A large issue with carbon steel is corrosion, a chemical reaction between a metal and its environment that deteriorate the metal and its properties (Davis, 2000). This happens because steel have a natural tendency to react with other chemical elements and do so frequently with oxygen and water. In these reactions hydrated iron oxides creates, also known as rust. The load bearing capacity will as a consequence be reduced by a smaller effective cross section or pitting, i.e. small holes in the steel.

Despite the corrosion, carbon steel is often used as building material in bridges. Coating are in these cases used to protect the steel from corrosion by adding it on the steel area to isolate it from the corrosive environment (Davis, 2000). In that way the corrosion is reduced or eliminated which will extend the life of the bridge and also increase its reliability. A steel construction that are painted with coating according to Swedish AMA gets a working life of at least 80 years (Trafikverket, 2011b). With a fully repaint it's increased to 120 years.

The most important properties for a structural steel are strength, toughness and weldability (SBI, 2008). The strength is described by yield strength f_y and ultimate tensile strength f_u which can be shown in a steels stress-strain curve, see Figure 2.10. The peak of the curve illustrates the yield point, where after the steel get large increases in strain with little or no increase of stress called getting into plastic behaviour. Exact values are presented further down, see Table 2.1.

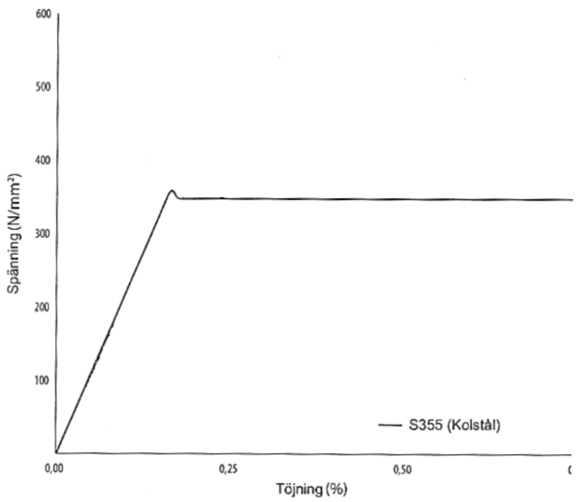

Figure 2.10 Stress-strain relationship for carbon steel (grade S355). Strain on x-axis and stress on y-axis (SBI, 2017).

The steels toughness says whether the material is brittle and crack before plastic deformation or not (SBI, 2008). A sufficient material doesn't crack until after this phase, but the risk increases with sinking temperature. Different classes divide steel according to this behaviour. Other qualities specific for carbon steel can be seen in Table 2.1.

Table 2.1 Properties for carbon steel grade S355 (SIS, 2005b; SBI, 2008).

Mechanical property		**S355**
Density ρ	$^{kg}/_{m^3}$	7 850
Thermal expansion coefficient $\propto$	C^{-1}	$1.2x10^{-5}$
Thermal conductivity λ	$^{W}/_{m°\text{C}}$	60
Specific heat capacity c	$^{J}/_{kg°\text{C}}$	450
Young's modulus E	GPa	210
Shear modulus G	GPa	81
Poisson's ratio v	$-$	0.3
Yield strength f_y	MPa	355
Ultimate tensile strength f_u	MPa	$470-630$

2.2.1.2 Design

Eurocode 3 consider designing with steel, which covers the grade S355 of carbon steel. The efficient material use for the design makes the total weight much less than for other building materials (SBI, 2008). Another advantage with steel bridges are the suitable way of being prefabricated where the construction elements are made under good conditions and will quickly be installed on place. This is very time efficient.

2.2.2 Stainless Steel

Stainless steel is a subcategory in the steel group for steels containing a minimum of 10,5% chromium (SBI, 2017). The increasing amount of chromium increases the corrosion resistance which is the characteristic for stainless steel and are the natural choice when it comes to bearing constructions in coast areas exposed to de-icing salt or compounds.

2.2.2.1 Material

The presence of chromium provides the steel surface with a thin protective film of oxide which protect the steel against corrosion attacks (Davis, 2000). If the film gets damaged and the steel is in an environment with access to air, the steel quickly heals itself by creating a new oxide layer. This protective mechanism against the atmosphere is very effective and a big advantage for stainless steel.

With increased chromium volume up to 20%, the corrosion resistance increase drastically as well (SBI, 2008). Also by adding other alloys, the steel will get different crystal structures and following different properties and will be suitable for different applications. This variety creates a big amount of grades of stainless steel and is therefore divided into families classified by their crystal structure; austenitic stainless steel, ferritic stainless steel, martensitic stainless steel, duplex stainless steel and precipitation hardening stainless steel (SBI, 2017). Within these families many grades exist with the main difference of amounts of chromium, nickel and other materials such as molybdenum, see Table 2.2.

Table 2.2 The different amount of alloys for the different families of stainless steel (SBI, 2017).

	Chromium [%]	Nickel [%]	Molybdenum [%]	Corrosion resistance	Area of use
Austenitic	$16.5 - 19.5$	$6 - 13.5$	$0 - 2.5$	Very good	Load bearing strutures
Ferritic	$10.5 - 21.5$	~ 0	$0 - 2.5$	Good	Indoor constructions
Martensitic	$11 - 13$	~ 0	~ 0	Moderate	Tools, e.g. knives
Duplex	$20 - 25$	$1 - 6.5$	$0.1 - 3.5$	Very good	Industrial vessels
Precipitation hardening	18	8	~ 0	Moderate	Airplanes, bolts

Austenitic steels are without hesitation the most used stainless steel for building applications (SBI, 2017). For infrastructure in particular, austenitic and duplex stainless steels are commonly used, and for structural members duplex stainless steels. Most stainless steels used in construction contain around 18% chromium and 10% nickel (SIS, 2006a).

The characteristic stress-strain curve for steel differs when it comes to stainless steel (SBI, 2017). Most importantly it's the shape of the curvature where there is no well-defined yield stress limit as for carbon steel, see Figure 2.11. For S355 the yield point is when the curvature has its peak before it flattens out.

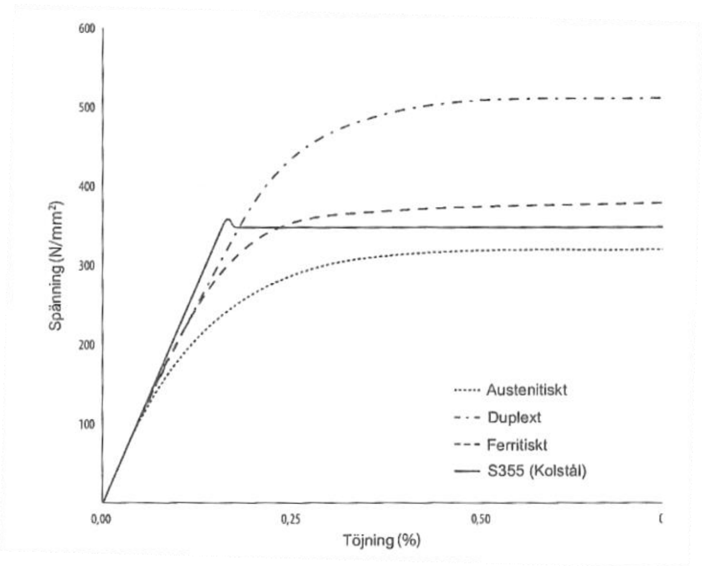

Figure 2.11 Stress-strain curves for austenitic-, duplex- and ferritic stainless steel in comparison to carbon steel grade S355. Strain on x-axis and stress on y-axis (SBI, 2017).

To give stainless steel a yield stress limit, a stress limit called 0.2-limit are defined which is the stress that will produce a 0.2% permanent strain after unloading (SBI, 2017).

Similar to carbon steel, specific qualities for stainless steel are presented in Table 2.3. But only austenitic, duplex and ferritic are represented since these are the families used for building constructions. Also, values for yield strength and ultimate tensile strength are given for hot rolled structural steel for the one or two most used standardised grades, i.e. 1.4301 and 1.4307 for austenitic stainless steel, 1.4462 for duplex stainless steel and 1.4003 and 1.4016 for ferritic stainless steel (SBI, 2017).

Table 2.3 Properties for the most commonly used grades in austenitic-, duplex- and ferritic stainless steel in comparison to carbon steel grade S355 (SIS, 2006a; SBI, 2017).

Mechanical property		Austenitic		Duplex	Ferritic		S355
		1.4301	1.4307	1.4462	1.4003	1.4016	
Density ρ	kg/m^3	7 900		7 800	7 700		7 850
Thermal expansion coefficient $\propto$	C^{-1}	$1.6x10^{-5}$		$1.3x10^{-5}$	$1x10^{-5}$		$1.2x10^{-5}$
Thermal conductivity λ	$W/m°C$	15		$13-15$	25		60
Specific heat capacity c	$J/kg°C$	500		500	$430-460$		450
Young's modulus E	GPa	200		200	200		210
Shear modulus G	GPa	76.9		76.9	76.9		81
Poisson's ratio v	$-$	0.3		0.3	0.3		0.3
Yield strength f_y	MPa	190	175	450	260	240	355
Ultimate tensile strength f_u	MPa	500	500	650	450	400	$470-630$

2.2.2.2 Design

Designing of stainless steel structures are treated in Eurocode 3, part 1-4 (SIS, 2006a). But only austenitic, ferritic and duplex stainless steel are treated. It's also only applicable for grades with nominal yield strength f_u below 480MPa. Values for yield strength and ultimate tensile strength are stated in tables depending on the thickness of the steel.

It's also described that the principal difference between stainless steel and carbon steel when doing structural design are that carbon steel deals with the protection for longer working life separately, afterwards as a supplement. For stainless steel it's included in the structural design, because the corrosion protection already is considered in the initial choice of material. As mentioned earlier in this chapter, in Section 2.2.1.1, carbon steel needs two full coat paintings but stainless steel nothing, for the same working life above 100 years.

The initial cost for stainless steel is higher than for carbon steel, but experience show that a corrosion resistant material with no need of maintenance could be more cost efficient (SBI, 2017). This life cycle analysis considers both initial- and maintenance cost as well as recycling and life expectancy.

2.2.3 Fibre Reinforced Polymer

A growing interest for more lightweight loadbearing material, applicable in civil engineering, resulted in the 1960's in development of the composite material called fibre reinforced polymer, short as FRP. It's a material structured with polymers that are reinforced with fibres and has an endless amount of compilations depending on desired qualities (Campbell, 2010). Composite material is defined as a combination of at least two materials with purpose to get better properties than for one material alone. The main objective with this reinforced polymer is to create a strong and stiff component with low weight.

2.2.3.1 Material

The two constituent for FRP is fibre and polymer, with the fibre providing strength and stiffness and the polymer binding the fibres to a unit, see Figure 2.12 (Campbell, 2010). The fibres, or reinforcement, are usually glass, carbon or aramid. Characteristic for the fibres is the length being considerably longer than the diameter. Layers of fibres are built upon each other and the product will get qualities depending on the direction of the fibres on each layer. The polymer, also called matrix, is a resin, either thermoplastics or thermosets. A thermoplastic resin can after cure convert back to liquid form. This won't happen to a thermoset resin, which is why it's more appropriate to use in civil engineering. Typical thermosets are epoxy, vinyl ester or polyester. The matrix maintains the fibres in their orientation and protect it from the environment. Also, it transmits loads from the matrix to the reinforcement. The total amount of fibres can be up to 70% in a composite without risking the polymer to fully enfold the matrix.

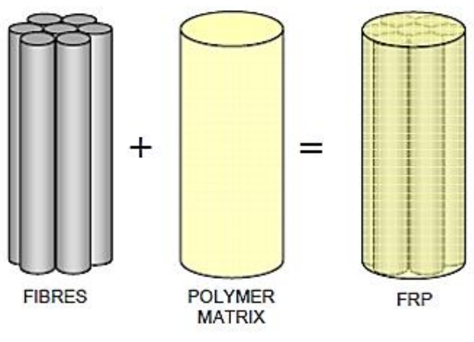

Figure 2.12 *Basic components in a FRP composite with the fibers providing strength and the matrix binding it to a unit (I.E. Comittee, 2006).*

The mechanical properties for an FRP-product depends on both orientation of fibre, production method and proportion between matrix and polymer (Hollaway and Head, 2001). A structural element of FRP are made of several layers, merging singular laminas, or plies, with a thickness around 0.1 mm or thicker, to become a final laminate. The orientation of the reinforcement in a lamina can either be unidirectional, bi-directional or randomly oriented, and are then attached together in the laminate, see Figure 2.13.

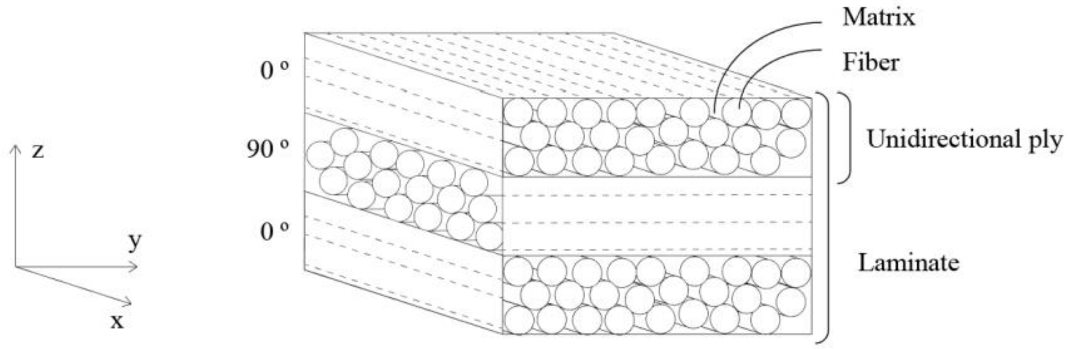

Figure 2.13 *Illustration of a laminate built up by unidirectional lamina. The 0° refers to the angle between the reinforcement to the x-axis, meaning they lie in the same direction. The 90° means it's perpendicular to the x-axis (Giger Johansson and Seebergs, 2018).*

For producing FRP, manual-, semi-automatic- and automatic processes are the three different methods. They provide different adaptions of shape, quality, production volume, cost and production time (Agarwal, Broutman and Chandrashekhara, 2018). The manual method is the most used one and is suitable for odd shapes and low production volumes. For a hand lay-up, a die mold of wood, steel or plastic is prepared with polishing and coating before the reinforcement fiber is placed layer wise inside it together with the resin matrix to finally being cured. For a spray-up, which is faster and cheaper than the hand lay-up, the reinforcement is instead sprayed into the die mold.

Because of the layer structure, FRP composites are counted as having an anisotropic material behaviour, meaning that one direction has different properties than the other. To be able to design and analyse structural element made of FRP laminates, the mechanical properties of each lamina must be known (Agarwal, Broutman and Chandrashekhara, 2018). That is time consuming, and the factor with the biggest impact on the properties are the relative proportion of fiber and matrix, the volume fraction V (Zoghi, 2014). The volume fraction of fibers V_f depend on the volume of fibers and total volume of composite, see Equation 2.1. It works the same way for the volume fraction of matrix V_m depending on volume of matrix and total volume of composite, see Equation 2.2.

$$V_f = \frac{v_f}{v_c} \tag{2.1}$$

$$V_m = \frac{v_m}{v_c} \tag{2.2}$$

Composites with fibers in unidirectional directions are most commonly used within infrastructural applications, and are an orthotropic material because of the anisotropic layers with equal properties transversally, see the z-axis in Figure 2.13. For a unidirectional FRP with epoxy resin and either fibres of e-glass-epoxy or carbon-epoxy, some important mechanical properties are seen in Table 2.4.

Table 2.4 Properties for unidirectional FRP with epoxy resin and e-glass-epoxy or carbon-epoxy fibers respectively (Agarwal, Broutman and Chandrashekhara, 2018).

Mechanical Property		**E-glass-epoxy**	**Carbon-epoxy**		**Steel S355**
Density, ρ	$^{kg}/_{m^3}$	1 800	1 500		7 850
Fibre volume fraction, V_f	–	0.45	0.60		–
Longitudinal modulus, E_1	GPa	38.6	148		210
Transverse modulus, E_2	GPa	8.27	9.65		210
Longitudinal tensile strength, X_t	MPa	1 062	1 314		470 − 630
Longitudinal compressive strength, X_c	MPa	610	1 220		470 − 630
Transverse tensile strength, Y_t	MPa	31	43		470 − 630
Transverse compressive strength, Y_c	MPa	118	168		470 − 630

2.2.3.2 Design

Yet there are no design codes and guidelines for FRP composites in Europe. Because of the many combinations of fibre reinforcement, polymer matrix, suppliers and producing techniques, the final properties may vary to much (Kolstein, 2008). This big variation complicates the application of a general design guideline for FRP in comparison to steel which don't meet this problem.

But generally, the greatest advantages with FRP are high strength, corrosion resistance, easy shaping, lightness, long service life and low maintenance. This leads to a steadily increase of usage of the material.

2.3 Dimensioning

The basic for dimensioning is the limit state where the construction reach different stages and becomes unable to fulfil the functional requirements (SBI, 2017). This refers to resistance and comfort criteria.

2.3.1 Static

For static analysis, general requirements are first of all stated in Eurocode – Basic of structural design (SIS, 2001). The limit state design is done either in ultimate limit state or serviceability state, which focus on the failure of the bridge or the required demand during use respectively. For verification of the limit states related to the working life of the construction, the codes also recommend values for these. For bridges it's 100 years, see Figure 2.14.

Design working life category	Indicative design working life (years)	Examples
1	10	Temporary structures (1)
2	10 to 25	Replaceable structural parts, e.g. gantry girders, bearings
3	15 to 30	Agricultural and similar structures
4	50	Building structures and other common structures
5	100	Monumental building structures, bridges, and other civil engineering structures
(1) Structures or parts of structures that can be dismantled with a view to being re-used should not be considered as temporary.		

Figure 2.14 Indicative design working life according to Eurocode. For bridges 100 years are recommended (SIS, 2001).

To verify the requirements in the limit states, the relevant situations and values for loads, material properties and geometric data needs to be known to get reliable outcome.

Beyond the basic design code, Eurocode 3 covers the design of steel structures. Part 1-1 handle the general rules, part 1-4 the supplementary rules for stainless steel and part 2 the design of steel bridges. As mentioned in Section 2.2.3.2, no codes are yet available for FRP.

2.3.1.1 Ultimate Limit State

Ultimate limit state, ULS, is associated with the collapse or other failures of the bridge (SIS, 2001). It concerns both the safety of people and of the structure itself. The objectives that needs to be verified are loss of equilibrium, failure caused by to big deformations and failure due to time-dependent effects such as fatigue.

For loss of equilibrium, the design value for the effect of actions destabilising the structure $E_{d,dst}$ needs to be less than the design value for the effect of stabilising actions $E_{d,stb}$, see Equation 2.3.

$$E_{d,dst} \leq E_{d,stb} \tag{2.3}$$

Similar for failure due to deformation, the design value for the effect of different actions E_d should be less than the design value of the resistance for the corresponding action R_d, see Equation 2.4. Different actions can for example be internal forces and moment.

$$E_d \leq R_d \tag{2.4}$$

2.3.1.2 Serviceability Limit State

Serviceability limit state, SLS, correspond to conditions beyond the specific service requirements of the bridge (SIS, 2001). It covers the functioning of the structure under normal use, peoples comfort and the appearance of the construction. These aspects are verified through limits for deformations, vibrations and damages that affect the functions of the bridge. For all requirements in SLS, it should be verified that the design value of the effects of actions specified in the serviceability criterion E_d is less than the limiting design value of the serviceability criterion C_d, see Equation 2.5.

$$E_d \leq C_d \tag{2.5}$$

According to Krav Brobyggande for bridges in Sweden, the general demand for vertical deformation of variable loads, such as traffic loads, is not to exceed 1/400 of the theoretical span L, see Equation 2.6 (Trafikverket, 2011a). This demand applies to the span both in longitudinal and transverse direction. It's also stated that the vertical movements at the bridge edge due to traffic loads can't exceed 5 mm.

$$Vertical\ deformation\ \leq \frac{L}{400} \tag{2.6}$$

Horizontal deformations are treated for the element that supports the bridge such as a column or a wall, which can't have deformations over 1/200 of the length of the column L, see Equation 2.7.

$$Horizontal\ deformation\ \leq \frac{L}{200} \tag{2.7}$$

2.3.2 Dynamic

As mentioned earlier in this chapter, in Section 2.3.1.2, dynamic behaviour comes under serviceability limit state. The dynamic phenomena on footbridges are the movements of the bridge due to different loads, but with pedestrian load as paramount. The bridge starts to vibrate, which is the movement of the bridge when oscillations starts around a fixed point, with unit hertz (Hz) (Sétra, 2006). The vibrations will have an acceleration who describes the speed behaviour in unit m/s^2. It's both the movement itself and the speed that can be experienced uncomfortable.

Dynamic loading applied to a stiff and massive structure won't give large vibrations, but the developments of lighter and more flexible footbridges challenges the dynamic behaviour and needs more thorough analysis (Sétra, 2006). However, the dynamics do rarely cause any structural failure, in fact, lightweight structures do often exceed the limits of comfort requirements without any complaints (fib, 2005). But it's still very important to check the natural frequencies for lightweight pedestrian bridges.

2.3.2.1 Dynamic performance

The vibrations in a bridge can occur in three directions; vertical, transverse horizontal and longitudinal horizontal, see Figure 2.15 (fib, 2005). The longitudinal component that aren't represented in the figure goes along the bridge, perpendicular to the other two.

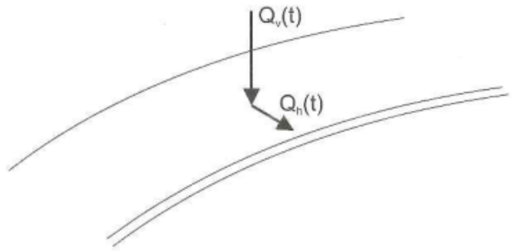

Figure 2.15 *Vertical $Q_v(t)$ and transverse horizontal $Q_h(t)$ components of forces from a pedestrian. The longitudinal component $Q_l(t)$ goes along the bridge (fib, 2005).*

The reasons why a bridge starts to move is several, with the pedestrian induced vibration as the dominating one (fib, 2005). That imply when pedestrian traffic is acting on the bridge and influences the dynamic response. A high pedestrian density means lack of space which leads to pedestrians walking pattern merging together and the frequency of the pace gets synchronised. This group effect increases the vibrations. A low pedestrian density works in the opposite way with individual walking and frequencies.

But also the structure itself create frequencies and are considered in the design process. The behaviour will depend on four factors; the stiffness, mass, magnitude of external force that oscillate on the structure and the damping. These factors give the bridge a natural frequency called eigenfrequency (Sétra, 2006).

If the frequency of the pedestrian induced vibration matches the eigenfrequency of the bridge, resonance will occur (Sétra, 2006). This phenomenon result in distinct movements and can be felt as uncomfortable for pedestrians. Therefore, when designing a footbridge to act stable with regard to dynamic behaviour, the basic method is to prevent resonance by avoiding eigenfrequencies within the range of pedestrian walking frequency. If modification of the natural frequency of the bridge doesn't avoid the resonance situation, the structural damping needs to be increased. Also, if resonance occurs in an existing bridge, the cheapest solution is to increase the damping as well (Sétra, 2006).

Structural damping is methods to eliminate oscillations and helps the vibrations in a bridge to stop. A natural damping can be material damping, such as heat dissipation for steel elements and cracking of concrete (fib, 2005). Damping of footbridges mainly depends on material properties, type of bridge structure and bearing conditions, and a bridge can be over-, critically- and underdamped depending on the damping ratio ξ , see Equation 2.8 and Figure 2.16 (Sétra, 2006).

$$\xi = \frac{c}{2\sqrt{km}} \tag{2.8}$$

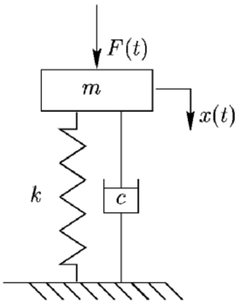

Figure 2.16 *Simple oscillator consisting of mass m connected to a support through a spring with stiffness k and a linear damper with viscosity c. The mass are loaded with an external force $F(t)$ (Sétra, 2006).*

A ratio above one indicates an overdamped situation where the structure doesn't oscillate. A ratio below one means an underdamped situation where the structure sway back and forth before it reaches its equilibrium. Finally a ratio equal to one is the scenario in between called critically damped, see Figure 2.17. The damping ratio cannot be calculated but has to be measured from test on the existing bridge. Because of this, it's hard to know the damping behaviour unless the designers have prior experiences.

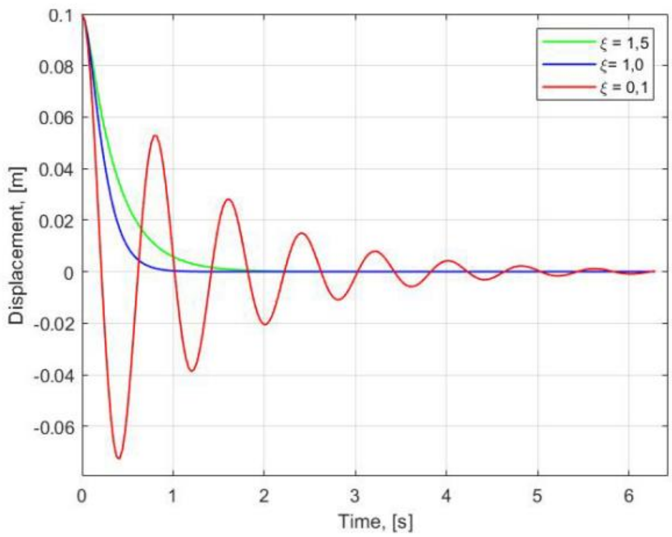

Figure 2.17 *Effect of damping. Green line represent an overdamped structure, blue a critically damped and red an underdamped (Bond and Hjelmgren, 2018).*

2.3.2.2 Eurocode

Eurocode are used for structural design in Sweden and rest of Europe, which also includes dynamic limits. It's stated that for pedestrian comfort, the criteria needed to be fulfilled is mainly a maximal limit for acceleration (SIS, 2001). These limiting values are below 0.7 m/s^2 for vertical acceleration and 0.2 m/s^2 for horizontal, see Table 2.5.

Table 2.5 *Limiting values for acceleration stated in Eurocode (SIS, 2001).*

Vertical	$< 0.7\, m/s^2$
Horizontal	$< 0.2\, m/s^2$

Except the acceleration, the comfort criteria should be verified by the critical natural frequencies for the bridge. They are limited in Eurocode as above 5 Hz for vertical frequencies and 2.5 Hz for horizontal, see Table 2.6.

Table 2.6 Limiting values for natural frequencies stated in Eurocode (SIS, 2001).

Vertical	$> 5Hz$
Horizontal	$> 2.5Hz$

In Eurocode 3 part 2, which specialises on steel bridges, it's noted that footbridges with excessive vibrations above the limiting value could cause discomfort for pedestrians (SIS, 2006b). To avoid this the design of the bridge should be remade to bring it appropriate natural frequencies, or it should be provided with sufficient dampers.

2.3.2.3 Sétra

Except the demands stated in Eurocode, constructing companies use a manual made by Sétra which supplies information, methodologies and tools for dynamic analysis to improve the quality of these (Sétra, 2006). The guidelines are in line with limits stated in Eurocode and are seen as a more expanded guidance with design recommendations. The methodology contains of five steps to in the end have a conclusion about the expected comfort of the bridge, see Figure 2.18. It starts with classifying the footbridge to eliminate bridges in class four which don't need a dynamic analysis. After the following calculation of the bridge's natural frequencies, the result is evaluated for risk of resonance. If there's a risk, dynamic load cases need to be studied to get the maximum accelerations by the structure. By comparing these to the comfort limits, a conclusion regarding the bridge dynamics and expected comfort can be made.

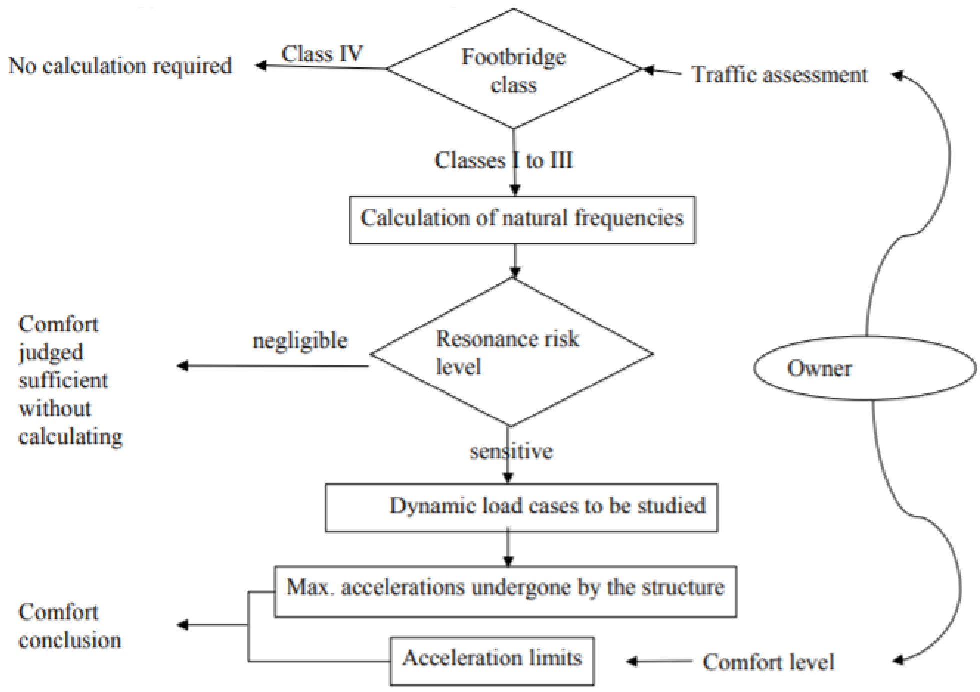

Figure 2.18 Dynamic design chart for footbridges according to Sétra, starting with classification of the bridge and ending with conclusions about the expected comfort (Sétra, 2006).

According to Sétra, the resonance is the big issue for the dynamic of footbridges in class one to three. To determine if the eigenfrequencies indicates resonance or not, the frequencies are compared to four ranges, from range one with maximum risk of resonance to range four with negligible risk. For vertical and longitudinal vibrations, see Figure 2.19, and for transverse horizontal vibrations, see Figure 2.20.

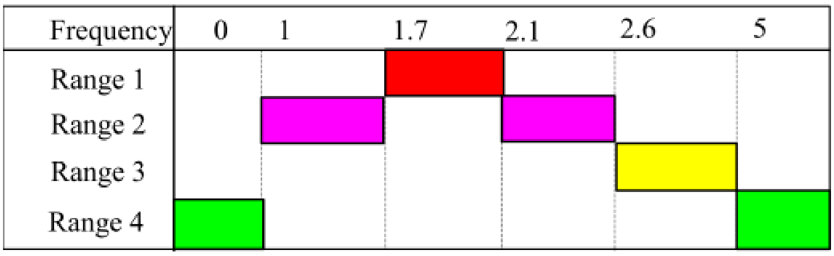

Figure 2.19 *Frequency ranges (Hz) of vertical and longitudinal vibrations. Range 1 indicate maximum risk of resonance and range 4 negligible risk (Sétra, 2006).*

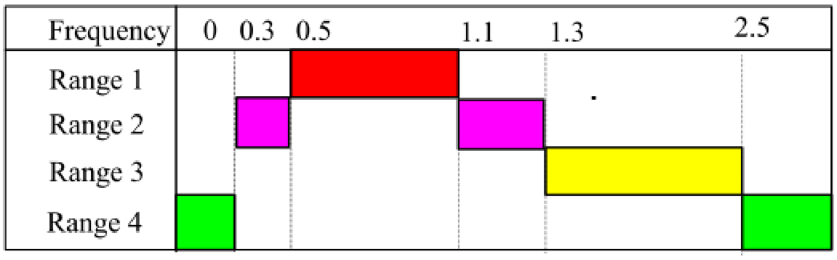

Figure 2.20 *Frequency ranges (Hz) of transverse horizontal vibrations. Range 1 indicate maximum risk of resonance and range 4 negligible risk (Sétra, 2006).*

2.4 Acting loads

Acting loads on structures in general is both permanent and variable ones, with the difference whether or not the load always is working.

2.4.1 Permanent loads

The permanent load for a bridge is the self-weight, including the weight of the load bearing beams and the deck system. The forces f are calculated with material weight g_{part} and length of each profile L_{part}, see Equation 2.9.

$$f\ [kN] = 9.807\ \left[\frac{m}{s^2}\right] \cdot g_{part}\ \left[\frac{kg}{m}\right] \cdot L_{part}\ [m] \qquad (2.9)$$

For a parametric point of view with different geometries, the self-weight can also be stated per meter in the longitudinal direction $[kN/m]$ by dividing g with the length of the bridge L.

2.4.2 Variable loads

Variable loads taken into consideration for analysis of a pedestrian bridge is traffic load from pedestrians and service vehicles, snow load and wind load.

Demands for traffic load on bridges are found in Eurocode 1 part 2 “Traffic loads on bridges”. Chapter 5 covers loads in footbridges which are divided into three load models for vertical loads; uniformly distributed load q_{fk}, concentrated load Q_{fwk} and service vehicle Q_{serv}.

For load model one, a recommended national value for the uniformly load are stated in the codes as $q_{fk} = 5\ kN/m^2$ (SIS, 2003b). But due to geometry conditions, the value can be reduced, see Equation 2.10 and 2.11.

$$q_{fk\left[\frac{kN}{m^2}\right]} = 2.0 + \frac{120}{L+30} \tag{2.10}$$

L is the loaded length [m]

$$2.5\frac{kN}{m^2} \leq q_{fk} \leq 5.0\frac{kN}{m^2} \tag{2.11}$$

The concentrated load in load model number two are of size $Q_{fwk} = 10\ kN$ distributed over an area of $100 \times 100\ mm^2$, but can according to Eurocode be neglected in load considerations if a service vehicle is prescribed on the bridge (SIS, 2003b). Finally load case number three which only is needed to be considered if the bridge will be loaded by service vehicles. If so, a load model with a two-axle load group of 80 and 40 kN with specific distances will be handled, see Figure 2.21. Notable is the statement in Eurocode saying that the uniformly distributed pedestrian load and load from service vehicle won’t appear at the same time (SIS, 2003b).

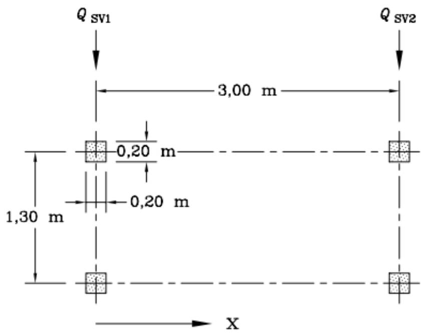

$Q_{SV1} = 80\ kN$
$Q_{SV2} = 40\ kN$

Figure 2.21 Load model for service vehicle, configurated with a two-axle load group (SIS, 2003b).

For the snow load a climate in Gothenburg Sweden are considered, with equations and demands for calculation stated in Eurocode 1 Part 1-3 “General actions – Snow load” (SIS, 2003a). Also here Eurocode states that snow don’t needs to be combined with traffic loads for pedestrian bridges (SIS, 2001).

Requirements for wind load are found in Eurocode 1 Part 1-4 “ General actions – Wind actions” (SIS, 2005a). As well as for snow conditions, the geographical values for wind loads are taken for Gothenburg Sweden.

Another pedestrian load other than the one stated in Eurocode is the one mentioned in Sétra, which only is used when calculation of eigenfrequencies and not combined in load combinations when dimensioning the bridge. It consider pedestrian crowds with Category II representing a dense crowd with 0.8 pedestrians/m^2 (Sétra, 2006). The number of pedestrians involved on the specific bridge N is then calculated, see Equation 2.12.

$$N = S \times d \tag{2.12}$$

S is the area of the footbridge [m^2]

The total weight of the crowd on the bridge W is then obtained with the pedestrian weight of 70 kg, see Equation 2.13. This weight is however smaller than the pedestrian load from Eurocode, but is as mentioned only applied when doing the dynamic analyse.

$$W\ [kg] = N \times 70kg \tag{2.13}$$

3 Designing with Linear Finite Elements

The following chapter describes the important aspects of designing with linear finite elements. The later on FE-analyse are done in FEM-Design, a modelling software for load-bearing structures according to Eurocode (StruSoft, 2019).

3.1 Element types

For analyses using Finite element software there are three types of elements that can describe the problem: structural elements, continuum elements and special elements (Broo, Lundgren and Plos, 2008). Structural elements contain beams, shells and other fabricated elements and are the used types for this thesis. These elements have six degrees of freedom, including rotations and translations of two and four degrees respectively, see Figure 3.1.

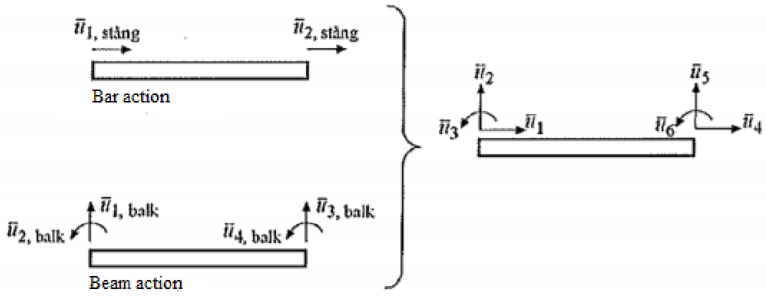

Figure 3.1 The six degrees of freedoms in a structural element, two rotations and four translations.

3.2 Equivalent Stiffness in Orthotropic Steel Deck

As described in Chapter 2, and in particular Section 2.1.2, the concept of an orthotropic steel deck is to get different stiffening elements to act as one unit. By spreading out the stiffness of the longitudinal and transversal beams over the entire deck plate, the whole structure gets an equivalent stiffness which is seen as a simplification of reality, see Figure 3.2. But with lower level of details and coarser mesh, the FE-modelling will run faster. A high level of details gets a massive and complex output (Blaauwendraad, 2010).

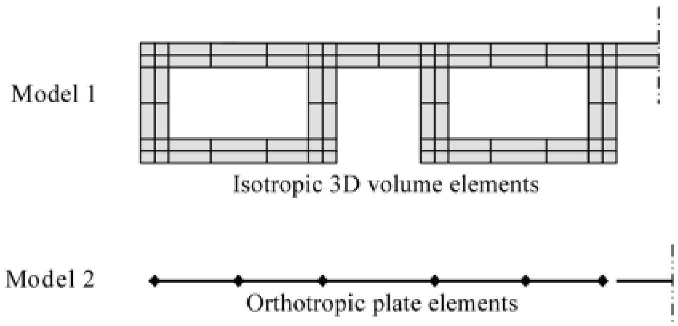

Figure 3.2 Two different detail levels of a FE model, with a high level in Model 1 and a low in Model 2 (Blaauwendraad, 2010).

The method used to implement the orthotropic properties into the 2D plate is to implement it in the rigidities of the plate. Another way had been to do it in the geometry. For calculation, the longitudinal direction of the bridge lays in x-axis while the transversal direction is in y-axis, see Figure 3.3. Also the definitions of width and area of stiffeners are presented.

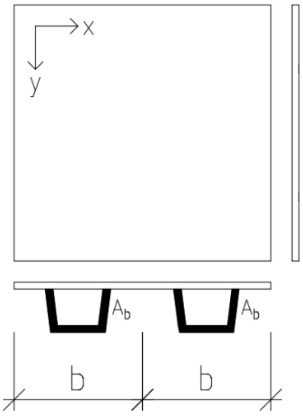

Figure 3.3 *Parameters used for calculation of equivalent stiffness. The x-axis refers to the longitudinal direction of the bridge, and the y-direction to the transverse direction (Håkansson and Wallerman, 2015).*

To get the equivalent stiffness for the deck, the cross-sectional properties needs to be defined in the two directions x and y. When analysing in FEM-Design, a fictitious shell can be chosen to represent the deck, which needs a definition of the rigidity matrix $\boldsymbol{D}$, see Equation 3.1. The blue box represents the membrane stiffness $\boldsymbol{D_m}$, also called axial rigidity, and the green box represents the bending stiffness $\boldsymbol{D_b}$, also called flexural rigidity. By this method, instead of entering the thicknesses of members, the rigidities of the members are chosen.

$$\boldsymbol{D} = \begin{bmatrix} d_{xx} & d_{\boldsymbol{v}} & 0 & 0 & 0 & 0 \\ & d_{yy} & 0 & 0 & 0 & 0 \\ & & d_{xy} & 0 & 0 & 0 \\ & & & D_{xx} & D_{\boldsymbol{v}} & 0 \\ & & & & D_{yy} & 0 \\ & & & & & D_{xy} \end{bmatrix} \tag{3.1}$$

For the bending stiffness $\boldsymbol{D_b}$ placed in the green box in the rigidity matrix in Equation 3.1, D_{xy} is replaced by an average value D_{av} between D_{xx} and D_{yy} since the torsion rigidity in an OSD may differ in x- and y-direction, with the following relationship $D_{xy} \neq D_{yx}$, see Equation 3.2 and 3.3 (Blaauwendraad, 2010).

$$\boldsymbol{D_b} = \begin{bmatrix} D_{xx} & D_{\boldsymbol{v}} & 0 \\ 0 & D_{yy} & 0 \\ 0 & 0 & D_{av} \end{bmatrix} \tag{3.2}$$

$$\boldsymbol{D} = \begin{bmatrix} d_{xx} & d_{\boldsymbol{v}} & 0 & 0 & 0 & 0 \\ & d_{yy} & 0 & 0 & 0 & 0 \\ & & d_{xy} & 0 & 0 & 0 \\ & & & D_{xx} & D_{\boldsymbol{v}} & 0 \\ & & & & D_{yy} & 0 \\ & & & & & D_{av} \end{bmatrix} \tag{3.3}$$

The second stiffness matrix to be defined in FEM-Design is for the shear stiffness $\boldsymbol{D_s}$, see Equation 3.4.

$$\boldsymbol{D_s} = \begin{bmatrix} D_{sx} & 0 \\ 0 & D_{sy} \end{bmatrix} \tag{3.4}$$

3.2.1 Membrane Stiffness

For a homogenous isotropic plate, i.e. a plate with same properties in all directions, the effect of the stiffeners needs to be added to the membrane rigidity $\boldsymbol{D_m}$, see original and additional rigidity matrices in Equation 3.5 and 3.6 respectively (Blaauwendraad, 2010). The blue box represents longitudinal stiffeners in the bridge and the green box represents the transvers stiffeners.

$$\boldsymbol{D_m} = \begin{bmatrix} \frac{E\cdot t}{1-\nu^2} & \nu \cdot \frac{E\cdot t}{1-\nu^2} & 0 \\ \nu \cdot \frac{E\cdot t}{1-\nu^2} & \frac{E\cdot t}{1-\nu^2} & 0 \\ 0 & 0 & \frac{1}{2\cdot(1-\nu)} \cdot \frac{E\cdot t}{1-\nu^2} \end{bmatrix} \tag{3.5}$$

$$\boldsymbol{D_{m.add}} = \begin{bmatrix} \frac{E\cdot A_a}{a} & 0 & 0 \\ 0 & \frac{E\cdot A_b}{b} & 0 \\ 0 & 0 & 0 \end{bmatrix} \tag{3.6}$$

But since the deck in Figure 3.3 only consists of trapezoidal ribs in transvers direction of the bridge without stiffeners in longitudinal direction, that addition will be removed from the matrix, see Equation 3.7 (Blaauwendraad, 2010).

$$\boldsymbol{D_m} = \begin{bmatrix} \frac{E\cdot t}{1-\nu^2} & \nu \cdot \frac{E\cdot t}{1-\nu^2} & 0 \\ \nu \cdot \frac{E\cdot t}{1-\nu^2} & \frac{E\cdot t}{1-\nu^2} & 0 \\ 0 & 0 & \frac{1}{2\cdot(1-\nu)} \cdot \frac{E\cdot t}{1-\nu^2} \end{bmatrix} + \begin{bmatrix} 0 & 0 & 0 \\ 0 & \frac{E\cdot A_b}{b} & 0 \\ 0 & 0 & 0 \end{bmatrix} =$$

$$= \begin{bmatrix} \frac{E\cdot t}{1-\nu^2} & \nu \cdot \frac{E\cdot t}{1-\nu^2} & 0 \\ \nu \cdot \frac{E\cdot t}{1-\nu^2} & \frac{E\cdot t}{1-\nu^2} \cdot \frac{E\cdot A_b}{b} & 0 \\ 0 & 0 & \frac{1}{2\cdot(1-\nu)} \cdot \frac{E\cdot t}{1-\nu^2} \end{bmatrix} \tag{3.7}$$

3.2.2 Bending Stiffness

For the longitudinal direction of the bridge, only the upper deck plate contributes to the flexural stiffness D_{xx} and depends on the plates thickness t, Young's modulus E and Poisson's ratio ν, see Equation 3.8 (Blaauwendraad, 2010).

$$D_{xx} = \frac{E \cdot t^3}{12 \cdot (1 - \boldsymbol{\nu}^2)} \tag{3.8}$$

For the transverse direction where the trapezoidal ribs are placed, the bending stiffness D_{yy} are calculated and can be smeared out over the width, see Equation 3.9.

$$D_{yy} = \frac{E \cdot I_y}{b} \tag{3.9}$$

For off-diagonal rigidity $D_{\boldsymbol{\nu}}$,which is related to the stiffness of the deck plate because of the occurrence of lateral contraction in that part, the definition comes from multiplying the bending stiffness in longitudinal direction D_{xx} by Poisson's ratio, see Equation 3.10.

$$D_{\nu} = \nu \cdot D_{xx} = \nu \cdot \frac{E \cdot t^3}{12 \cdot (1 - \nu^2)} \tag{3.10}$$

As mention before, D_{av} is an average value between D_{xx} and D_{yy} and is calculated with their average torsional moment of inertia, see Equation 3.11.

$$D_{av} = G \cdot \frac{i_{av}}{2} \tag{3.11}$$

Finally the full bending rigidity matrix $\boldsymbol{D_b}$ is completed, see Equation 3.12.

$$\boldsymbol{D_b} = \begin{bmatrix} \frac{E \cdot t^3}{12 \cdot (1 - \nu^2)} & \nu \cdot \frac{E \cdot t^3}{12 \cdot (1 - \nu^2)} & 0 \\ \nu \cdot \frac{E \cdot t^3}{12 \cdot (1 - \nu^2)} & \frac{E \cdot I_y}{b} & 0 \\ 0 & 0 & G \cdot \frac{i_{av}}{2} \end{bmatrix} \tag{3.12}$$

3.2.3 Shear Stiffness

The transverse shear stiffness matrix $\boldsymbol{D_s}$ are defined with different rigidities depending on direction and cross sections of the stiffeners, see Equation 3.13. (Blaauwendraad, 2010).

$$\boldsymbol{D_s} = \begin{bmatrix} D_{sx} & 0 \\ 0 & D_{sy} \end{bmatrix} \tag{3.13}$$

The equation for the shear stiffness $\boldsymbol{D_s}$ depends on the thickness of the stiffener and the shape factor η , which is 6/5 for a rectangular cross-section, see Equation 3.14

$$D_s = G \cdot \frac{t}{\eta} = G \cdot \frac{5t}{6} \tag{3.14}$$

For a direction not sensitive to transverse shear distortion, the shear rigidity D_s will be calculated with area and spacing between the stiffeners instead, see Equation 3.15.

$$D_s = G \cdot \frac{A_s}{b} \tag{3.15}$$

3.3 Initial rotational stiffness

The stiffness in truss joints has a big impact on its different behaviour in further FEM analyses, with the buckling behaviour as one important aspect. Since one aim with this master's thesis is to evaluate an optimised steel truss with better material efficiency, a new design format will appear with varying cross sections for the bars in the truss. The compressed top chord will require a big cross-sectional area while the tensioned bottom chord doesn't, and even less the diagonals. For optimal material efficiency, the joints between the diagonals and the chords won't match in sizes, see Figure 3.4.

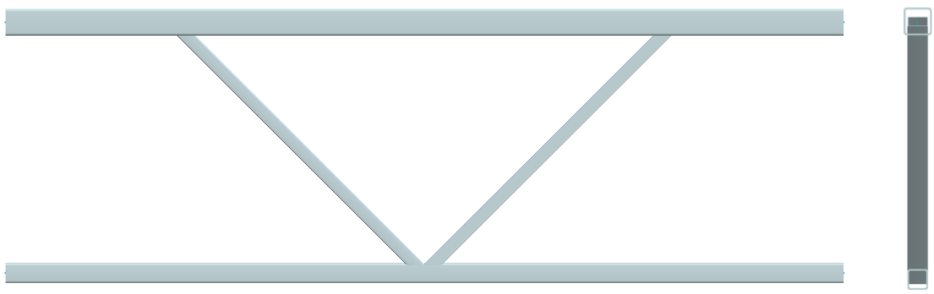

Figure 3.4 *The joint between top chord and diagonal has different cross-sectional sizes resulting in a stiffness neither hinged nor fixed, but something in between.*

These different dimensions of bar profiles are considered in factor β, see Equation 3.16 and Figure 3.5 (Garifullin *et al.*, 2017).

$$\beta = \frac{b_1}{b_0} \tag{3.16}$$

where

b_1 is the width of the connected member
b_0 is the width of the main member

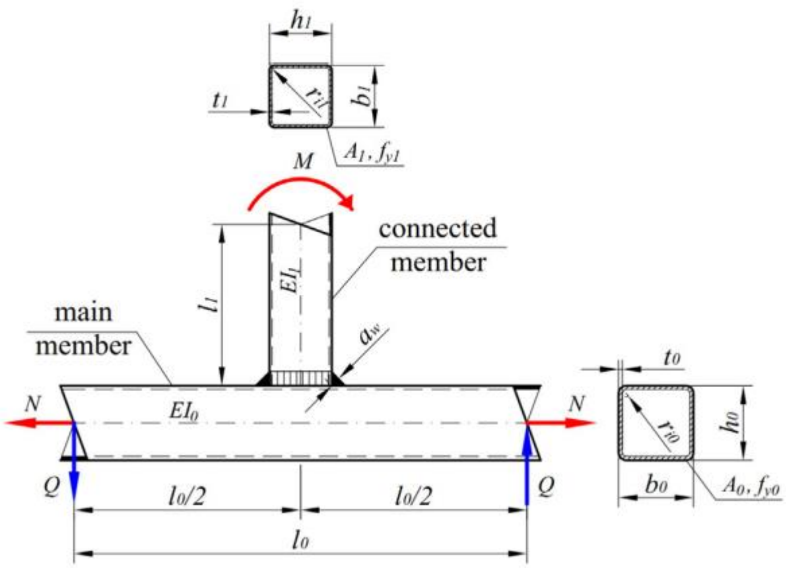

Figure 3.5 Dimensions and forces acting in a RHS T-joint with bar 0 as main member and bar 1 as connecting member (Garifullin et al., 2017).

This results in a connection being neither hinged nor fixed but something in between. The joint can be classified as rigid, normally pinned or semi-rigid according to its initial rotational stiffness $S_{j.ini}$, which later on has a major impact on the buckling behaviour of the bars (Garifullin *et al.*, 2017). Eurocode 3 Part 1-8 "Design of joints" only covers the initial rotational stiffness for these types of joints between H- and I-profiles, not between hollow sections, which will be the case in this study. The equation in Eurocode applicable for H- and I-profiles is based on the component method, see Equation 3.17 (SIS, 2005c).

$$S_{j.ini} = \frac{E \cdot z^2}{\sum_i \frac{i}{k_i}} \tag{3.17}$$

where

k_i is the stiffness coefficient for basic component i
z is the level arm

This initial rotational stiffness is in an article in the Journal of Construction Steel Research evaluated for welded RHS T-joints loaded by the in-plane bending moment (Garifullin *et al.*, 2017). It's shown that Equation 3.17 significantly underestimates the values for RHS-profiles and a proposed equation for these joints are presented, see Equation 3.18.

$$S_{j.ini} = \frac{E \cdot z^2}{\sum_i \frac{i}{k_i}} = \frac{E \cdot z^2}{\frac{2}{k_{cf}} + \frac{2}{k_{cw}} + \frac{1}{k_{sh}}} \tag{3.18}$$

The different stiffness coefficients to be considered for RHS joints are the coefficient for deformation of the surface of the main member k_{cf}, the coefficient for compression and tension deformation of the webs in the main member k_{cw} and finally the coefficient for shear deformation of the webs in the main member k_{sh}. Other coefficient than these three are not considered but may exist for weld and axial deformations (Garifullin *et al.*, 2017).

The coefficient for deformation of the surface of the main member k_{cf} are defined in the article, see Equation 3.19. With this equation the coefficient can be used both for compressive and tensile parts and that's why there's two addends for this coefficient in Equation 3.18.

$$k_{cf} = \frac{20 \cdot t_0^3 \cdot l_{eff,cf}}{(1-\beta)^3 \cdot b_0^3} \cdot \frac{1}{2+\frac{6 \cdot \beta}{1-\beta}} \tag{3.19}$$

where

$$l_{eff,cf} = t_1 + 2 \cdot b_0 \cdot \sqrt{1-\beta}$$

The coefficient for compression and tension deformation of the webs in the main member k_{cw} is defined as well, see Equation 3.20. Also with this equation the coefficient is the same for compression and tension and are taken twice in the initial rotational stiffness equation, see Equation 3.18.

$$k_{cw} = \frac{2 \cdot t_0 \cdot b_{eff,cw,el}}{h_0 - 3 \cdot t_0} \tag{3.20}$$

where

$$b_{eff,cw,el} = 2 \cdot 0.7 \cdot l_{eff,cw} + t_1$$

$$l_{eff,cw} = max \begin{cases} t_0 \cdot \sqrt{\frac{b_0}{2 \cdot t_0}} \leq 2.5 \cdot t_0 \\ \frac{b_0}{2} \cdot \sqrt{1-\beta} \leq \frac{h_0}{2} \end{cases}$$

Finally, the coefficient for shear deformation of the webs in the main member k_{sh} is defined, see Equation 3.21. This coefficient only contributes to the total stiffness coefficient one time in Equation 3.18.

$$k_{sh} = 0.38 \cdot \frac{A_{VC}}{r \cdot z} \tag{3.21}$$

where

$$r \approx 1$$

$$A_{VC} = 2 \cdot t_0 \cdot (h_0 - t_0)$$

The equations for the different coefficients are with three tests valid with more accurate predictions (Garifullin *et al.*, 2017). At least for butt-welded joints, while filled welds still are getting underestimated results, see illustrations of welds in Figure 3.6. It's also noticed that joints with filled welds have higher initial stiffness, with the conclusion of weld types affecting the stiffness.

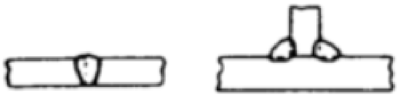

Figure 3.6 Butt-weld and filled weld respectively.

Even though the axial forces acting in the main member aren't considered in the coefficients, these are usually decreasing the resistance of the joint, and also its initial rotational stiffness (Garifullin *et al.*, 2017). This is taken into consideration with coefficient $k_{sn,ip}$, see Equation 3.22.

$$S_{j.ini} = \frac{k_{sn,ip} \cdot E \cdot z^2}{\sum_i \frac{i}{k_i}} = \frac{k_{sn,ip} \cdot E \cdot z^2}{\frac{2}{k_{cf}} + \frac{2}{k_{cw}} + \frac{1}{k_{sh}}} \tag{3.22}$$

where

$$k_{sn,ip} = \begin{cases} 1.3 - \frac{0.4 \cdot |n|}{\beta} & n > 0 \\ 1.0 & n < 0 \end{cases}$$

$$n = \frac{N_0}{A_0 \cdot f_{y0}}$$

A negative n indicates compression in the main member, and a positive n tension in the main member, which means a compressive main member don't get affected by axial forces. This is opposite to the definitions in Eurocode.

To summarise it, Equation 3.22 gives the correct initial rotational stiffness for a joint of hollow sections, without underestimating the forces.

4 Case study – Optimisation

A case study is made for a couple of bridge designs to be able to evaluate whether optimised trusses saves enough steel to invest in other innovative deck systems. This without exceeding the cost for a conventional bridge design with carbon steel. The alternative deck systems are expected to have higher initial costs from production and manufacturing, but lower for maintenance.

The five types of bridge designs investigated in the study are four with carbon steel as main material, and one with duplex stainless steel, see Figure 4.1. The first one is a typical solution for a pedestrian truss bridge with a steel trapezoidal deck system (TRP). The second one is similar to the previous one with a deck system of plates on top of transverse beams. The remaining three solutions with fiber reinforced polymer (FRP) are designs with new material approaches with a deck of lightweight composite material and transverse beams either in carbon steel or stainless steel.

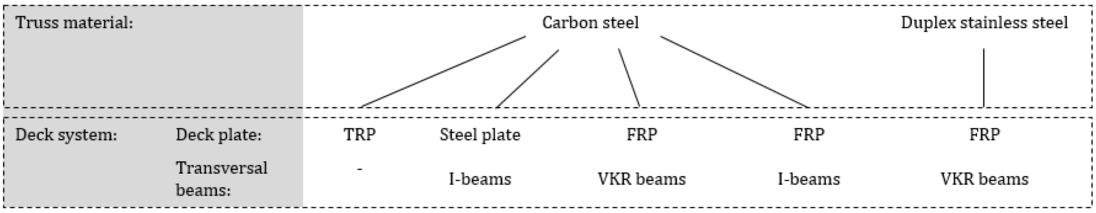

Figure 4.1 The five cases studied, four with carbon steel and one with stainless steel.

4.1 Material optimisation

The first step in the case study is to evaluate whether the trusses in the bridge can be enough material effective or not, for a material and economic gain. To obtain this, the utilisations ratios in ultimate limit state should be as close to 100 % as possible, meaning the capacity of the steel bars are equal to the actual load case and fully utilised. Earlier studies, presented in Chapter 2, and in particular Section 2.1.1, indicates that the warren truss is both the most material and production efficient truss form, and is the type used for this study.

4.1.1 Truss divisions

Due to length limitation in production and transportation, the 30-meter bars in the chords needs to be divided into smaller parts less than 12 meter. Both the top and bottom chords are divided into $8.8 + 12 + 9.2\ m$ together covering the 30-meter span, see Figure 4.2. The asymmetric division is chosen to avoid connections in the junctions between chords and web members.

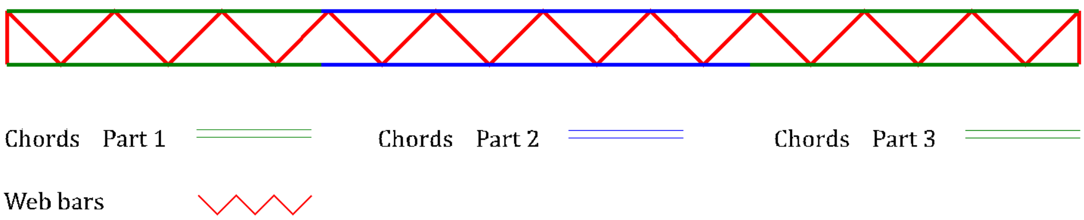

Figure 4.2 Truss divisions with three parts for chords and one part for web members.

An advantage with three parts instead of one in the chords are the possibility of using different profiles instead of one along the 30-meter span. This is useful since the internal forces in the bars varies along the bridge as well as the sequent utilisation ratios. By using unique profiles who better matches the forces in each section, a more optimised design solution appears. But to many profiles complicates the production and the cost will increase again. The three parts division is seen reasonable in that aspect.

4.1.2 Geometry and guidelines

The different solutions will be studied for a truss geometry typical for this kind of bridge, see Table 4.1. The length, width, height and angle between diagonal bars in the truss are the same for all five cases. Profiles used are hot-rolled hollow sections, VKR, either square or rectangular.

Table 4.1 Geometry for bridges in case study.

Length	Width	Height	Angle diagonal bar	⇒ Length of panel	⇒ Number of panels
30	3	1.5	45°	3	10

The significant for the conventional truss design is the desire to have dimensions of the chords and web members matching, see left picture in Figure 4.3. This is preferable for the rotational stiffness of the connection which will act stiff, almost rigid, since the webs of the chord profiles will contribute to the stiffness.

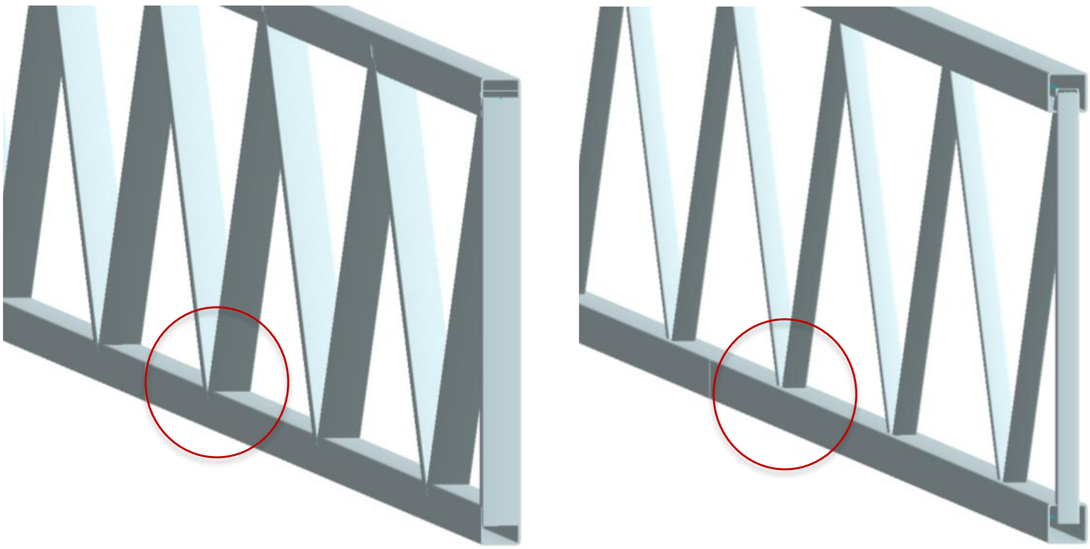

Figure 4.3 The left truss is a truss with chords and web bars with matching dimensions. The right truss is a truss with bars with variating dimensions.

The guideline for the conventional truss are:

- The chord profiles for both top and bottom will be the same for all three divisions along the bridge.

- For rotational stiffening reasons, the height of the web members needs to be equal to the width of the chords, see Equation 4.1.

$$h_{web\ member} = b_{chords} \tag{4.1}$$

For the optimised design, the conventional truss is developed to get higher optimisation ratios in the bars. For these solutions the dimensions will vary and the chord webs are no longer increasing the stiffness of the connection, see right picture in Figure 4.3. Only the top flange of the chord is acting towards the bar and the rotational stiffness will instead be lower than one and seen as something in between fixed and hinged. This optimisation will save material, but require further work with the rotational stiffness of the bar connections.

The following guidelines applies when optimising the truss:

- For aesthetical reasons the outer dimensions of the top- and bottom chord will be the same over all three divisions, only varying with thickness. With a uniform outer appearance, only the cross-sectional area towards the inside will vary with different capacities.

- The height of the web members doesn't need to be equal to the width of the chords, see Equation 4.2.

$$h_{web\ member} \neq b_{chords} \tag{4.2}$$

The study covers the superstructure of the bridge, which is a simply supported structure without rotations in the supports and only movement in the longitudinal x-direction. The movement in y- and z-direction are locked, see Figure 4.4. The joints between web bars and chords are rigid without rotations and movements in all three directions.

Figure 4.4 Boundary conditions for the simply supported beams with locked motions in y- and z-direction, represented by a red and blue arrow respectively.

4.1.3 Critical sections

For top and bottom chord, the most loaded part is in mid-section $x = 15\ m$. Regarding the web members, the second diagonal from the edges are the ones with highest internal forces, see Figure 4.5.

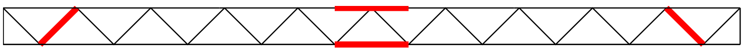

Figure 4.5 *The most loaded parts in the truss marked with red, both for top- and bottom chord and for web members.*

To get the maximum load effects for these sections, a method with influence lines are used to understand the effect from a moving load. This method gives the placement of the vehicle which is necessary for the maximum load effect. The principle is to use a curvature with the same scale as the deflected shape of the beam, showing the effect for a specific load situation. The unit value along the influence line under the load says in what grade the effect should be scaled, with value one giving the maximum load effect.

For the load situation with maximum bending moment at mid-section, the resultant force from the two load axels of $40\ kN$ and $80\ kN$ in the vehicle should be placed at that specific position, see left picture in Figure 4.6. For maximum load effect in diagonal, the resultant should be placed $3\ m$ from the support were the diagonal connects to the top chord, see right picture in Figure 4.6.

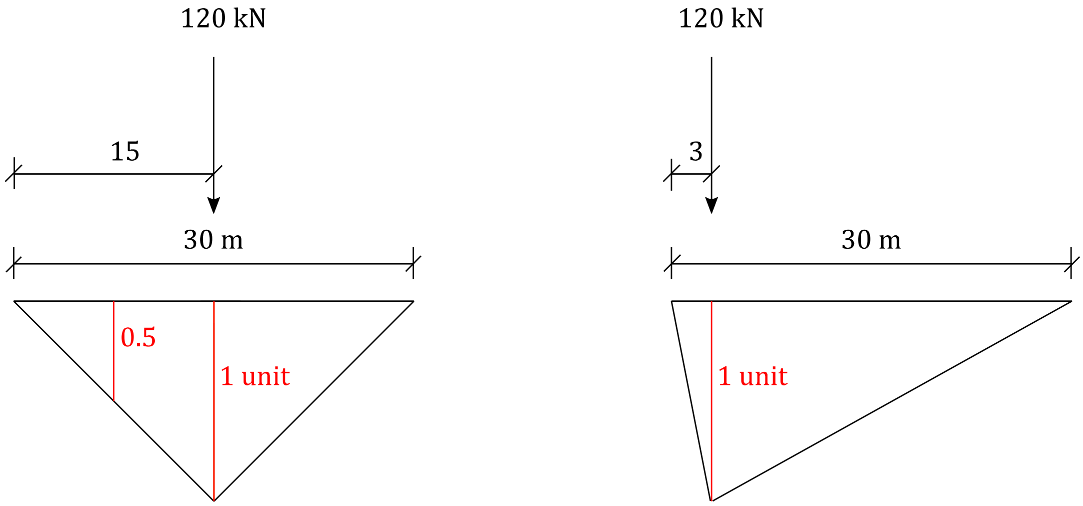

Figure 4.6 *Influence lines for bending moment at midspan or at 3 meters from support for beam loaded with a concentrated load.*

For the correct placement of the resultant force in between the two vehicle axels, calculations show this is at a $2\ m$-distance from the $40\ kN$-axel and $1\ m$ from the $80\ kN$-axel, see Figure 4.7 and Equations 4.3 to 4.5. For configuration of service vehicle, see Chapter 2, and in particular Section 2.4.2.

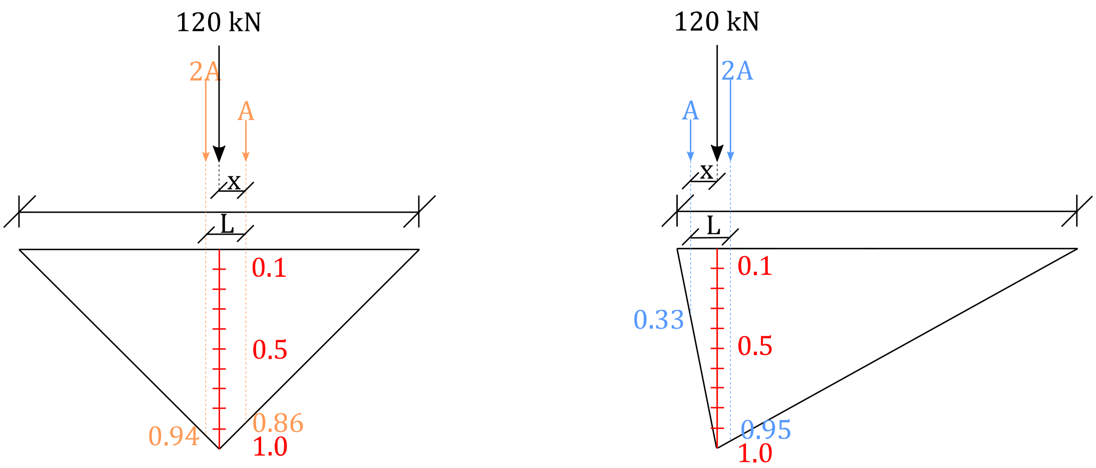

Figure 4.7 *The placement of the resultant force from the two axels in the service vehicle.*

$$A = 40\ kN$$
$$B = 80\ kN = 2A$$

$$A = (A + B) \cdot \frac{(L - x)}{L} \quad \rightarrow \quad A = 3A \cdot \frac{(L - x)}{L} \quad \rightarrow$$
$$x = L - \frac{L}{3} = \frac{2L}{3} \tag{4.3}$$

$$B = (A + B) \cdot \frac{x}{L} \quad \rightarrow \quad 2A = 3A \cdot \frac{x}{L} \quad \rightarrow$$
$$x = \frac{2L}{3} \quad \rightarrow \quad Check\ OK \tag{4.4}$$

$$L = 3m \quad \rightarrow \quad x = \frac{2 \cdot 3}{3} = 2m \tag{4.5}$$

These two placements of the service vehicle are useful for maximum bending moments in the two critical sections of the truss and used when analysing the truss capacity for the most critical load combination.

4.1.4 Actions on bridge

The considered loads in the analysis are the permanent and variable loads stated in Chapter 2, and in particular Section 2.4, except the snow load. This is disregarded since the variable traffic load and snow load doesn't need to be combined, with traffic load being the biggest. ψ-factors are taken from Eurocode with specific values for traffic and wind forces applied for footbridges, see Figure 4.8 (SIS, 2001).

Action	Symbol	ψ_0	ψ_1	ψ_2
Traffic loads	gr1 Q_{fwk} gr2	0,40 0 0	0,40 0 0	0 0 0
Wind forces	F_W	0,3	0,2	0
Thermal actions	T	0,6[1]	0,6	0,5
Snow loads	Sn (during execution)	0,8	-	0
Construction loads	Q_c - Working personal, staff and visitors with small equipment (Q_{ca}) - Storage of construction material, precast elements, etc. (Q_{cb}) - Heavy equipment etc. (Q_{cc}) - Cranes, lifts, vehicles etc. (Q_{cd})	 1,0 1,0 1,0 1,0	 - - - -	 0,2 1,0 1,0 -
1) The recommended ψ_0 value for thermal actions may in most cases be reduced to 0 for ultimate limit states EQU, STR and GEO. See however the design Eurocodes				

Figure 4.8 Recommended values of ψ-factors for footbridges with used factors highlighted (SIS, 2001).

With self-weight SW, traffic load from pedestrians TR, traffic load from service vehicles SV and wind load WI, different combinations are generated. The combined loads are done with ψ-factors in groups of:

- Self-weight, wind
- Self-weight, wind, pedestrians
- Self-weight, wind, service vehicle at $x = 15\ m$
- Self-weight, wind, service vehicle at $x = 3\ m$

As described earlier in Section 2.4.2, a concentrated load Q_{fwk} isn't taken into account, neither are the snow load. Combinations including both pedestrians and service vehicle aren't made since they won't appear at the same time. The pedestrian load is through its 30 m-geometry reduced to $4.0 \frac{kN}{m^2}$. With these conditions at analyse, the most critical load combination for the truss is shown to be the second combination with self-weight, wind and pedestrian traffic, see Equation 4.6. The combination sets the self-weight as an unfavourable permanent action, the traffic load as the leading variable action and the wind force as an accompanying variable action.

$$\begin{aligned} &0.89 \times 1.35 \times SW + 1.5 \times TR + 1.5 \times \psi_0 \times WI = \\ &0.89 \times 1.35 \times SW + 1.5 \times TR + 1.5 \times 0.3 \times WI \end{aligned} \tag{4.6}$$

When analysing the transverse beams in the deck on the other hand, the fourth combination with self-weight, wind and a service vehicle placed closed to the support is the most critical, see Equation 4.7. Here the combination sets the self-weight as an unfavourable permanent action, the wind force as the leading variable action and the service vehicle load as an accompanying variable action.

$$\begin{aligned} &0.89 \times 1.35 \times SW + 1.5 \times WI + 1.5 \times \psi_0 \times SV_{x=3} = \\ &0.89 \times 1.35 \times SW + 1.5 \times WI + 1.5 \times 0.4 \times SV_{x=3} \end{aligned} \tag{4.7}$$

4.1.5 Connections

The two different types of connections in the bridge making effective joints for are:

- VKR/VKR – joint between bars in the truss, and also between bottom chord and transverse beams

- VKR/I-beam – joint between bottom chords and transverse beams

Both these connections will be welded, see sketches in Figure 4.9 and Figure 4.10.

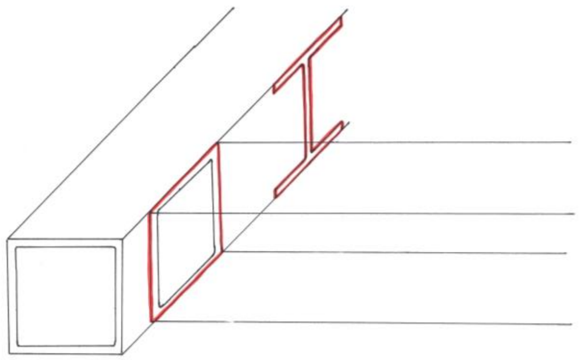

Figure 4.9 Sketch of joints between VKR/VKR and VKR/I-beam between bottom chord and transverse beams.

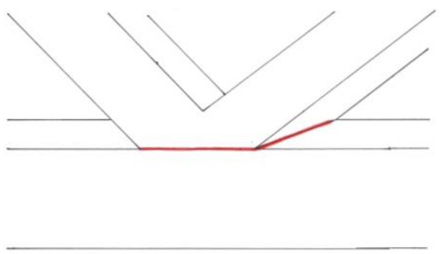

Figure 4.10 Sketch of joint between three VKR profiles, two diagonal members and a bottom chord, in a truss system.

4.2 Results

When building the design models in FEM-Design, the structural elements are modelled, loads applied and load combinations defined. The structural elements have an impact on the stiffness of the bridge, but the deck plate has been removed and substituted with an element with load but no stiffening effect. This to eliminate the stiffness of the plate when dimensioning the truss at a worst-case scenario.

As a start, a first order analysis is done which calculate the stresses for a scenario where all the bars in the truss still are straight. From that result the dimensioning of the profile is made. With this final configuration of profiles, a second order analysis are also done for the worst load combination for the truss. The stresses are in this analysis checked for the scenario when the bridge is loaded together with the displacement, i.e. checked when loaded after exposed to buckling, with the compressive top chord as the most critical bar.

When the dimensioning of the bridge is done, the dynamic analysis is made with check of natural frequencies. The first five eigenmodes are picked out from FEM-Design and compared to specific limits, see limits in Chapter 2 and in particular Section 2.3.2. If the frequencies are below the limit, the acceleration is calculated by hand and controlled as well. This is only necessary for the vertical vibrations, since these are the most critical.

After analysing the conventional design, the same truss is remade with other profiles to maximize the capacities of the bars in the truss in line with the guidelines presented in Section 4.1.2. The same analysing procedure as for the conventional design is then followed. The results presented in the following sections are for the most critical parts in the truss, see Section 4.1.3.

4.2.1 No.1 – TRP deck

The first design alternative is the warren truss together with a trapezoidal steel deck. This deck consists of a top plate with stiffening U-beams underneath, laying in the transverse direction of the bridge, i.e. y-direction, see illustration in Figure 4.11 and Figure 4.12.

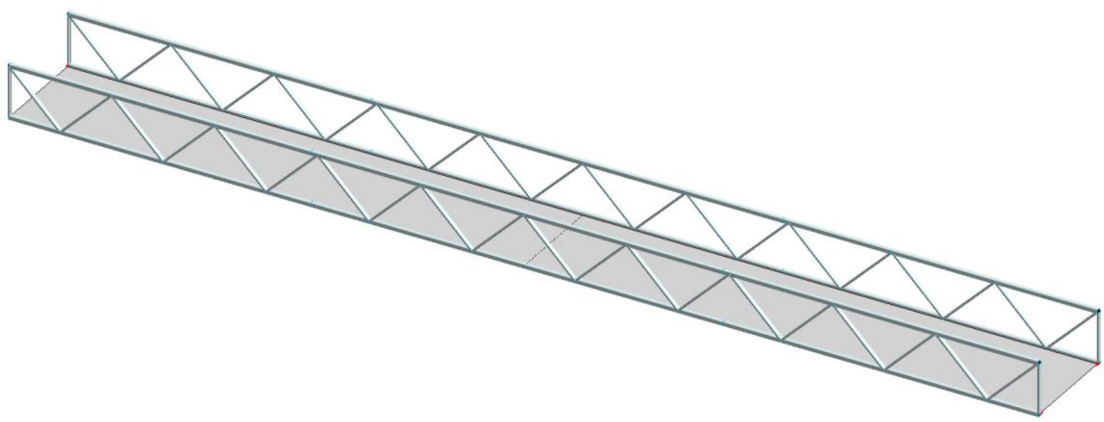

Figure 4.11 Bridge solution number one with warren trusses and a trapezoidal steel deck.

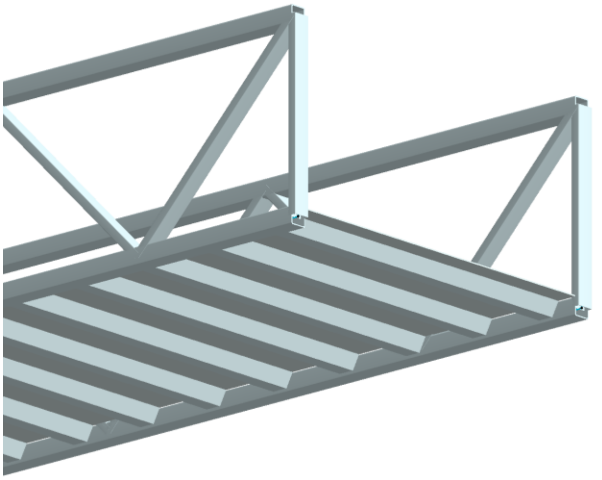

Figure 4.12 *The trapezoidal steel deck seen from below with transverse beams in y-direction, connected to a steel plate.*

The thickness of the top plate is $10\,mm$ and the spacing between the U-beams $640\,mm$, see Figure 4.13. For this specific configuration, the selfweight becomes $g = 106\,\frac{kg}{m^2} = 1.04\,\frac{kN}{m^2}$ for steel density $\rho = 7850\,\frac{kg}{m^3}$. Since there is no need of further elements in the deck system, this is the total weight for it.

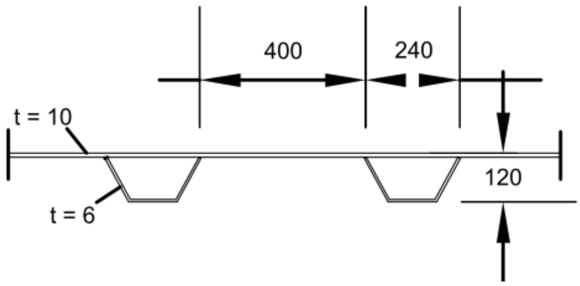

Figure 4.13 *Sectional illustration of the TRP deck.*

When defining a TRP deck in FEM-Design, two approaches are possible. The most accurate way is to model it by hand with different structural parts to simulate its exact appearance, as in Figure 4.12. This is however time consuming. The other approach is to calculate the equivalent stiffness of the deck, as described in Chapter 3, and in particular Section 3.2, to define a simple flat plate with. This is a faster process but a simplification of the stiffening behaviour of the plate. Both these approaches will be used for modelling the TRP deck to be evaluated against each other. First out is the hand modelling method.

After analysing and designing of steel bars in FEM-Design, results are produced and compiled. Chosen profiles are presented, as well as capacity utilisation ratios [%] in ULS for the different bars and the five first shapes of the eigenfrequencies [Hz]. For later economic evaluations, quantity estimations are also presented in form of steel weight [t], needed painted steel area [m^2] and needed welding length [m]. These numbers give the foundation for further analyses of the bridge. All results are presented for both the conventional and optimised design and compared against each other, see Table 4.2. The column to the right shows the difference between the conventional and optimised truss in [%]. A positive green value indicates profit for the optimised truss and a negative red value loss. Dimensioning load cases varies between the compressed top chord and diagonals and the tensioned bottom chord. The compressed members are dimensioned for interaction between normal force and bending, while the tensioned members is dimensioned for normal capacity.

Table 4.2 *Results for analysed conventional and optimised truss designs respectively, with a TRP deck system. Presented are the stated profiles, utilisation ratios for bar capacities, eigenfrequencies and different quantity estimations.*

	Conventional truss		**Optimised truss**		
	Profile types in truss - VKR				
Top Chord	Part 1-3	140 × 140 × 6.3	Part 1 Part 2 Part 3	140 × 140 × 5 140 × 140 × 6.3 140 × 140 × 5	
Bottom Chord	Part 1-3	140 × 140 × 5	Part 1 Part 2 Part 3	140 × 140 × 5 140 × 140 × 5 140 × 140 × 5	
Diagonals	Part 1-3	140 × 70 × 4	Part 1-3	100 × 60 × 4	
	Utilisation ratio in bars, ULS Should be $\leq$ 100 %				**diff.**
Top Chord	Part 1 Part 2 Part 3	72 % 96 % 72 %	Part 1 Part 2 Part 3	89 % 95 % 89 %	17 % -1 % 17 %
Bottom Chord	Part 1 Part 2 Part 3	48 % 65 % 48 %	Part 1 Part 2 Part 3	50 % 66 % 50 %	2 % 1 % 2 %
Diagonals	Part 1-3	59 %	Part 1-3	93 %	34 %
	Eigenfrequencies Should be $\geq$ 2.5 Hz for horizontal (H) vibrations Should be $\geq$ 5.0 Hz for vertical (V) vibrations **Acceleration** Should be $\leq$ 0.2 m/s^2 for horizontal (H) acceleration Should be $\leq$ 0.7 m/s^2 for vertical (V) acceleration				
Shape 1	3.232 Hz (V) Acceleration: 0 m/s^2 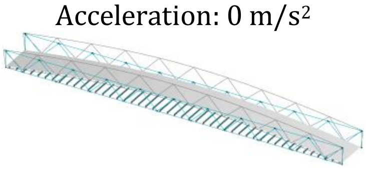		3.131 Hz (V) Acceleration: 0 m/s^2 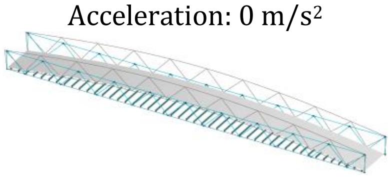		
Shape 2	3.713 Hz (H) 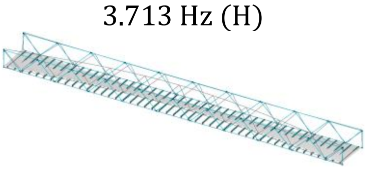		3.671 Hz (H) 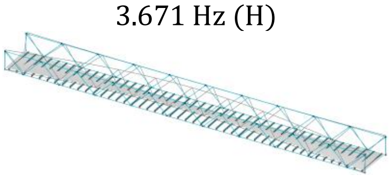		

Shape 3	7.343 Hz (V) 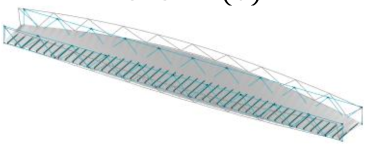	7.189 Hz (V) 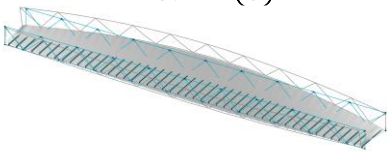	
Shape 4	9.802 Hz (V) 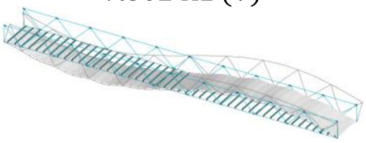	8.467 Hz (H) 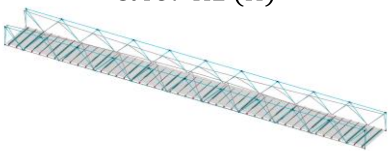	
Shape 5	10.817 Hz (H) 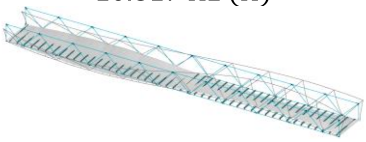	9.156 Hz (H) 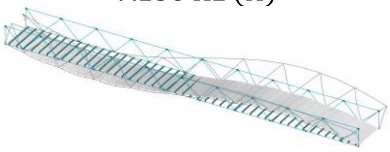	
	Quantity estimations Weight [t], Painted area [m²] and Welding length [m]		**diff.**
Weight [t]			
Truss	$3.966\ t$ Top: 1.567 Bottom: 1.259 Diagonals: 1.14	$3.496\ t$ Top: 1.382 Bottom: 1.259 Diagonals: 0.855	11.9 %
Deck	$9.016\ t$ Steel plate: 6.735 Transversal beams: 2.281	$9.016\ t$ Steel plate: 6.735 Transversal beams: 2.281	0 %
TOTAL	$13.0\ t$	$12.5\ t$	3.8 %
Painted Area [m²]			
Truss	$102.676\ m^2$ Top: 32.627 Bottom: 32.827 Diagonals: 37.222	$93.711\ m^2$ Top: 32.747 Bottom: 32.827 Diagonals: 28.137	8.7 %
Deck	$270.931\ m^2$ Steel plate: 172.257 Transversal beams: 98.674	$270.931\ m^2$ Steel plate: 172.257 Transversal beams: 98.674	0 %
TOTAL	$373.6\ m^2$	$364.6\ m^2$	2.4 %
Welding Length [m]			
TRP	$47 \times 2 \times 3 = 282\ m$	$47 \times 2 \times 3 = 282\ m$	0 %
TRP/ Bottom chord	$2 \times (30 + 47 \times 0.370) = 94.78\ m$	$2 \times (30 + 47 \times 0.370) = 94.78\ m$	0 %
Diagonals/ Chords	$2 \times 40 \times \begin{pmatrix} 2 \times 0.140 + \\ 2 \times 0.099 \end{pmatrix} = 38.24\ m$	$2 \times 40 \times \begin{pmatrix} 2 \times 0.100 + \\ 2 \times 0.085 \end{pmatrix} = 29.6\ m$	22.6 %

Verticals/ Chords	$2 \times 4 \times \binom{2 \times 0.140 +}{2 \times 0.070} = 3.36\ m$	$2 \times 4 \times \binom{2 \times 0.100 +}{2 \times 0.060} = 2.56\ m$	23.8 %
Parts Top chord	$2 \times 2 \times (4 \times 0.140) = 2.24\ m$	$2 \times 2 \times (4 \times 0.140) = 2.24\ m$	0 %
Parts Bottom chord	$2.24\ m$	$2.24\ m$	0 %
TOTAL	$422.9\ m$	$413.4\ m$	6.7 %
	Conventional truss	**Optimised truss**	

The results show a big profit of the capacity utilisation for the bars after optimising the design. Mostly in the top chord and diagonals since the bottom chord already has the smallest profile thickness possible in the conventional design and can't be thinner. The first vertical eigenfrequency is below acceptable limit but has acceptable acceleration resulting in a good expected dynamic behaviour. The total weight and painted steel area were similar with a slightly benefit to the optimised design. The same difference applies for the total length of welding.

A second order calculation is also made for the compressed top chord which is exposed to bending. Both the conventional and optimised design pass this analysis and obtains lower stresses and utilisation ratios than from the first order analysis, see Table 4.3. Dimensioning load case for this analysis is, as equal to the first order analysis, the interaction between normal force and bending.

Table 4.3 Utilisation ratios in top chord for second order analysis.

	Conventional truss		**Optimised truss**	
	Utilisation ratio top chord for Second Order Analysis Should be ≤ 100 %			
Top Chord	Part 1	71 %	Part 1	87 %
	Part 2	79 %	Part 2	79 %
	Part 3	71 %	Part 3	87 %

The results have this far been for the hand modelling method for the TRP deck. To compare the results, particularly the utilisation ratios in ULS and eigenfrequencies, the equivalent stiffness in form of membrane-, flexural- and shear stiffness, are by hand calculated to define a flat shell representing the deck, see Figure 4.14. Also weight and centre of gravity are defined.

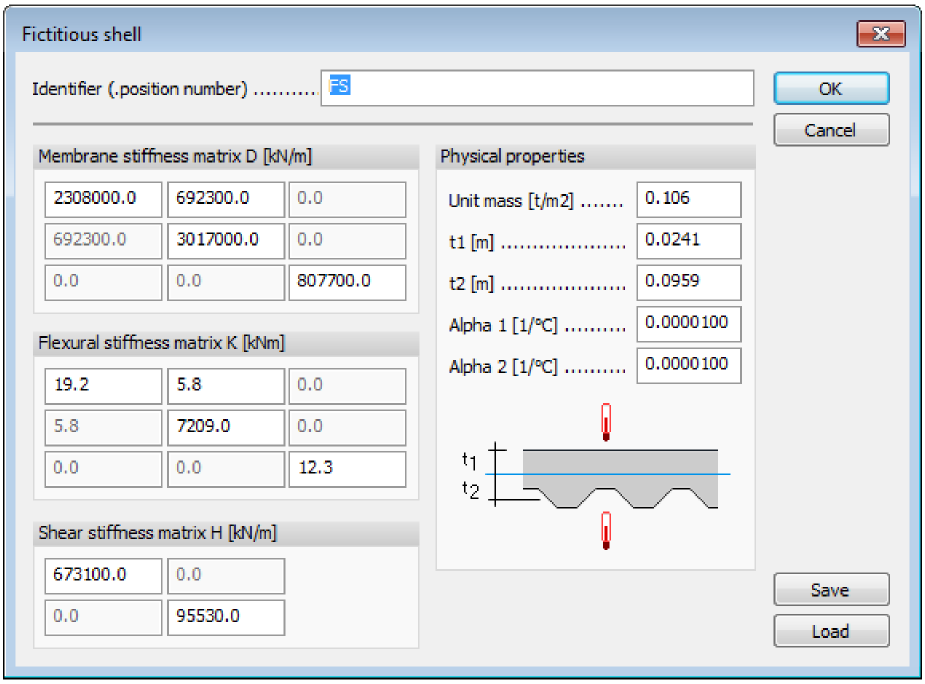

Figure 4.14 *The defined shell with specified membrane-, flexural- and shear stiffness as well as weight and centre of gravity.*

With this simplified deck plate, the same analysis procedure in FEM-Design is done as for the conventional truss from before. For a perfect comparison the two approaches should give the same results, but it's shown to differ, see Table 4.4.

Table 4.4 *Results for analysed conventional truss design with a TRP deck modelled by two different approaches. One modelled by hand and the other by a simplified shell with defined equivalent stiffness matrix.*

	TRP modelled by hand		**TRP with equivalent stiffness matrix**		
	Profile types in truss - VKR				
Top Chord	Part 1-3	140 × 140 × 6.3	⊣⊦	⊣⊦	
Bottom Chord	Part 1-3	140 × 140 × 5	⊣⊦	⊣⊦	
Diagonals	Part 1-3	140 × 70 × 4	⊣⊦	⊣⊦	
	Utilisation ratio in bars, ULS Should be ≤ 100 %				**diff.**
Top Chord	Part 1 Part 2 Part 3	72 % 96 % 72 %	Part 1 Part 2 Part 3	70 % 91 % 70 %	-2 % -5 % -2 %

Bottom Chord	Part 1 Part 2 Part 3	48 % 65 % 48 %	Part 1 Part 2 Part 3	36 % 39 % 36 %	-12 % -26 % -12 %
Diagonals	Part 1-3	59 %	Part 1-3	57 %	-2 %
	Eigenfrequencies Should be $\geq 2.5\ Hz$ for horizontal (H) vibrations Should be $\geq 5.0\ Hz$ for vertical (V) vibrations **Acceleration** Should be $\leq 0.2\ m/s^2$ for horizontal (H) acceleration Should be $\leq 0.7\ m/s^2$ for vertical (V) acceleration				
Shape 1	3.232 Hz (V) Acceleration: 0 m/s² 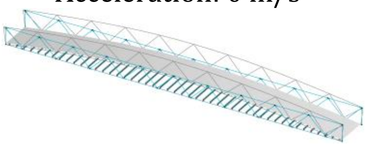		3.412 Hz (V) Acceleration: 0 m/s² 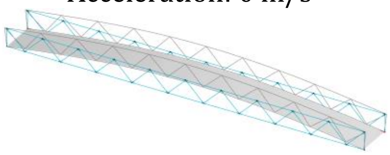		
Shape 2	3.713 Hz (H) 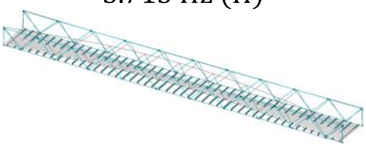		3.716 Hz (H) 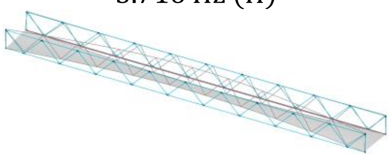		
Shape 3	7.343 Hz (V) 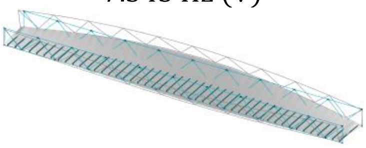		7.823 Hz (V) 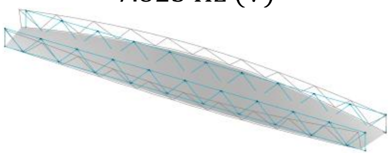		
Shape 4	9.802 Hz (V) 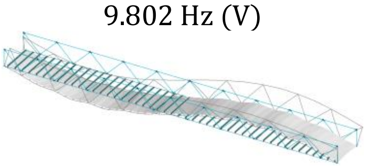		10.718 Hz (V) 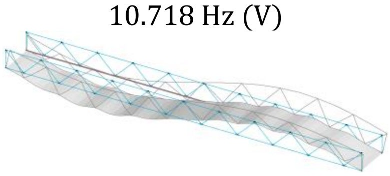		
Shape 5	10.817 Hz (H) 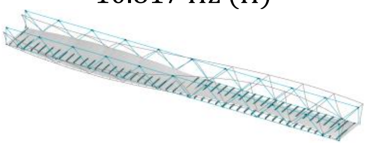		11.169 Hz (H) 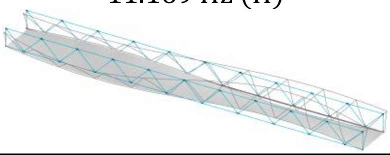		
	TRP modelled by hand		**TRP with equivalent stiffness matrix**		

The comparison shows the equivalent stiffness method getting lower utilisation in the bars, and this method can be assumed not being on the safer side. Also looking at the eigenfrequencies with shape number 1 being the critical vertical shape, the results are similar to each other but slightly higher for the case with equivalent stiffness matrix. For both utilisation and vibration aspects, the hand modelling method can be assumed being more on the safer side than the equivalent stiffness method.

4.2.2 No.2 – Steel plate with transverse I-beams

The second design alternative is the same warren truss as before, but with a steel deck consisting of a plate and transversal I-beams, see Figure 4.15. This system will have the same stiffening mechanism as the TRP, but with two different components instead of one. The spacing between the transversal beams are 1.5 m, which can be compared to the 640 mm spacing for the TRP deck.

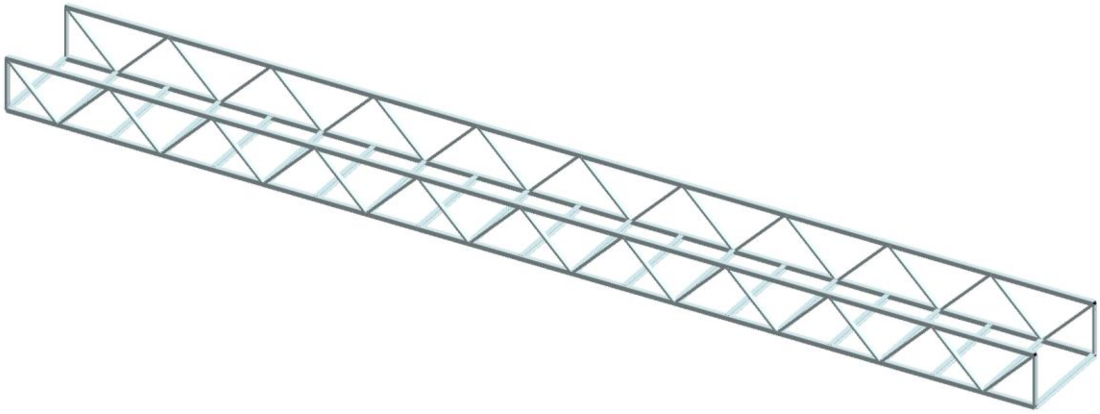

Figure 4.15 Bridge solution number two with warren trusses and a deck system of a steel plate and transversal I-beams.

The plate has a 10 mm thickness which with density $\rho = 7850\ \frac{kg}{m^3}$ result in a selfweight of $g = 78.5\ \frac{kg}{m^2} = 0.770\ \frac{kN}{m^2}$. This plate is initially analysed for not being too thin, and the normal stresses are shown being far below the 355 MPa-limit for steel grade $S355$, see Figure 4.16. Also the deflection check for the plate is okay.

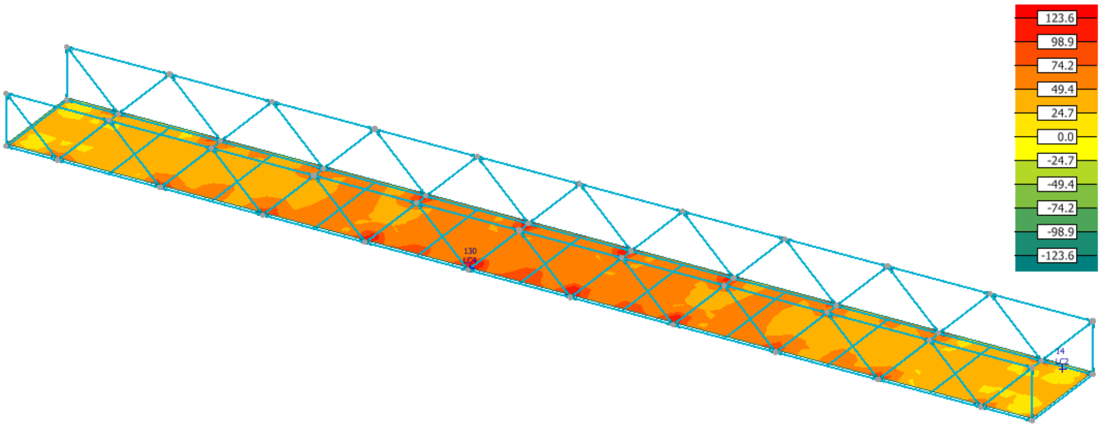

Figure 4.16 130 MPa as maximum normal stress for a steel plate with thickness 10mm.

To choose adequate transverse beams, a beam design is initially made for these. With intention to use I-beams, the range is from IPE as the weakest to HEM as the strongest with HEA and HEB in between. For each step the weight and cross-sectional area increases and improves the capacity of the bars and also the dynamic behaviour of the bridge. The dimension is chosen to match the height of the bottom chord which the beams will be welded to. If the capacity of the beam is too small in comparison to the internal forces, it’s replaced to the next one. For enough capacity, the beams need to be of sort HEB with dimension 140 mm for normal capacity as dimensioning load case, see Table 4.5.

Table 4.5 Profile and utilisation ratio for transverse beams in conventional and optimised truss respectively.

	Conventional truss		**Optimised truss**		
	Profile types in deck – I-beams				
Transverse beams	Part 1-3	HEB 140	Part 1-3	HEB 140	
	Utilisation ratio in bars Should be ≤ 100 %				**diff.**
Transverse beams	Part 1-3	82 %	Part 1-3	82 %	0 %

Same analyse procedure and design of steel bars are made as for the previous bridge solution. Profiles, utilisation ratios, eigenfrequencies and quantity values are compiled and compared for the conventional and optimised truss, see Table 4.6. The column to the right shows the difference between the two trusses in [%]. A positive green value indicates profit for the optimised truss and a negative red value loss. Dimensioning load cases varies between the compressed top chord and diagonals and the tensioned bottom chord. The compressed members are dimensioned for interaction between normal force and bending, while the tensioned members is dimensioned for normal capacity. Noteworthy are the outer dimensions of the chords that's being forced to be 140 mm due to the required size of transverse beams.

Table 4.6 Results for analysed conventional and optimised truss designs respectively, with a deck of HEB beams and a thin steel plate. Presented are the stated profiles, utilisation ratios for bar capacities, eigenfrequencies and different quantity estimations.

	Conventional truss		**Optimised truss**		
	Profile types in truss - VKR				
Top Chord	Part 1-3	140 × 140 × 6.3	Part 1 Part 2 Part 3	140 × 140 × 5 140 × 140 × 6.3 140 × 140 × 5	
Bottom Chord	Part 1-3	140 × 140 × 6.3	Part 1 Part 2 Part 3	140 × 140 × 5 140 × 140 × 6.3 140 × 140 × 5	
Diagonals	Part 1-3	140 × 70 × 4	Part 1-3	100 × 60 × 3.6	

	Utilisation ratio in bars, ULS Should be $\leq$ 100 %				**diff.**
Top Chord	Part 1	72 %	Part 1	90 %	18 %
	Part 2	96 %	Part 2	96 %	0 %
	Part 3	72 %	Part 3	90 %	18 %
Bottom Chord	Part 1	72 %	Part 1	89 %	17 %
	Part 2	83 %	Part 2	82 %	-1 %
	Part 3	72 %	Part 3	89 %	17 %
Diagonals	Part 1-3	57 %	Part 1-3	99 %	42 %
	Eigenfrequencies Should be $\geq 2.5\ Hz$ for horizontal (H) vibrations Should be $\geq 5.0\ Hz$ for vertical (V) vibrations **Acceleration** Should be $\leq 0.2\ m/s^2$ for horizontal (H) acceleration Should be $\leq 0.7\ m/s^2$ for vertical (V) acceleration				
Shape 1	1.125 Hz (H) 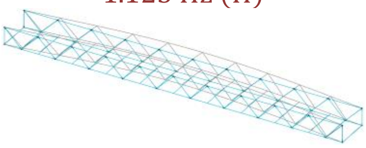		1.119 Hz (H) 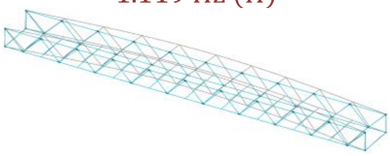		
Shape 2	2.440 Hz (H) 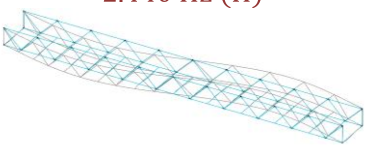		2.439 Hz (H) 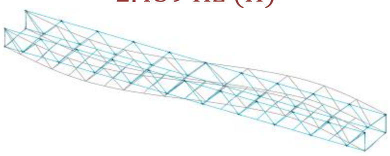		
Shape 3	2.697 Hz (V) Acceleration: 0 m/s^2 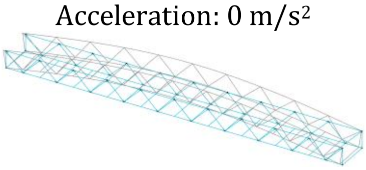		2.609 Hz (V) Acceleration: 0 m/s^2 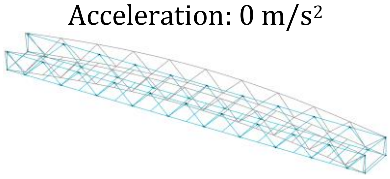		
Shape 4	3.755 Hz (H) 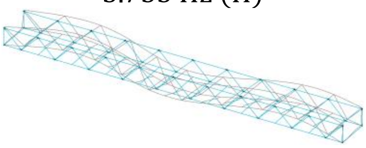		3.709 Hz (H) 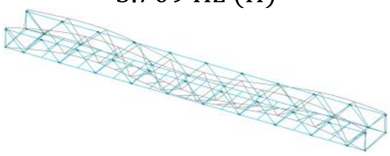		
Shape 5	3.919 Hz (V) Acceleration: 0 m/s^2 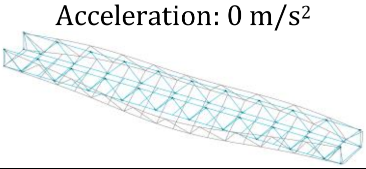		3.797 Hz (V) Acceleration: 0 m/s^2 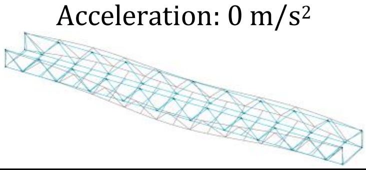		

	Quantity estimations Weight [t], Painted area [m²] and Welding length [m]		diff.
Weight [t]			
Truss	$4.274\ t$ Top: 1.567 Bottom: 1.567 Diagonals: 1.14	$3.539\ t$ Top: 1.382 Bottom: 1.382 Diagonals: 0.775	17.2 %
Deck	$8.859\ t$ Steel plate: 6.735 Transversal beams: 2.124	$8.859\ t$ Steel plate: 6.735 Transversal beams: 2.124	0 %
TOTAL	$13.1\ t$	$12.4\ t$	5.3 %
Painted Area [m²]			
Truss	$102.476\ m^2$ Top: 32.627 Bottom: 32.627 Diagonals: 37.222	$93.725\ m^2$ Top: 32.747 Bottom: 32.747 Diagonals: 28.231	8.5 %
Deck	$222.997\ m^2$ Steel plate: 172.257 Transversal beams: 50.74	$222.998\ m^2$ Steel plate: 172.258 Transversal beams: 50.74	0 %
TOTAL	$325.5\ m^2$	$316.7\ m^2$	2.7 %
Welding Length [m]			
Transversal beams/ Bottom chord	$2 \times 21 \times 0.826 = 34.692\ m$	$2 \times 21 \times 0.826 = 34.692\ m$	0 %
Transversal beams/ Deck plate	$Joint\ \rightarrow 0\ m$	$Joint\ \rightarrow 0\ m$	0 %
Diagonals/ Chords	$2 \times 40 \times \begin{pmatrix} 2 \times 0.140 + \\ 2 \times 0.099 \end{pmatrix} = 38.24\ m$	$2 \times 40 \times \begin{pmatrix} 2 \times 0.100 + \\ 2 \times 0.085 \end{pmatrix} = 29.6\ m$	22.6 %
Verticals/ Chords	$2 \times 4 \times \begin{pmatrix} 2 \times 0.140 + \\ 2 \times 0.070 \end{pmatrix} = 3.36\ m$	$2 \times 4 \times \begin{pmatrix} 2 \times 0.100 + \\ 2 \times 0.060 \end{pmatrix} = 2.56\ m$	23.8 %
Parts Top chord	$2 \times 2 \times (4 \times 0.140) = 2.24\ m$	$2 \times 2 \times (4 \times 0.140) = 2.24\ m$	0 %
Parts Bottom chord	$2.24\ m$	$2.24\ m$	0 %
TOTAL	$80.8\ m$	$71.3\ m$	11.8 %
	Conventional truss	**Optimised truss**	

The results when optimising the truss for this design, show a big profit in utilisation of bars when varying the chord thickness, equally between top and bottom. The capacity of diagonals is when decreasing the sizes even more utilised with over 40 %. Both the weight of the truss and total welding length have great benefits for the optimised design with a big decrease. Finally the painted steel area were similar with a slightly benefit to the optimised truss.

A second order calculation is also made for the compressed top chord which is exposed to bending. Both the conventional and optimised design pass this analysis and obtains lower or equal stresses and utilisation ratios than from the first order analysis, see Table 4.7. Dimensioning load case for this analysis is, as equal to the first order analysis, the interaction between normal force and bending.

Table 4.7 Utilisation ratios in top chord for second order analysis.

	Conventional truss		Optimised truss	
	Utilisation ratio top chord for Second Order Analysis Should be ≤ 100 %			
Top Chord	Part 1	69 %	Part 1	88 %
	Part 2	91 %	Part 2	96 %
	Part 3	69 %	Part 3	88 %

4.2.3 No.3 – FRP deck with transverse VKR beams

This third design solution consists of warren trusses and a deck system with a plate of fiber reinforced polymer and VKR transverse beams, see Figure 4.17. The deck plate is thereof switched from steel to the more lightweight composite material. Also this design have a deck built up of two different structural elements with the transverse VKR beams chosen to have the same height as the bottom chord, with 1.5 m spacing.

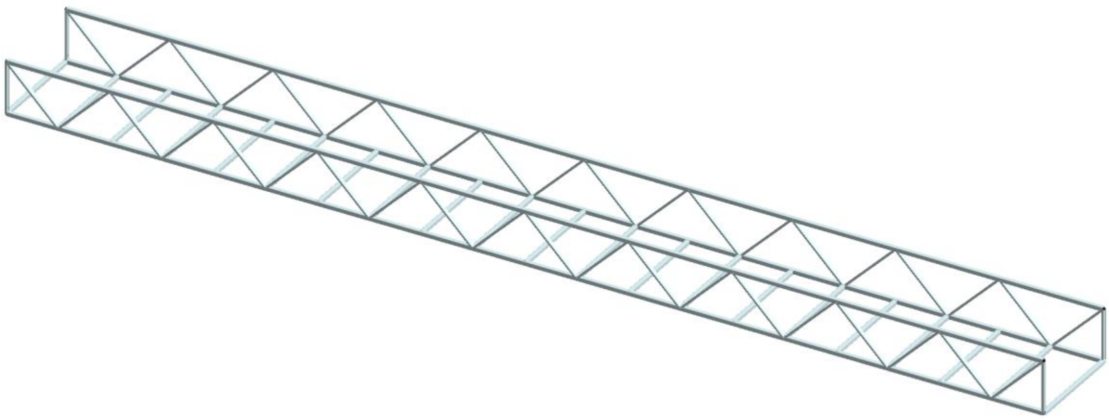

Figure 4.17 Bridge solution number three with warren trusses and a deck system of FRP and VKR transversal beams.

Material properties for the FRP deck are taken from Fiberline Composites product Fiberline Plank HD which is their product recommended and most used for pedestrian bridges (Fiberline Composites, 2019). It's made of glass fiber polymer with a self-weight of $g = 17.06\ \frac{kg}{m^2} = 0.167\ \frac{kN}{m^2}$, which is approximately $\frac{1}{5}$ of the weight of the previous 10 mm steel plate. It’s built up of a plate with stiffeners underneath, see Figure 4.18. See Appendix A for product specification.

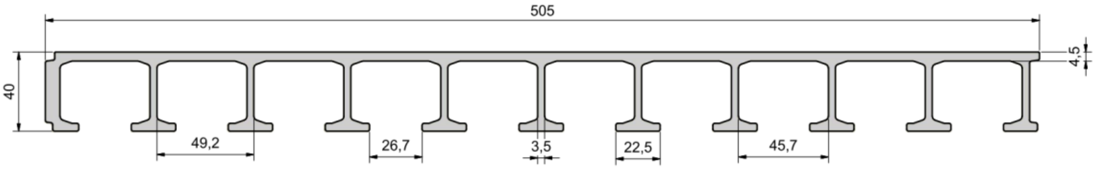

Figure 4.18 Sectional illustration of the FRP deck Fiberline Plank HD (Fiberline Composites, 2019).

Regarding installation of the modules, accessories are available from the same manufacturer made to fit the module Fiberline Plank HD, see Figure 4.19 (Fiberline Composites, 2019). Everything is made of stainless steel and, as seen in the figure, most accessories are made to connect the modules to I-beams, with only one solution available for VKR beams. A pedestrian bridge can simply be produced at a manufacturing plant and be lifted on place on site, see Figure 4.20.

Clamp: For connecting FRP to transverse I-beams

Clip: For connecting FRP to transverse I-beams

Baseplate: For connecting FRP to transverse I-beams

Angle: For connecting FRP to transverse VKR-beams

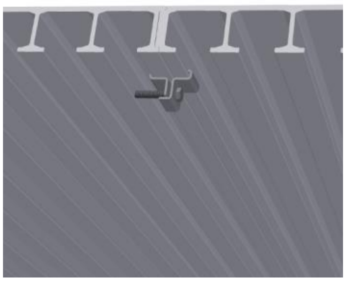

Clip: For connecting two FRP modules transversely

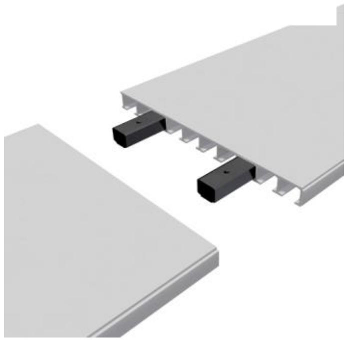

Joint profile: For connecting two FRP modules longitudinally

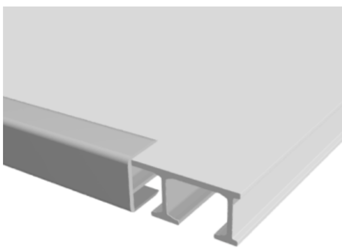

Edge U-profile: For finishing edges of HD planks

Figure 4.19 Accessories for Fiberline HD Plank (Fiberline Composites, 2019).

Figure 4.20 A bridge with FRP deck lifted on place at building site (Fiberline Composites, 2019).

This FRP deck are in tables stated to exceed the deflection limits for spans over $2.5m$, see limits for bridges in Chapter 2, and in particular Section 2.3.1. The transverse beams are due to that placed every $1.5m$.

To choose adequate transverse beams, a beam design is initially made for these. With intention to use VKR beams, the $120\ mm$ dimension is needed for enough capacity with normal capacity as dimensioning load case, see Table 4.8.

Table 4.8 Profile and utilisation ratio for transverse beams in conventional and optimised truss respectively.

	Conventional truss		**Optimised truss**		
	Profile types in deck – VKR				
Transverse beams	Part 1-3	$120 \times 120 \times 6.3$	Part 1-3	$120 \times 120 \times 6.3$	
	Utilisation ratio in bars Should be $\leq$ 100 %				**diff.**
Transverse beams	Part 1-3	93 %	Part 1-3	93 %	0 %

Same analysing procedure and designing of steel bars are made as for the two previous bridge solutions. Profiles, utilisation ratios, eigenfrequencies and quantity values are compiled and compared for the conventional and optimised truss, see Table 4.9. The column to the right shows the difference between the two trusses in [%]. A positive green value indicates profit for the optimised truss and a negative red value loss. Dimensioning load cases varies between the compressed top chord and diagonals and the tensioned bottom chord. The compressed members are dimensioned for interaction between normal force and bending, while the tensioned members is dimensioned for normal capacity.

Table 4.9 *Results for analysed conventional and optimised truss designs respectively, with a deck of VKR beams and a FRP plate. Presented are the stated profiles, utilisation ratios for bar capacities, eigenfrequencies and different quantity estimations.*

	Conventional truss		**Optimised truss**		
	Profile types in truss - VKR				
Top Chord	Part 1-3	$120 \times 120 \times 8$	Part 1 Part 2 Part 3	$120 \times 120 \times 6.3$ $120 \times 120 \times 8$ $120 \times 120 \times 6.3$	
Bottom Chord	Part 1-3	$120 \times 120 \times 6.3$	Part 1 Part 2 Part 3	$120 \times 120 \times 5$ $120 \times 120 \times 6.3$ $120 \times 120 \times 5$	
Diagonals	Part 1-3	$120 \times 60 \times 3.6$	Part 1-3	$100 \times 60 \times 3.6$	
	Utilisation ratio in bars, ULS Should be $\leq$ 100 %				**diff.**
Top Chord	Part 1	67 %	Part 1	83 %	16 %
	Part 2	90 %	Part 2	89 %	-1 %
	Part 3	67 %	Part 3	83 %	16 %
Bottom Chord	Part 1	76 %	Part 1	94 %	18 %
	Part 2	86 %	Part 2	85 %	-1 %
	Part 3	76 %	Part 3	94 %	18 %
Diagonals	Part 1-3	77 %	Part 1-3	91 %	14 %
	Eigenfrequencies Should be $\geq$ 2.5 Hz for horizontal (H) vibrations Should be $\geq$ 5.0 Hz for vertical (V) vibrations **Acceleration** Should be $\leq$ 0.2 m/s^2 for horizontal (H) acceleration Should be $\leq$ 0.7 m/s^2 for vertical (V) acceleration				
Shape 1	1.363 Hz (H) 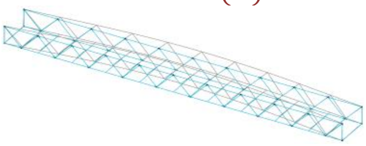		1.347 Hz (H) 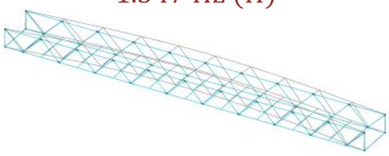		
Shape 2	2.931 Hz (H) 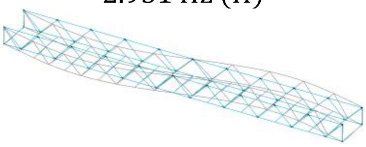		2.937 Hz (H) 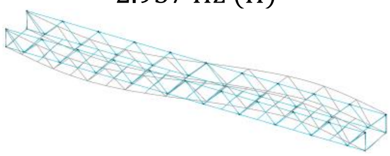		
Shape 3	3.214 Hz (V) Acceleration: 0 m/s^2 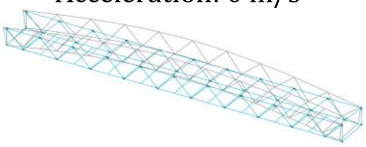		3.134 Hz (V) Acceleration: 0 m/s^2 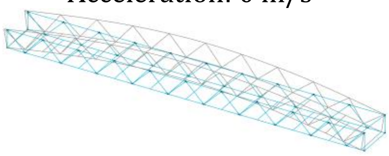		

Shape 4	4.325 Hz (V) Acceleration: 0 m/s² 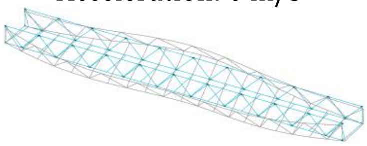	4.222 Hz (V) Acceleration: 0 m/s² 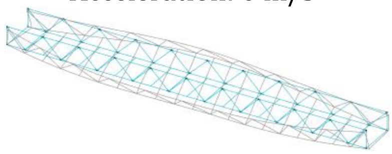	
Shape 5	4.509 Hz (H) 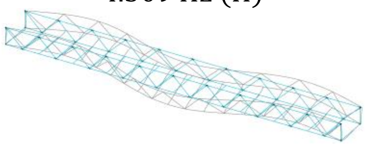	4.476 Hz (H) 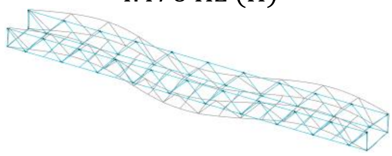	
	Quantity estimations Weight [t], Painted area [m²] and Welding length [m]		**diff.**
Weight [t]			
Truss	$3.862\ t$ Top: 1.656 Bottom: 1.329 Diagonals: 0.877	$3.409\ t$ Top: 1.46 Bottom: 1.174 Diagonals: 0.775	11.7 %
Deck	$2.870\ t$ FRP: 1.474 Transversal beams: 1.396	$2.870\ t$ FRP: 1.474 Transversal beams: 1.396	0 %
TOTAL	$6.7\ t$	$6.3\ t$	6.0 %
Painted Area [m²]			
Truss	$87.256\ m^2$ Top: 27.564 Bottom: 27.827 Diagonals: 31.865	$83.899\ m^2$ Top: 27.721 Bottom: 27.947 Diagonals: 28.231	3.8 %
Deck	$29.218\ m^2$ FRP: 0 Transversal beams: 29.218	$29.218\ m^2$ FRP: 0 Transversal beams: 29.218	0 %
TOTAL	$116.5\ m^2$	$113.1\ m^2$	2.9 %
Welding Length [m]			
Transversal beams/ Bottom chord	$2 \times 21 \times (4 \times 0.120) = 20.16\ m$	$2 \times 21 \times (4 \times 0.120) = 20.16\ m$	0 %
Transversal beams/ Deck plate	$Glued \rightarrow 0\ m$	$Glued \rightarrow 0\ m$	-
Diagonals/ Chords	$2 \times 40 \times \begin{pmatrix} 2 \times 0.120 + \\ 2 \times 0.085 \end{pmatrix} = 32.8\ m$	$2 \times 40 \times \begin{pmatrix} 2 \times 0.100 + \\ 2 \times 0.085 \end{pmatrix} = 29.6\ m$	9.8 %
Verticals/ Chords	$2 \times 4 \times \begin{pmatrix} 2 \times 0.120 + \\ 2 \times 0.060 \end{pmatrix} = 2.88\ m$	$2 \times 4 \times \begin{pmatrix} 2 \times 0.100 + \\ 2 \times 0.060 \end{pmatrix} = 2.56\ m$	11.1 %

Parts Top chord	$2 \times 2 \times (4 \times 0.120) = 1.92\ m$	$2 \times 2 \times (4 \times 0.120) = 1.92\ m$	0 %
Parts Bottom chord	$1.92\ m$	$1.92\ m$	0 %
TOTAL	$59.7\ m$	$56.2\ m$	5.9 %
	Conventional truss	**Optimised truss**	

The results show a big profit in utilisation of bars when varying the chord thickness, equally between top and bottom. The capacity of diagonals is also better utilised when decreasing the sizes with the same magnitude as for the chords. The weight of the truss has great benefits for the optimised design with a big decrease, and finally the painted steel area and total length of welding were similar with a slightly benefit to the optimised truss.

A second order calculation is also made for the compressed top chord which is exposed to bending. Both the conventional and optimised design pass this analysis and obtains lower stresses and utilisation ratios than from the first order analysis, see Table 4.10. Dimensioning load case for this analysis is, as equal to the first order analysis, the interaction between normal force and bending.

Table 4.10 Utilisation ratios in top chord for second order analysis.

	Conventional truss		**Optimised truss**	
	Utilisation ratio top chord for Second Order Analysis Should be ≤ 100 %			
Top Chord	Part 1 Part 2 Part 3	64 % 73 % 64 %	Part 1 Part 2 Part 3	82 % 76 % 82 %

4.2.4 No.4 – FRP deck with transverse I-beams

An alternative solution to the bridge design above is to simply replace the VKR transverse beams with I-beams and have the truss remained as it is, see Figure 4.21. This switch is interesting in the weight aspect, but will for sure increase the needed painted area and welding length because of the sectional shape. But the big advantage with an open profile instead of a closed is the easy inspections.

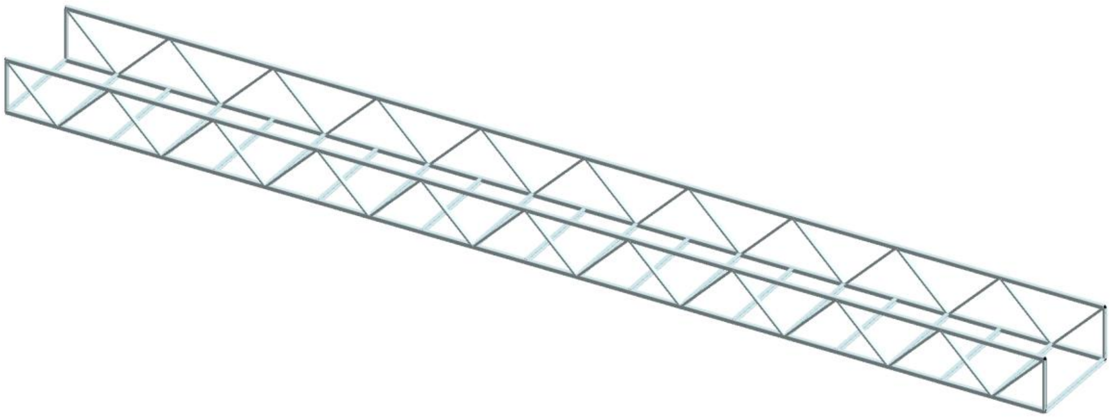

Figure 4.21 Bridge solution number four with warren trusses and a deck system of FRP and transverse I-beams.

To choose adequate transverse I-beams, a beam design is initially made for these. The range is from IPE as the weakest to HEM as the strongest with HEA and HEB in between. For each step the weight and cross-sectional area increases and improves the capacity of the bars and also the dynamic behaviour of the bridge. The dimensions are chosen to match the height of the bottom chord which the beams will be welded to. If the capacity of the beam is too small in comparison to the internal forces, it's replaced to the next one. For enough capacity, the beams in both designs needs to be of sort HEM with dimension 100 (corresponds to $120\,mm$ height) for normal capacity as dimensioning load case, see Table 4.11.

Table 4.11 Profile and utilisation ratio for transverse beams in conventional and optimised truss respectively.

	Conventional truss		**Optimised truss**		
	Profile types in deck – I-beams				
Transverse beams	Part 1-3	HEM 100	Part 1-3	HEM 100	
	Utilisation ratio in bars Should be ≤ 100 %				**diff.**
Transverse beams	Part 1-3	85 %	Part 1-3	85 %	0 %

Since the purpose of this design is to have the truss intact from the previous FRP design, no changes in profile dimensions are done for the conventional truss. Only the optimised one are developed to its specific favour. The same analysing procedure and designing of steel bars are made as for the three previous bridge solutions. Profiles, utilisation ratios, eigenfrequencies and quantity values are compiled and compared for the conventional and optimised truss, see Table 4.12. The column to the right shows the difference between the two trusses in [%]. A positive green value indicates profit for the optimised truss and a negative red value loss. Dimensioning load cases varies between the compressed top chord and diagonals and the tensioned bottom chord. The compressed members are dimensioned for interaction between normal force and bending, while the tensioned members is dimensioned for normal capacity.

Table 4.12 *Results for analysed conventional and optimised truss designs respectively, with a deck of I-beams and a FRP plate. Presented are the stated profiles, utilisation ratios for bar capacities, eigenfrequencies and different quantity estimations.*

	Conventional truss		**Optimised truss**		
	Profile types in truss - VKR				
Top Chord	Part 1-3	$120 \times 120 \times 8$	Part 1	$120 \times 120 \times 6.3$	
			Part 2	$120 \times 120 \times 8$	
			Part 3	$120 \times 120 \times 6.3$	
Bottom Chord	Part 1-3	$120 \times 120 \times 6.3$	Part 1	$120 \times 120 \times 5$	
			Part 2	$120 \times 120 \times 6.3$	
			Part 3	$120 \times 120 \times 5$	
Diagonals	Part 1-3	$120 \times 60 \times 3.6$	Part 1-3	$100 \times 60 \times 3.6$	
	Utilisation ratio in bars, ULS Should be ≤ 100 %				**diff.**
Top Chord	Part 1	70 %	Part 1	86 %	16 %
	Part 2	93 %	Part 2	93 %	0 %
	Part 3	70 %	Part 3	86 %	16 %
Bottom Chord	Part 1	78 %	Part 1	96 %	18 %
	Part 2	88 %	Part 2	88 %	0 %
	Part 3	78 %	Part 3	96 %	18 %
Diagonals	Part 1-3	80 %	Part 1-3	94 %	14 %
	Eigenfrequencies Should be $\geq 2.5\ Hz$ for horizontal (H) vibrations Should be $\geq 5.0\ Hz$ for vertical (V) vibrations **Acceleration** Should be $\leq 0.2\ m/s^2$ for horizontal (H) acceleration Should be $\leq 0.7\ m/s^2$ for vertical (V) acceleration				
Shape 1	1.128 Hz (H) 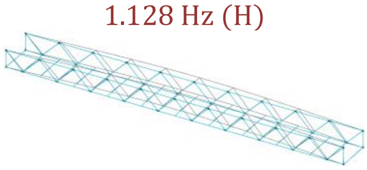		1.120 Hz (H) 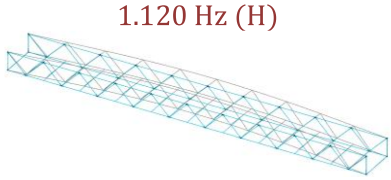		

Shape 2	2.432 Hz (H) 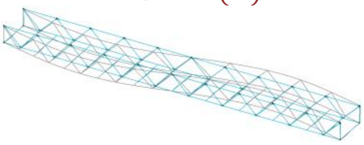	2.437 Hz (H) 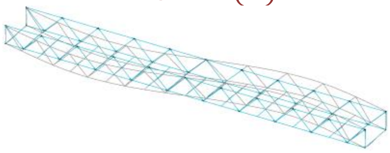	
Shape 3	3.076 Hz (V) Acceleration: 0 m/s² 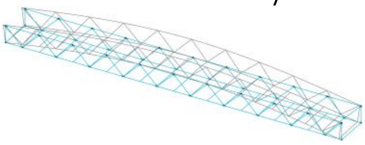	2.996 Hz (V) Acceleration: 0 m/s² 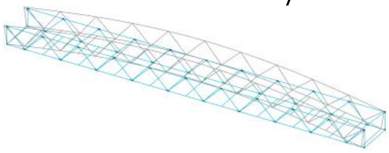	
Shape 4	3.774 Hz (H) 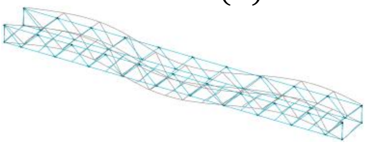	3.760 Hz (H) 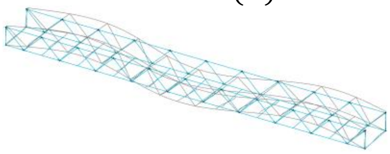	
Shape 5	4.114 Hz (V) Acceleration: 0 m/s² 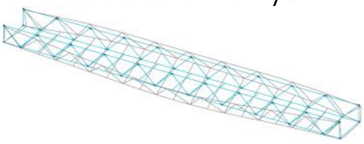	3.987 Hz (V) Acceleration: 0 m/s² 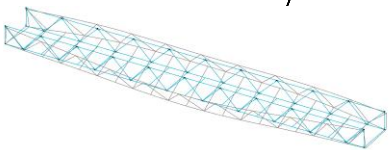	
	Quantity estimations Weight [t], Painted area [m²] and Welding length [m]		**diff.**
Weight [t]			
Truss	$3.862\ t$ Top: 1.656 Bottom: 1.329 Diagonals: 0.877	$3.409\ t$ Top: 1.46 Bottom: 1.174 Diagonals: 0.775	11.7 %
Deck	$4.107\ t$ FRP: 1.474 Transversal beams: 2.633	$4.107\ t$ FRP: 1.474 Transversal beams: 2.633	0 %
TOTAL	$8.0\ t$	$7.5\ t$	6.3 %
Painted Area [m²]			
Truss	$87.256\ m^2$ Top: 27.564 Bottom: 27.827 Diagonals: 31.865	$83.899\ m^2$ Top: 27.721 Bottom: 27.947 Diagonals: 28.231	3.8 %
Deck	$39.022\ m^2$ FRP: 0 Transversal beams: 39.022	$39.022\ m^2$ FRP: 0 Transversal beams: 39.022	0 %
TOTAL	$126.3\ m^2$	$122.9\ m^2$	2.7 %

Welding Length [m]			
Transversal beams/ Bottom chord	$2 \times 21 \times 0.640 = 26.88\ m$	$2 \times 21 \times 0.640 = 26.88\ m$	0 %
Transversal beams/ Deck plate	$Glued\ \rightarrow 0\ m$	$Glued\ \rightarrow 0\ m$	-
Diagonals/ Chords	$2 \times 40 \times \binom{2 \times 0.120 +}{2 \times 0.085} = 32.8\ m$	$2 \times 40 \times \binom{2 \times 0.100 +}{2 \times 0.085} = 29.6\ m$	9.8 %
Verticals/ Chords	$2 \times 4 \times \binom{2 \times 0.120 +}{2 \times 0.060} = 2.88\ m$	$2 \times 4 \times \binom{2 \times 0.100 +}{2 \times 0.060} = 2.56\ m$	11.1 %
Parts Top chord	$2 \times 2 \times (4 \times 0.120) = 1.92\ m$	$2 \times 2 \times (4 \times 0.120) = 1.92\ m$	0 %
Parts Bottom chord	$1.92\ m$	$1.92\ m$	0 %
TOTAL	$66.4\ m$	$62.9\ m$	5.3 %
	Conventional truss	**Optimised truss**	

The results when optimising the truss for this design show a big profit in utilisation of bars when varying the chord thickness, equally between top and bottom. The capacity of diagonals is also better utilised when decreasing the sizes with the same magnitude as for the chords. The weight of the truss has great benefits for the optimised design with a big decrease, and finally the painted steel area and total length of welding were similar with a slightly benefit to the optimised truss.

When comparing the conventional truss to the results for the FRP deck with VKR transverse beams in Table 4.9, the forces in the truss bars are similar between the two trusses with below three percent differ. Weight, painted steel area and welding length are equal. But when changing from VKR transverse beams to HEM profiles, the weight of the deck increased from below three tonnes to over four tonnes, i.e. a heavier deck with over 40 %. Also the painted steel area and welding length where increased with just over 30 % for the deck when changing to I-beams.

A second order calculation is also made for the compressed top chord which is exposed to bending. Both the conventional and optimised design pass this analysis and obtains lower stresses and utilisation ratios than from the first order analysis, see Table 4.13. Dimensioning load case for this analysis is, as equal to the first order analysis, the interaction between normal force and bending.

Table 4.13 Utilisation ratios in top chord for second order analysis.

	Conventional truss		Optimised truss	
	Utilisation ratio top chord for Second Order Analysis Should be ≤ 100 %			
Top Chord	Part 1	61 %	Part 1	85 %
	Part 2	85 %	Part 2	77 %
	Part 3	61 %	Part 3	85 %

4.2.5 No.5 – Solution with stainless steel

When deciding which design alternatives to remake in stainless steel instead of carbon steel, the previous four ones have been compared and evaluated. Already from start, one of the two designs with FRP deck were considered interesting. When comparing the two ones, it's clear that the design with VKR transverse beams are much lighter, needs less steel corrosion paint and welding work, see Table 4.14. That's enough reason for choosing bridge design No.3 to further remake in stainless steel, both trusses and transverse beams.

Table 4.14 Comparison between the two bridge designs with trusses of carbon steel and FRP deck.

Design No.	Deck plate	Transverse beams	Max UR	Min UR	Weight	Painted Area	Welding Length
			[%]	[%]	[t]	[m^2]	[m]
No.3 Convent.	FRP	VKR	90	67	6.7	116.5	59.7
No.3 Optim.	FRP	VKR	94	83	6.3	113.1	56.2
No.4 Convent.	FRP	I-beam	93	70	8.0	126.3	66.4
No.4 Optim.	FRP	I-beam	96	86	7.5	122.9	62.9

When deciding whether to analyse one of the two bridge designs entirely made of carbon steel, the big amount of steel and heavy weight were reasons enough not to remake it in stainless steel, see Table 4.15. The extra tonnes of steel in comparison to the bridges in Table 4.14 would be too expensive to do stainless than using other materials as deck plate, such as FRP.

Table 4.15 Comparison between the two bridge designs with trusses and deck made of carbon steel.

Design No.	Deck plate	Transverse beams	Max UR	Min UR	Weight	Painted Area	Welding Length
			[%]	[%]	[t]	[m²]	[m]
No.1 Convent.	TRP	-	96	48	13.0	373.6	422.9
No.1 Optim.	TRP	-	95	50	12.5	364.6	413.4
No.2 Convent.	Steel plate	I-beam	96	57	13.1	325.5	80.8
No.2 Optim.	Steel plate	I-beam	99	82	12.4	316.7	71.3

To sum up, it's decided to do a stainless-steel alternative for bridge No.3 – the FRP deck with transverse VKR beams.

When applying material on the different elements in FEM-Design, stainless steel needs to be created by the user since only carbon steel of different sorts are predefined in the library. This can be done and parameters are by hand changed, see specific values in Section 2.2.2, and in particular Table 2.3. The duplex stainless steel 1.4462 will be used with yield strength $f_y = 450\ MPa$ and ultimate tensile strength $f_u = 650\ MPa$. Also the modulus of elasticity E, Poison's ratio v and density ρ are taken directly from the same table. The partial factors differs from carbon steel as well with $\gamma_{M0} = 1.1 \quad \gamma_{M1} = 1.1 \quad \gamma_{M2} = 1.25$ (SIS, 2006a).

Another change to consider when using stainless steel in FEM-Design is the buckling curves when calculating the flexural buckling. The χ_{LT}-factor in the buckling force equation takes the curves into consideration, see Equation 4.8 and 4.9. Buckling curves depends on cross section and geometry and gives a value for the imperfection factor α_{LT}.

$$\chi_{LT} = \frac{1}{\phi_{LT}+\sqrt{\phi_{LT}^2-\lambda_{LT}^2}} \tag{4.8}$$

$$\phi_{LT} = 0.5 \times \left[1 + \alpha_{LT} \times (\lambda_{LT} - \lambda_0) + \lambda_{LT}^2\right] \tag{4.9}$$

The limit slenderness λ_0 are equal to 0.2 for carbon steel and this value is difficult and very time consuming to change in the program. For stainless steel the limit slenderness is equal to $\lambda_0 = 0.4$, and to overcome the restriction in FEM-Design, a brief study has been made to find a way to get reliable results when still using the default value $\lambda_0 = 0.2$.

In Eurocode 3 part 1-4, which covers dimensioning with stainless steel, the imperfection factor and limit slenderness factor are stated and equal for all types of cross sectional geometries, see Table 4.16 (SIS, 2006a).

Table 4.16 Imperfection factor α_{LT} and limit slenderness factor λ_0 for flexural buckling analysis for stainless steel (SIS, 2006a).

Stainless steel	
α_{LT}	0.49
λ_0	0.40

All profiles used in the research are welded sections with limit $\frac{h}{b} \leq 2$, which for carbon steel gives buckling curve c and the following imperfection factor $\alpha_{LT} = 0.49$, i.e. the same as for stainless steel, see Table 4.17 (SIS, 2005b).

Table 4.17 Imperfection factor α_{LT} and limit slenderness factor λ_0 for flexural buckling analysis for stainless and carbon steel (SIS, 2005b).

	Stainless steel	Carbon steel
α_{LT}	0.49	0.49
λ_0	0.40	0.20

These different factors will for sure give different values for χ_{LT}. To overcome this, the buckling curve b will be used instead with the decreased imperfection factor $\alpha_{LT} = 0.34$, see Table 4.18.

Table 4.18 Adjusted imperfection factor α_{LT} for carbon steel marked with red and limit slenderness factor λ_0 for flexural buckling analysis.

	Stainless steel	Adjusted Carbon steel
α_{LT}	0.49	0.34
λ_0	0.40	0.20

The purpose of the following study is to valid the results of factor χ_{LT} for four different profiles, to show whether this adjustment in calculation are reliable or not. A difference below 5.0 % are considered acceptable.

The first buckling mode to check the results for are the flexural buckling. Two quadratic and two rectangular profiles are analysed, see Table 4.19. All four get a difference below 5.0 % and the adjustment in design are considered reliable.

Table 4.19 *Results for the χ_{LT}-factor for flexural buckling mode of carbon and stainless steel with difference in [%] in the right column.*

	$\boldsymbol{\alpha_{LT}}$	$\boldsymbol{\lambda_0}$	$\boldsymbol{\chi}$	**diff.**
Carbon steel $120 \times 120 \times 8$	0.34 Curve (b)	0.2 Default	0.599	1.94 %
Stainless steel $120 \times 120 \times 8$	0.49	0.4	0.588	
Carbon steel $140 \times 140 \times 8$	0.34 Curve (b)	0.2 Default	0.697	-0.14 %
Stainless steel $140 \times 140 \times 8$	0.49	0.4	0.698	
Carbon steel $120 \times 60 \times 3.6$	0.34 Curve (b)	0.2 Default	0.563	2.51 %
Stainless steel $120 \times 60 \times 3.6$	0.49	0.4	0.549	
Carbon steel $100 \times 60 \times 3.6$	0.34 Curve (b)	0.2 Default	0.456	3.70 %
Stainless steel $100 \times 60 \times 3.6$	0.49	0.4	0.44	

The second buckling mode are the torsional-flexural buckling. Also here, the same two quadric and rectangular profiles are analysed, see Table 4.20. The difference is below the 5.0 %-limit for this mode as well.

Table 4.20 *Results for the χ_{LT}-factor for torsional-flexural buckling mode for carbon and stainless steel with difference in [%] in the right column.*

	$\boldsymbol{i_1}$ **or** $\boldsymbol{i_2}$	$\boldsymbol{\alpha_{LT}}$	$\boldsymbol{\lambda_0}$	$\boldsymbol{\chi}$	**diff.**
Carbon steel $120 \times 120 \times 8$	45.5	0.34 Curve (b)	0.2 Default	0.6	1.93 %
Stainless steel $120 \times 120 \times 8$	45.5	0.49	0.4	0.588	
Carbon steel $140 \times 140 \times 8$	53.6	0.34 Curve (b)	0.2 Default	0.696	-0.13 %
Stainless steel $140 \times 140 \times 8$	53.6	0.49	0.4	0.697	
Carbon steel $120 \times 60 \times 3.6$	24.9	0.34 Curve (b)	0.2 Default	0.247	4.26 %
Stainless steel $120 \times 60 \times 3.6$	24.9	0.49	0.4	0.237	
Carbon steel $100 \times 60 \times 3.6$	24.4	0.34 Curve (b)	0.2 Default	0.239	4.24 %
Stainless steel $100 \times 60 \times 3.6$	24.4	0.49	0.4	0.229	

For the two buckling modes, the χ-value used in FEM-Design gets slightly higher with the approximate method, when using values for carbon steel, than the more correct method with correct values for stainless steel. A higher value gives a scenario on the unsafe side, but the difference is small enough to let it pass and the approximate approach will be used in the following calculations for the stainless bridge design.

To choose adequate transverse beams, a beam design is initially made for these. For enough capacity, VKR beams of dimension 120 mm is needed with normal capacity as dimensioning load case, see Table 4.21. In comparison to the carbon steel design in Table 4.8, thinner profiles are used and the capacity it better utilised. This is possible since both yield and tensile strength is better for stainless steel than carbon.

Table 4.21 Profile and utilisation ratio for transverse beams in conventional and optimised truss of stainless steel respectively.

	Conventional truss		**Optimised truss**		
	Profile types in deck – VKR				
Transverse beams	Part 1-3	120 × 120 × 5	Part 1-3	120 × 120 × 5	
	Utilisation ratio in bars Should be ≤ 100 %				**diff.**
Transverse beams	Part 1-3	99 %	Part 1-3	98 %	-1 %

Same analyse procedure and design of steel bars are made as for the previous bridge solutions. Profiles, utilisation ratios in ULS, eigenfrequencies and quantity values are compiled and compared for the conventional and optimised truss, see Table 4.22. The column to the right shows the difference between the two trusses in [%]. A positive green value indicates profit for the optimised truss and a negative red value loss. Dimensioning load cases varies between the compressed top chord and diagonals and the tensioned bottom chord. The compressed members are dimensioned for interaction between normal force and bending, while the tensioned members are dimensioned for normal capacity. In comparison to the carbon steel design in Table 4.9, the thinnest VKR profiles of 5 mm are used along the entire bottom chords and the capacity is better utilised also here. All other profiles are identical to the carbon steel design.

Table 4.22 Results for analysed conventional and optimised truss designs of stainless steel respectively, with a deck of VKR beams and a FRP plate. Presented are the stated profiles, utilisation ratios for bar capacities, eigenfrequencies and different quantity estimations.

	Conventional truss		**Optimised truss**		
	Profile types in truss - VKR				
Top Chord	Part 1-3	120 × 120 × 8	Part 1 Part 2 Part 3	120 × 120 × 6.3 120 × 120 × 8 120 × 120 × 6.3	
Bottom Chord	Part 1-3	120 × 120 × 5	Part 1 Part 2 Part 3	120 × 120 × 5 120 × 120 × 5 120 × 120 × 5	
Diagonals	Part 1-3	120 × 60 × 3.6	Part 1-3	100 × 60 × 3.6	

	Utilisation ratio in bars, ULS Should be $\leq$ 100 %				**diff.**
Top Chord	Part 1 Part 2 Part 3	70 % 94 % 70 %	Part 1 Part 2 Part 3	87 % 94 % 87 %	17 % 0 % 17 %
Bottom Chord	Part 1 Part 2 Part 3	80 % 91 % 80 %	Part 1 Part 2 Part 3	81 % 91 % 81 %	1 % 0 % 1 %
Diagonals	Part 1-3	85 %	Part 1-3	97 %	12 %
	Eigenfrequencies Should be $\geq 2.5\ Hz$ for horizontal (H) vibrations Should be $\geq 5.0\ Hz$ for vertical (V) vibrations **Acceleration** Should be $\leq 0.2\ m/s^2$ for horizontal (H) acceleration Should be $\leq 0.7\ m/s^2$ for vertical (V) acceleration				
Shape 1	1.240 Hz (H) 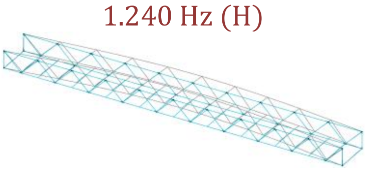		1.247 Hz (H) 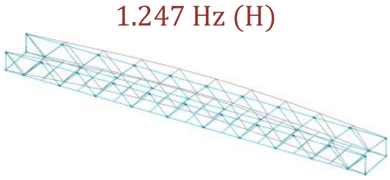		
Shape 2	2.681 Hz (H) 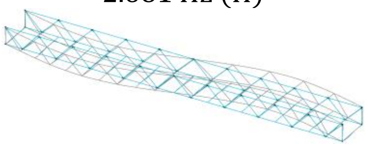		2.706 Hz (H) 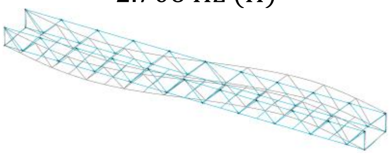		
Shape 3	3.023 Hz (V) Acceleration: 0 m/s^2 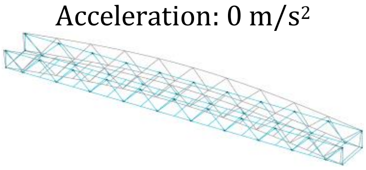		2.998 Hz (V) Acceleration: 0 m/s^2 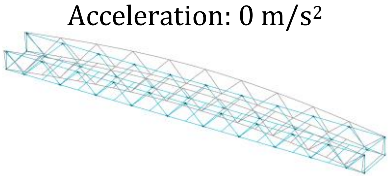		
Shape 4	4.046 Hz (V) Acceleration: 0 m/s^2 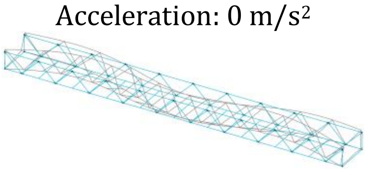		4.060 Hz (V) Acceleration: 0 m/s^2 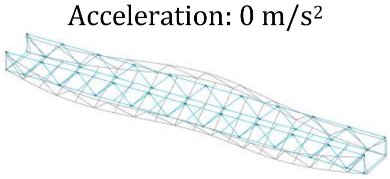		
Shape 5	4.182 Hz (H) 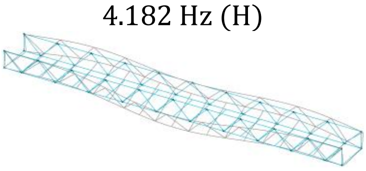		4.154 Hz (H) 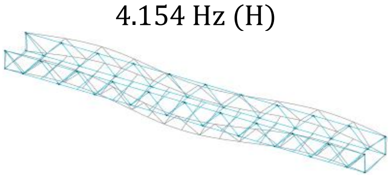		

	Quantity estimations Weight [t], Painted area [m²] and Welding length [m]		**diff.**
Weight [t]			
Truss	$3.58\ t$ Top: 1.645 Bottom: 1.064 Diagonals: 0.872	$3.285\ t$ Top: 1.451 Bottom: 1.064 Diagonals: 0.77	8.2 %
Deck	$2.591\ t$ FRP: 1.474 Transversal beams: 1.117	$2.591\ t$ FRP: 1.474 Transversal beams: 1.117	0 %
TOTAL	$6.2\ t$	$5.9\ t$	4.8 %
Painted Area [m²]			
Truss	$0\ m^2$ Top: 0 Bottom: 0 Diagonals: 0	$0\ m^2$ Top: 0 Bottom: 0 Diagonals: 0	-
Deck	$0\ m^2$ FRP: 0 Transversal beams: 0	$0\ m^2$ FRP: 0 Transversal beams: 0	-
TOTAL	$0\ m^2$	$0\ m^2$	-
Welding Length [m]			
Transversal beams/ Bottom chord	$2 \times 21 \times (4 \times 0.120) = 20.16\ m$	$2 \times 21 \times (4 \times 0.120) = 20.16\ m$	0 %
Transversal beams/ Deck plate	$Glued\ \rightarrow 0\ m$	$Glued\ \rightarrow 0\ m$	-
Diagonals/ Chords	$2 \times 40 \times \begin{pmatrix} 2 \times 0.120 + \\ 2 \times 0.085 \end{pmatrix} = 32.8\ m$	$2 \times 40 \times \begin{pmatrix} 2 \times 0.100 + \\ 2 \times 0.085 \end{pmatrix} = 29.6\ m$	9.8 %
Verticals/ Chords	$2 \times 4 \times \begin{pmatrix} 2 \times 0.120 + \\ 2 \times 0.060 \end{pmatrix} = 2.88\ m$	$2 \times 4 \times \begin{pmatrix} 2 \times 0.100 + \\ 2 \times 0.060 \end{pmatrix} = 2.56\ m$	11.1 %
Parts Top chord	$2 \times 2 \times (4 \times 0.120) = 1.92\ m$	$2 \times 2 \times (4 \times 0.120) = 1.92\ m$	0 %
Parts Bottom chord	$1.92\ m$	$1.92\ m$	0 %
TOTAL	$59.7\ m$	$56.2\ m$	5.9 %
	Conventional truss	**Optimised truss**	

The results show a big profit in utilisation of bars when varying the thickness of the top chord. The bottom one couldn't be thinner and were intact all the way. The capacity of diagonals is also better utilised when decreasing the sizes with the same magnitude as for the top chord. The weight of the truss and total length of welding were similar with a slightly benefit to the optimised truss, and finally the painted steel area where zero for both design.

A second order calculation is also made for the compressed top chord which is exposed to bending. Both the conventional and optimised design pass this analysis and obtains lower stresses and utilisation ratios than from the first order analysis, see Table 4.23. Dimensioning load case for this analysis is, as equal to the first order analysis, the interaction between normal force and bending.

Table 4.23 Utilisation ratios in top chord for second order analysis.

	Conventional truss		Optimised truss	
	Utilisation ratio top chord for Second Order Analysis Should be ≤ 100 %			
Top Chord	Part 1	56 %	Part 1	72 %
	Part 2	69 %	Part 2	68 %
	Part 3	56 %	Part 3	72 %

4.2.6 Summary

Here follows a summarise of the result values for each design, both the conventional one and the optimised, see Table 4.24. Presented are the type of deck components since these are the only varying members in the bridge, as well as maximum and minimum utilisation ratios in ULS for truss bars, the total weight of the bridge, the amount of painted steel area and finally the total welding length for the bridge.

Table 4.24 A summary of the results for the five bridge designs, four of carbon steel and one of stainless steel. The green boxes highlight the best result for each category.

Design No.	Deck plate	Transverse beams	Max UR	Min UR	Weight	Painted Area	Welding Length
			[%]	[%]	[t]	[m^2]	[m]
Carbon steel designs							
No.1 Convent.	TRP	-	96	48	13.0	373.6	422.9
No.1 Optim.	TRP	-	95	50	12.5	364.6	413.4
No.2 Convent.	Steel plate	I-beam	96	57	13.1	325.5	80.8
No.2 Optim.	Steel plate	I-beam	99	82	12.4	316.7	71.3
No.3 Convent.	FRP	VKR	90	67	6.7	116.5	59.7
No.3 Optim.	FRP	VKR	94	83	6.3	113.1	56.2
No.4 Convent.	FRP	I-beam	93	70	8.0	126.3	66.4
No.4 Optim.	FRP	I-beam	96	86	7.5	122.9	62.9
Stainless steel designs							
No.5 Convent.	FRP	VKR	94	70	6.2	0	59.7
No.5 Optim.	FRP	VKR	94	81	5.9	0	56.2

As seen and marked with green boxes, the most efficient bridge when it comes to weight, steel painting and welding is the FRP solutions. This was expected since the FRP is $\frac{1}{5}$ more light weight than steel, doesn't need any corrosion paint and are fastened on top of the transversal beams with accessories instead of welds. When a more detailed weight comparison is done between the optimised bridges, it's even more clear that the truss becomes lighter with the use of FRP decks, see Table 4.25.

Table 4.25 A detailed summary showing the exact amount of steel or FRP in truss, deck plate and transverse beams respectively for the optimised designs.

Design No.	Deck plate	Transverse beams	Weight truss	Weight deck plate	Weight transverse beams
			[t]	[t]	[t]
No.1 Optim.	TRP	-	3.496	6.735	2.281
No.2 Optim.	Steel plate	I-beam	3.539	6.735	2.124
No.3 Optim.	FRP	VKR	3.409	1.474	1.396
No.4 Optim.	FRP	I-beam	3.409	1.474	2.633
No.5 Optim.	FRP	VKR	3.285	1.474	1.117

When comparing designs No.1 and No.2, when replacing a trapezoidal plate with two elements acting in the same way, it's shown that the design with separate plate and beams have a more utilised truss, shorter welding length and also the benefits at inspection work with an open profile. The weight is however equivalent.

When comparing design No.3 and No.4, when only changing the transverse beams from VKR to I-beams and keeping the truss intact, it's shown that the bar capacity in the truss is more utilised when using I-beams. The deck got heavier though, resulting in a heavier bridge in total. The painted steel area and welding length increased as well.

The No.5 design has one major benefit from the others, the non-existing corrosion paint. The weight and short welding length is as well advantageous. See Appendix B for calculation sheet for weight, painted area and welding length for bridge design No.5 with a FRP deck.

5 Case study – Life Cycle Cost Analysis

A life cycle cost analysis is done to compare the economic aspects for the five bridge designs from the case study. The cost includes initial investments, maintenance costs, reparations and supervision, and is a tool to show investors the cost over the bridge's total life span to register the benefits of the new ideas compared to conventional ones. This LCC-analysis is for a life length of 50 year.

5.1 Costs

For this kind of analyse, the costs are divided into investment, maintenance, repair, user and demolition costs which affect either the investor, the users of the bridge or the society. The investor is mostly affected by the investment, maintenance, reparations and demolition costs while the user is connected to the user costs in form of delays during maintenance and reparation work. The society costs mostly refer to environmental impact and costs for traffic accidents.

5.1.1 Investment costs

The initial cost used in this LCC-analysis includes material prices from BE groups pricelist of 2019 as well as prices for installations and painting, see Table 5.1 (BE Group, 2019). Planning and design costs as well as transportation costs are neglected since these costs will work in favour for the FRP designs. First the design work is cheaper than for steel due to already defined modules and secondly there's beneficial shipping costs because of the light weight. Also, the biggest transportation cost refers to the trusses which are equal for all designs. Therefore, this neglection makes a comparison on the safe side.

Table 5.1 Initial costs used in the LCC-analysis (BE Group, 2019; Fiberline Composites, 2019).

Product	Unit	Price $[{SEK}/_{unit}]$
Material		
Carbon steel – S355	tonnes	25 000
Stainless steel – Duplex 1.4462	tonnes	65 000
FRP – Fiberline composites Plank HD	m^2	1 440
Connections		
Welding material – S355	kg	159
Welding material – 1.4462	kg	415
Installation – Plate/transverse beams	pcs	100
Installation – Plank HD	pcs	64
Painting		
Initial painting – S355	m^2	350

5.1.2 Maintenance and repair costs

The maintenance costs cover operation and inspection while reparation costs are falling under repair costs. Inspections on pedestrian bridges needs to be done periodically both for carbon steel and stainless steel, see Table 5.2 for expected frequency and costs (Javier Veganzones Munoz *et al.*, 2016). As seen inspection needs more often for carbon steel than stainless steel but has the same prices.

Table 5.2 Costs for maintenance and repair operations used in the LCC-analysis.

Inspection type	Interval $[year]$	Unit	Price $[SEK/unit]$	Days	Affected road length $[m]$
Inspection regarding patch painting – Carbon steel bridges	1	tonnes	3 240	0.5	0
Large inspections – All bridges	6	tonnes	18 900	0.5	500
Repainting – Carbon steel bridges	25	m^2	2 100	5	500

5.1.3 User costs

During inspection and reparation work, extra costs will appear due to disturbance in traffic under the bridge with increased value with increased traffic, see Table 5.3 for both needed parameters and costs (Javier Veganzones Munoz *et al.*, 2016). These cots are equal for all bridge cases in the study. ATD is the average daily traffic with 5 000, 10 000 and 15 000 vehicles representing low, medium and high ADT respectively. For this LCC-analysis a low ADT will be used.

Table 5.3 User costs used in LCC-analysis.

Inspection type	Value
Percentage of heavy vehicles	10 %
Affected road length	500 m
Speed reduction	-60 km/h for low ADT -40 km/h for medium ADT -30 km/h for high ADT
Time value heavy vehicles	540 SEK/h
Time value passenger vehicles	145 SEK/h

5.1.4 Demolition

The cost for disposal after the bridge's service life is approximated to be 2.28 % of the investment cost of each bridge for an 3.0 % interest rate.

5.2 Results

The total life cycle costs can effectively be compared against each other, but is very much depending on different applied parameters. These are studied in a so-called sensitivity analysis determining the reliability of the results.

5.2.1 Life cycle cost

The investment cost for every design alternatives are obtained from the LCC-sheet including the material costs for main beams (truss and transverse beams) and deck plate, cost for welding, installations when merging deck modules or attaching it to the transverse beams, and also the corrosion painting, see Figure 5.1. As seen in the picture the main beams are twice as expensive for the stainless-steel design than the four previous with carbon steel. However, in total the initial cost gets higher for the carbon steel bridges since the painting cost is remarkably high. Comparable are design No.2 and No.5 with approximately equal investment cost.

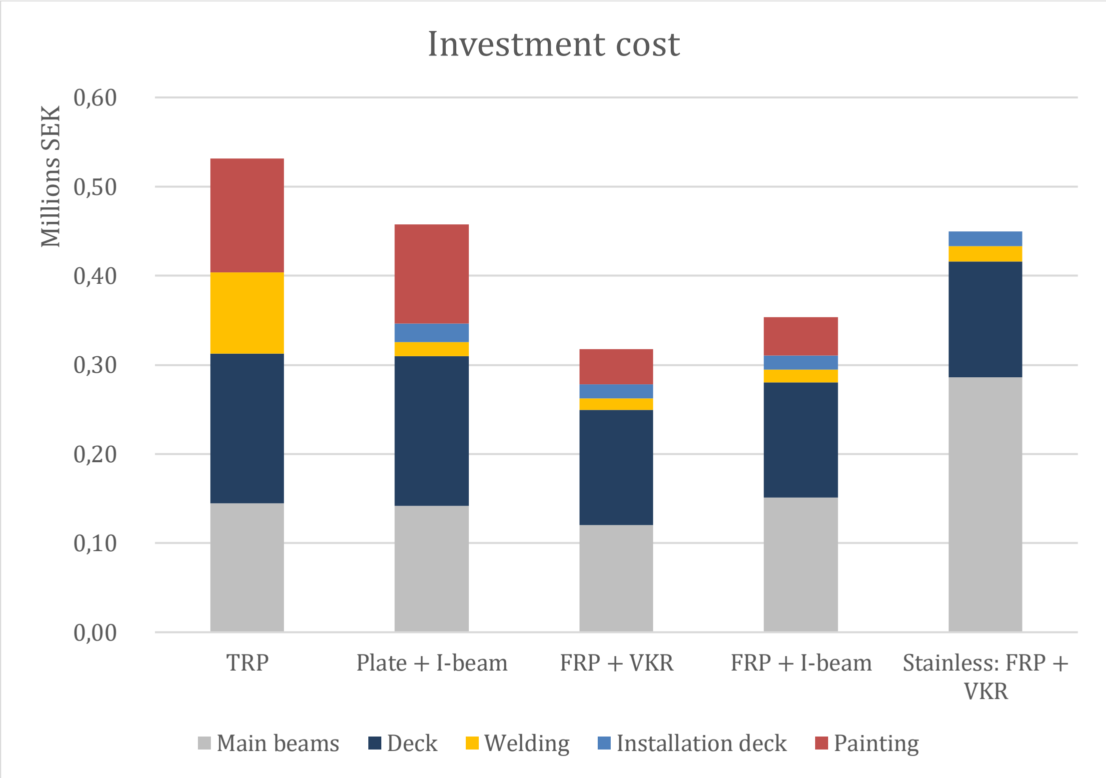

Figure 5.1 *Investment costs obtained from the LCC-analysis.*

The total cost in the LCC-analysis includes investment, maintenance, reparation, user costs and the final demolition, see Figure 5.2. The yearly interest rate used is 3 % meaning that's the rate the investor would get if investing the money in a bank account or stock with a certain rate. As seen in the stacks, same phenomenon happens for the total cost over the bridges 50-year life span as for the investment cost with the reparation cost having a remarkably big influence on the rising price. The stainless-steel bridge doesn't have any reparation costs since it doesn't need to be repainted.

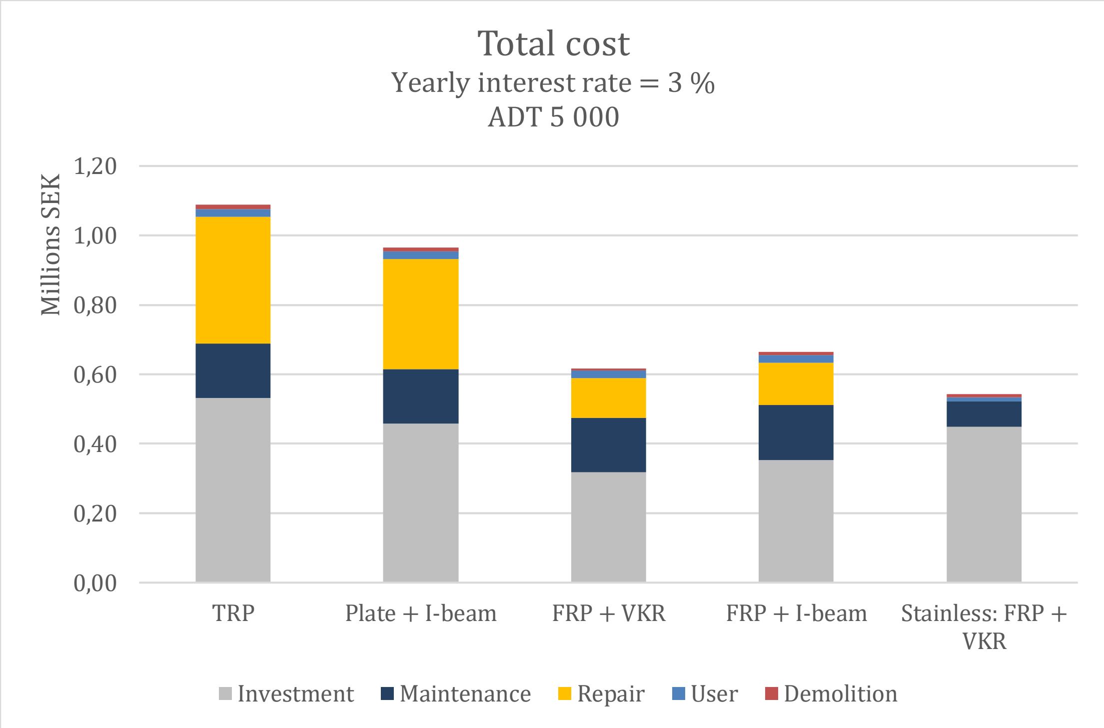

Figure 5.2 Total costs obtained from the LCC-analysis.

As seen in the figure, new materials such as stainless steel and FRP are more expensive initially than regular carbon steel, but gets cheaper in the long run when corrosion painting needs to be added every 25 years. Traffic disturbance and user costs are subsequent cost due to this maintenance work with increased value for a bigger road. However, the welding work for stainless steel is more expensive than for carbon steel, but that's a cost included in the LCC-calculation. See Appendix C for LCC-calculation sheet for bridge design No.1 with a trapezoidal deck, and Appendix D for exact values for investment- and total costs for each design respectively.

5.2.2 Sensitivity analysis

To see what effect different important parameters has on the total costs, a sensitivity analysis is made. The first important parameter is the average daily traffic, ADT, which affects the user costs, see Figure 5.3. Increased traffic increases the delay for the different users of the bridge. With low ADT the users have least impact on the total price and is reasonable to use for the analysis.

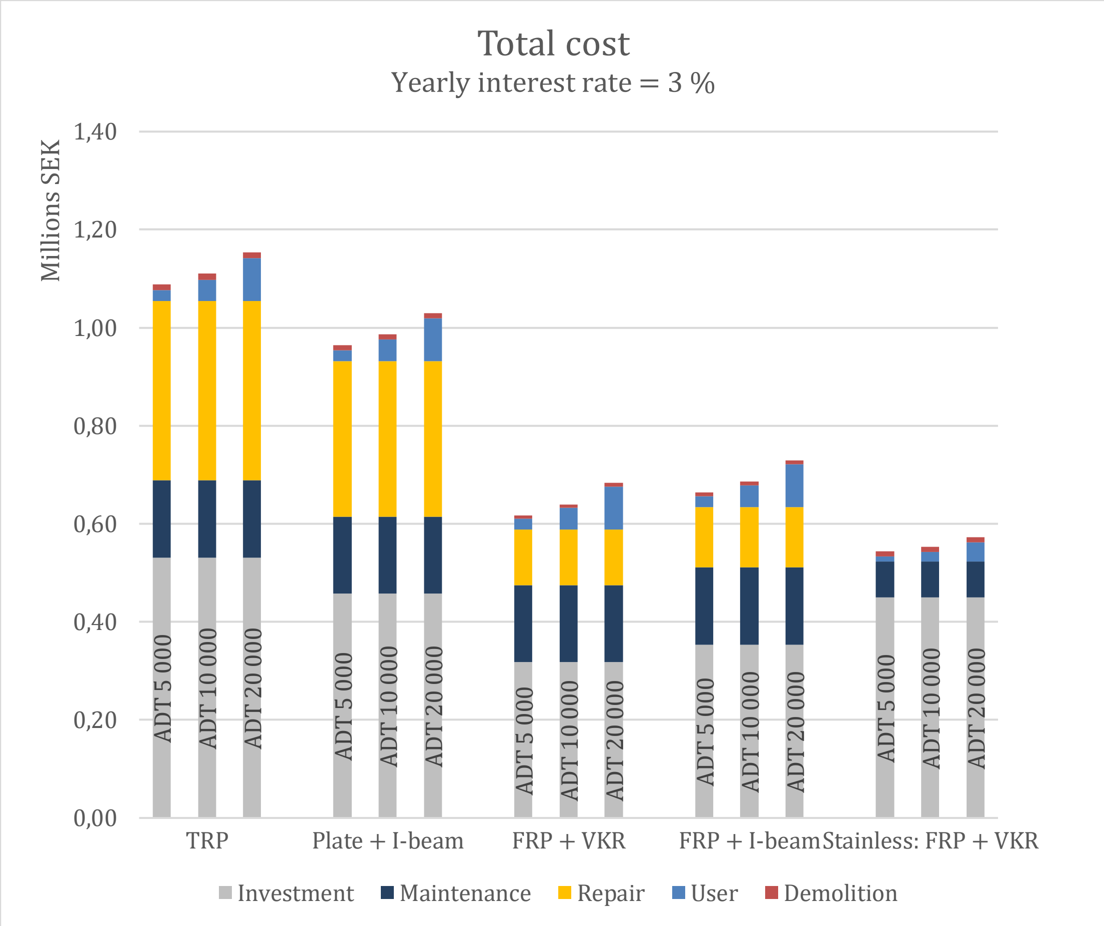

Figure 5.3 *Total costs for both low, medium and high ADT with variation only for the user cost.*

Another parameter to investigate for sensitivity is the interest rate. The investment costs will be the same regardless of the rate, but it will influence all future costs such as maintenance, repair, user and demolition. As seen in Figure 5.2 the three bridges interesting to study are No.3, No.4 and No.5 with low and similar prices. When comparing the total costs for interest rates between zero and seven, the rate is shown to have a big impact for the carbon steel bridges, see Figure 5.4. With zero interest rate, the stainless steel is clearly the cheapest alternative since the future costs are smaller than for carbon steel and won't be as affected of rate. At around six percent the total life time cost is almost equal for the three designs in question, independently of material used.

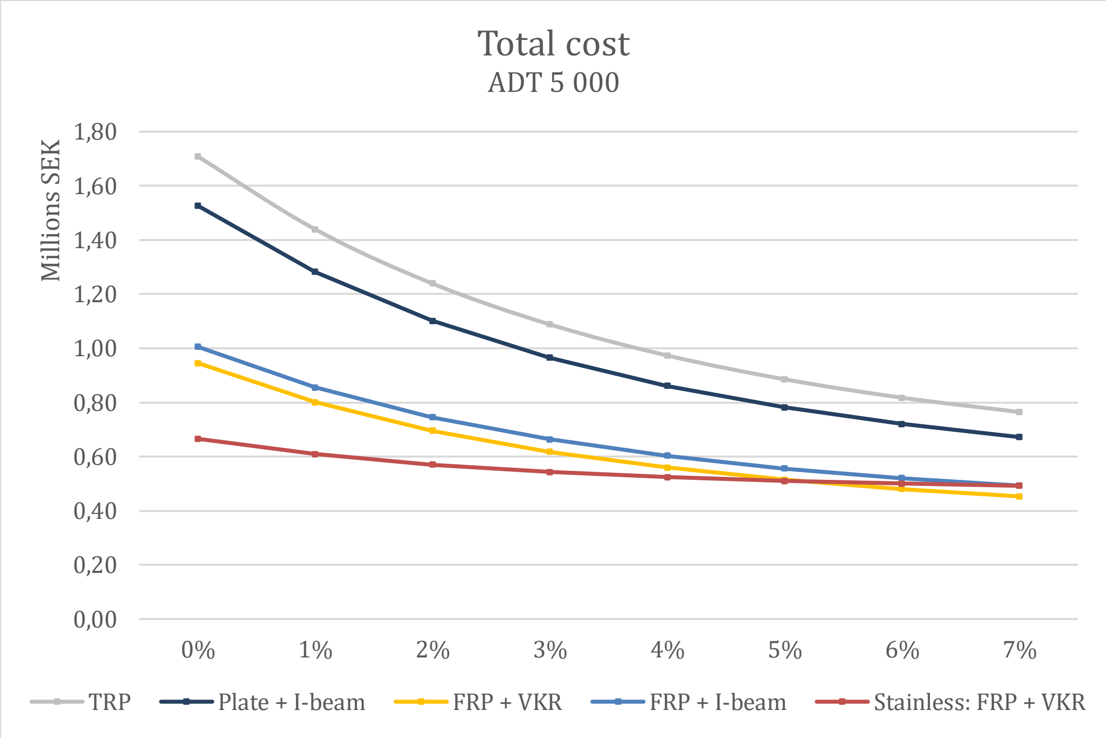

Figure 5.4 *Total costs for interest rates betweel zero and seven for all five bridge designs.*

See Appendix D for exact values from the sensitivity analysis for total costs for each design respectively.

5.2.3 Summary

The LCC analysis show that investors most likely will get lower total costs when using stainless steel and FRP instead of only carbon steel, looking at the bridges total life of 50 years. With longer service life, the benefits would be even bigger.

6 Case study – Life Cycle Assessment

Despite the economic aspect of a structure, it's interesting to look at the environmental aspect as well. This is done in life cycle assessment, looking at the production, use and disposal of the product. As well as for the LCC the life length is 50 years.

6.1 Carbon dioxide emissions

To investigate the environmental impact of the bridges, the most common categories to analyse are climate change, ozone depletion, terrestrial acidification, freshwater eutrophication and fossil depletion. This study is focusing on the climate change with amount of carbon dioxide emissions, which is an easy way to compare different alternatives against each other over their life cycle. Also, carbon dioxide emissions are the largest contributor to the greenhouse effect with around 75 % (Christian Holmström, 2019).

6.1.1 Life cycle stages

Life cycle assessments in other infrastructure projects clearly notes the production of material as the major source to the environmental impact (Li *et al.*, 2013). In a study for a 8m long and 1.5m wide bridge in Taiwan made of steel, concrete or FRP respectively, designed according to specific codes for equal performances, the production stage stands for 83 – 91 % of the total carbon dioxide emission, see Figure 6.1. The building stage has the second biggest impact and finally the transportation the smallest. This is reasonable also for other geometries and other projects in general. The building and transportation stages will however have similar impacts for all five bridge alternatives without contributing to any changes in the final results of total amount of CO_2 emission. The same will apply for energy generation- and disposal processes. Therefore, these will be neglected in this assessment study and the focus will only be on the production stage.

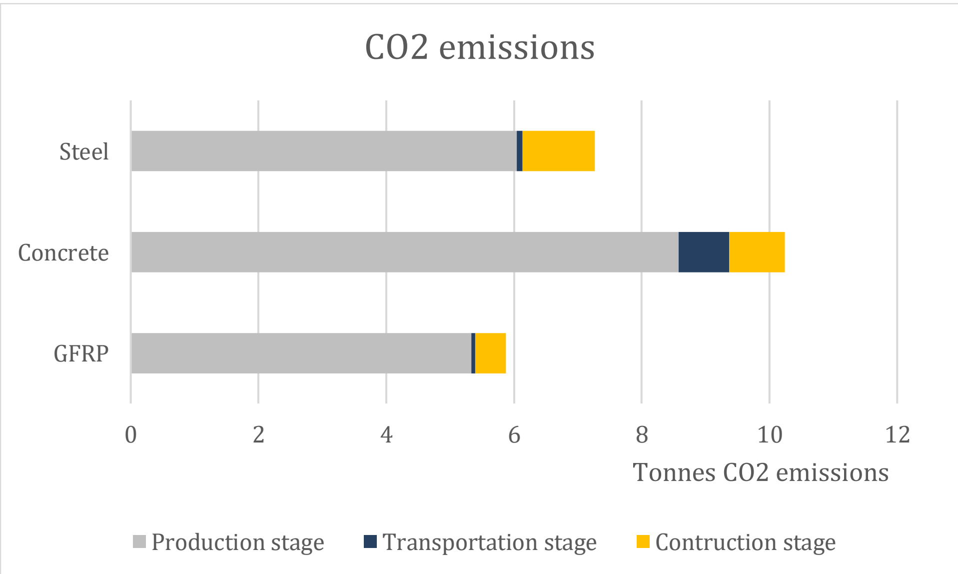

Figure 6.1 Comparison of CO_2 emissions for a pedestrian bridge in Taiwan designd for either steel, concrete or GFRP (Li et al., 2013).

6.1.2 Materials

Each material, and also necessary painting for carbon steel, have individual values for carbon dioxide emissions per measured unit, see Table 6.1. The values for regular and stainless steel are presented in a climate analysis work tool from Trafikverket, while the values for corrosion painting and reinforced polymer are taken from university studies. A high value of emissions refers to great environmental impact.

Table 6.1 Amounts of carbon dioxide emission per kg material used in LCA-study (Hammond and Jones, 2008; Mara, Haghani and Harryson, 2014; Trafikverket, 2019).

Material	**Carbon dioxide emissions** [kg CO^2 / kg]
Carbon steel – S355	1.5
Duplex stainless steel – 1.4662	4.5
FRP – Glass fibre reinforced polymer GRP	5.0
Painting	**Carbon dioxide emissions** [kg CO^2 / m^2]
Corrosion paint	1.6

A comparable value would be 4.5 tonnes as average CO_2 emissions per capita in Sweden and 6.8 tonnes for one average European inhabitant.

6.2 Amounts of material

The product analysed are the five different bridge designs, see Chapter 4 and in particular Section 4.2. It's five different superstructures with similar load bearing system but with different material used. These five designs will be compared to see whether or not one alternative stands out against the others, either in a good or bad way. The accuracy is rough, only taking the material production into consideration. The amounts of material are listed in [kg] and taken from the case study, see Table 6.2.

Table 6.2 Amounts of material for the five optimised bridge deigns.

Design No.	**Deck plate**	**Transverse beams**	**Carbon steel**	**Stainless steel**	**Glass fibre polymer**	**Painting**
			[kg]	[kg]	[kg]	[m^2]
No.1 Optim.	TRP	-	12 500	0	0	364.6
No.2 Optim.	Steel plate	I-beam	12 400	0	0	316.7
No.3 Optim.	FRP	VKR	4 805	0	1 474	113.1
No.4 Optim.	FRP	I-beam	6 042	0	1 474	122.9
No.5 Optim.	FRP	VKR	0	4 402	1 474	0

6.3 Results

The total amount of carbon dioxide emission can effectively be compared against each bridge design, see Figure 6.2. The production of the main material of the bridge (steel and FRP) is the major source for the carbon dioxide emissions, but also paint is considered in the analysis. As seen in the picture, the stainless steel emits way more carbon dioxide in comparison to regular carbon steel. See Appendix E for exact values for each design respectively.

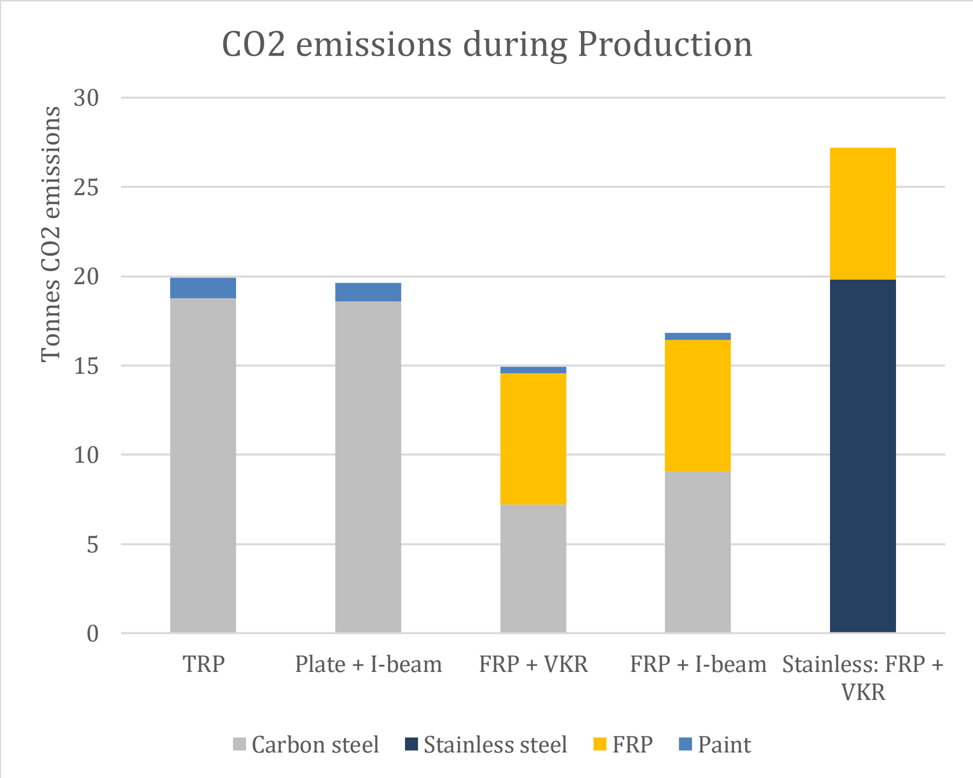

Figure 6.2 Total tonnes carbon dioxide emissions during production for each bridge respectively.

The picture shows that the bridges made of carbon steel releases less total amount of carbon dioxide when comparing all five designs. The use of FRP deck decreases the amount of steel needed and decrease the emissions even further.

From the previous LCC-study, see Chapter 5, the two similar bridges No.3 and No.5 with FRP deck and either carbon- or stainless steel for the truss and transverse VKR beams were shown to be the cheapest two alternatives with similar total cots over the bridge's service life. For this life cycle assessment on the other hand, the difference in total emission between the two solutions were the biggest possible, with the one of carbon steel emitting over 40 % less carbon dioxide than the one of stainless steel.

7 Discussion

The case study made in this thesis covers three main parts. First, it's investigated how beneficial it is to optimise the trusses for a pedestrian bridge. Later on, a life cycle cost analysis is made to look at the economical aspect of the design solutions. As last, the environmental impact in terms of carbon dioxide emissions are analysed. This chapter will discuss the reliability of results from the three parts.

7.1 Optimisation

The initial choice when designing the truss was to use a warren truss, because of its simple appearance and effective fabrication and manufacturing. When doing the dimensioning of bars for the conventional and optimised truss, the comparison clearly shows that big amounts of steel are saved when using profiles aiming to be fully utilised without choosing profiles with same dimensions, which would be the ordinary method. Depending on bridge design, $8.2 - 17.2\ \%$ steel was to be saved. It's also shown that big steel profits are made when varying the thickness of the chords. Both these choices when selecting bar profiles are rarely used and comes as approaches under the work with optimisation of the truss.

The big consequence of an optimised truss however, is the extra work with joints between bars. The extra strength from the flanges of the profiles are removed and these joints needs to be stiffened, as briefly mentioned in Chapter 4, and in particular Section 4.1.2.

The first two designs with either a deck of TRP or a steel plate on top of I-beams are considered as two correspondent systems. The two trusses are fairly similar in profile configuration, but the different deck systems show a big advantage for the I-beams when it comes to welding amount with only $\frac{1}{6}$ of the total welding needed for the TRP.

Design No.3 and No.4 are also seen as equivalent systems, both using a FRP deck but with different transverse beams. The major benefit with the use of this lightweight deck is the material reduction for steel in the truss, also including less steel area to paint. The truss configuration is identical for both solutions, as well as for the FRP modules, but the design using hot-rolled hollow sections as transverse beams gets significantly lighter than the design with I-beams. More exact 1.2 tonnes lighter. Also, the slightly less welding amount is beneficial for the system with VKR beams compared to I-sections.

These two comparisons between two equal systems resulted in the decision to only further investigate one of four bridge designs and remake it in stainless steel. This design was the one with a FRP deck on top of VKR transverse beams, since that design so far were the most efficient both in steel amount and welding length. When using stainless steel for all steel elements, the increased strength lowered the weight with further 0.4 tonnes. The even bigger difference is the absence of corrosion resistance paint, from over $100\ \mathrm{m}^2$ to $0\ \mathrm{m}^2$.

7.2 FRP deck

The use of a FRP deck is an innovative approach for the design of this bridge. A module from Fiberline Composites named Fiberline Plank HD is used, which is their deck system typically used for pedestrian bridges. Two other modules were also available, one less durable for medium loads and one even stronger for road bridges.

For installation of the deck on top of transverse beams, there are a lot more accessories available for open profiles (I-beams) than closed profiles (VKR), se Section 4.2.3 and in particular Figure 4.19. This may be a consequence of it being much easier to merge it to I-beams. For closed profiles the airtight climate inside is vital and drilling holes to fasten the profile is challenging. To ensure the sealing to be airtight, testing will be necessary.

But there are situations where the I-beam will be useful as well. The bridge in the case study is narrow with its 3 m width, and transverse VKR beams are found best suitable. This is expected since the normal force is the dimensioning load case for short transverse beams. But for an increased width, the moment in the beam will become dimensioning and that action is more efficient handled in I-beams.

7.3 LCC

The essential assumptions made for the life cycle cost analysis were to have planning-, designing- and transportation costs neglected. These were seen to be equal in sizes, or at least compensating. Planning and designing are beneficial for the three designs with FRP deck since modules are used without need for design work. Transportation costs will however be higher when products need to be shipped from outside Sweden.

Also, the service length of 50 years is a choice of great importance in the analysis. This is nevertheless a reasonable assumption for a pedestrian bridge, but the decision disregards the fact that different materials have different service lives. That will usually influence the total costs, since a short-lasting bridge is seen as more expensive than a long-lasting.

The study clearly shows the initial- and repair costs to be the most influencing parts. A solution with carbon steel is more priceworthy than stainless steel, initially. However, when adding the maintenance- and repair costs for the service life, the carbon steel solutions passes the one made of stainless steel and becomes more expensive. This indicates the material used for the bridges as an important and crucial choice, being the influencing factor for investment and repair costs.

In the sensitivity analysis some insights are made regarding what would happen when changing different parameters. It’s shown that changes in the interest rate have an important effect in the total cost, it decreases with increased rate. To postpone payments and place it on the stock before payment lowers the total cost, and is beneficial for the carbon steel design with a lot of reparation work. Bridge No.5 with stainless steel however, isn’t affected that much by the interest rate because of the big investment cost and low maintenance cost. The sensitivity study for average daily traffic only showed the original ADT 5 000 to be the most critical case since the increased number made the differences between the design even bigger.

The most valuable insight of the LCC-study was the importance of the initial decision-taking. The choice of material is decisive in the examination of total costs during the life cycle of a bridge.

7.4 LCA

The main choice in the life cycle assessment was to only have the carbon dioxide emissions investigated. Even though they are the biggest source to the greenhouse effect, other methods can be used to get a wider picture. The main assumption made for the estimation of emissions was to only look at the environmental impact from production. The stages after weren't taken into consideration.

The gathered values from Trafikverket show that production of stainless steel has three times more carbon dioxide emissions per kilo than carbon steel, which has major effects on the results of total emissions. FRP releases even more emissions but don't influence the results as much since the material amount is significant lower. The results clearly place the bridge made of stainless steel to be the less environmental friendly solution.

7.5 Overall

The results from optimisation as well as life cycle cost study indicates that a solution with stainless steel together with the advantageous FRP deck is the best solution economically. On the other hand, the service life assessment points out this design to be the one releasing most carbon dioxide emissions. The four designs with carbon steel shows to have less impact on the environment, but is more expensive. These contradictory results make the decision making hard and it has to be decided which aspect's the most important. A table listing advantages and disadvantages for each bridge design compile this study including optimisation, life cycle cost and life cycle assessment, and finalise the discussion, see Table 7.1.

Table 7.1 Listed advantages and disadvantages for each of the five bridge designs.

	Advantages	**Disadvantages**
No.1: Truss beams with a TRP-deck	– Optimisation – – LCC –	– Optimisation – High amounts of welding. Needs high amount of corrosion resistance paint every 25 years. – LCC – High investment cost. Mainly due to the high amount of welding and painting. High total cost. Mainly due to high reparation costs.

	– LCA – Low amount of CO_2 emissions.	– LCA –
No.2: Truss beams with a deck system of a steel plate with transverse I-beams	– Optimisation –	– Optimisation –
	– LCC –	– LCC – Needs high amount of corrosion resistance paint every 25 years. High investment cost. Mainly due to the painting. High total cost. Mainly due to high reparation costs.
	– LCA – Low amount of CO_2 emissions.	– LCA –
No.3: Truss beams with a deck system of a FRP deck and transverse VKR beams	– Optimisation – Lightweight deck which decreases the amount of steel in truss. Lower the total weight of the bridge as well.	– Optimisation – Installation of deck a bit complicated since closed profiles needs to be airtight. Only one accessory available for this product.
	– LCC – Low investments costs. Low total cost.	– LCC – Needs corrosion resistance paint every 25 years.
	– LCA – Low amount of CO_2 emissions.	– LCA –

No.4: Truss beams with a deck system of a FRP deck and transverse I-beams	– Optimisation – Lightweight deck which decreases the amount of steel in truss. Lower the total weight of the bridge as well. Easy installation of deck and many different accessories available for the product. – LCC – Low investments costs. Low total cost. – LCA – Low amount of CO_2 emissions.	– Optimisation – – LCC – Needs corrosion resistance paint every 25 years. – LCA –
No.5: Truss beams with a deck system of a FRP deck and transverse VKR beams, in stainless steel	– Optimisation – Lightweight deck which decreases the amount of steel in truss. Lower the total weight of the bridge as well. – LCC – Low total cost. Low (zero) reparation cost. – LCA –	– Optimisation – Installation of deck a bit complicated since closed profiles needs to be airtight. Only one accessory available for this product. – LCC – High investment cost. – LCA – High amount of CO_2 emissions. Due to the fact that stainless steel emits three times more emissions than carbon steel.
	Advantages	**Disadvantages**

8 Conclusions

In this final chapter, the conclusions made from the study are summed up. The aim of the thesis was to optimise a conventional steel truss footbridge by using innovative approaches to reduce the total amount of material used. This were done by making five different bridge solutions, designed with different deck systems with variable material. These were to be compared and evaluated against each other. Every assumption made before each analysis should be taken into consideration to be able to use the results in future decisions regarding use of stainless steel and FRP in these types of bridges.

The optimisation of the truss, for all five alternatives, saved $8.2 - 17.2$ % amount of steel depending on bridge type. The lower limit was bound to the predefined profiles used, not able to make it any smaller or thinner. The optimised truss for design No.1 with a TRP-deck for example, made an average 12 % saving, corresponding to almost 0.5 tonne steel. It's a result showing that extra work with strengthening of bar connections gives material efficiency of the steel.

From the LCC study, the three bridge designs with a deck made of FRP got surprisingly cheap in comparison to the two pure carbon steel designs. Even without an optimised truss it would be economically advantageous to use these types of solutions. It's worth mentioning that it's mainly the need of repainting of the carbon steel that is the cause for this outcome. It is clearly shown to be financially profitable to investigate innovative design solutions in contrast to conventional carbon steel bridges.

The decision to only do a stainless-steel version of one carbon steel bridge were made early in the study, due to the great profitable outcome in the comparison to the total weight between the bridges. The LCC-study confirmed it as well. This carbon steel design was bridge solution No.3 with a FRP deck on VKR transversal beams. But when analysing this bridge, made in carbon- or stainless steel, the later one became the less expensive one. The bridge with stainless steel ended up at a cost of $0.54\ MSEK$ in comparison to $0.62\ MSEK$ for the carbon steel, seen at its whole service life and not only at investment. The use of a FRP deck makes the construction way more economic independently of steel sort. But when looking at the environmental impact the results are shifting. The bridge with stainless steel releases $19.9\ tonnes$ carbon dioxide emissions in comparison to $14.9\ tonnes$ for the carbon steel, because of the three times more emissions per kilo material produced.

So, for the construction of a pedestrian bridge with a span of 30 meters, stainless steel can be considered as the most cost-efficient material. But at the same time the less environmental friendly choice. FRP are on the other hand working in favour for both total cost and total emissions. However, it's important to mention that the conclusions of this analysis were valid for this specific situation.

8.1 Further studies

Several topics that needs to be discussed within the subject with innovative steel pedestrian bridges exists, some of them are listed below.

- Further research regarding geometry of the bridge. In this case study the bridges are of specific length, width and height and it would be interesting to see the effects of results when changing these. Especially the width of the deck.

- Further research regarding stainless steel bridges. Which other design solutions than implementation of FRP decks would be beneficial both for economic and environmental impact.

- Look deeper into the initial rotational stiffness of the connections in the bars when optimised. The theory was treated but not the analyse of it.

- Designing of joints in the truss. An important aspect at dimensioning, which were neglected in this thesis.

9 References

Agarwal, B. D., Broutman, L. J. and Chandrashekhara, K. (2018) *Analyis and Performance of Fiber Composites*. 4th edn. Hoboken: John Wiley & Sons, Inc.

AISC (1963) *Design Manual for Orthotropic Steel Plate Deck Bridges*. New York.

Allen, E. and Zalewski, W. (2010) *Form and Forces: Designing efficient, expressive structures*. New Jersey: John Wiley & Sons, Inc.

BE Group (2019) *Pris 20190306*. Available at: https://www.begroup.se/om-be-group/ladda-ner-bestall/prislistor/.

Blaauwendraad, J. (2010) *Plates and FEM - Surprises and Pitfalls*. Delft: Springer.

Bond, J. and Hjelmgren, V. (2018) *Dynamic and Economic Aspects of Carbon Fiber Reinforced Polymer Footbridges*. Chalmers University of Technology. Available at: http://publications.lib.chalmers.se/records/fulltext/255631/255631.pdf.

Broo, H., Lundgren, K. and Plos, M. (2008) *A guide to non-linear finite element modelling of shear and torsion in concrete bridges*. Gothenburg.

Campbell, F. C. (2010) *Structural composite materials*. Ohio: ASM International.

Christian Holmström (2019) *Koldioxid per capita - internationellt*. Available at: https://www.ekonomifakta.se/Fakta/Miljo/Utslapp-internationellt/Koldioxid-per-capita/ (Accessed: 29 March 2019).

Comp, T. A., Jackson, D. C. and Jones, A. D. (1976) *Trusses*. Washington.

Davis, J. R. (2000) *Corrosion: Understanding the basics*. Ohio: ASM International.

DeCelle, J. *et al.* (2013) *WPI – Pedestrian Bridge Study*. Worcester. Available at: https://web.wpi.edu/Pubs/E-project/Available/E-project-031013-103455/unrestricted/WPI_-_Pedestrian_Bridge_Study.pdf.

Duan, L. (2017) *Truss bridge*. Access Science. doi: 10.1036/1097-8542.712890.

fib (2005) *Guidelines for the design of footbridges*. Lusanne: fib.

Fiberline Composites (2019) *Fiberline Plank HD*. Available at: https://fiberline.com/fiberline-plank-hd (Accessed: 15 January 2019).

Garifullin, M. *et al.* (2017) 'Initial in-plane rotational stiffness of welded RHS T joints with axial force in main member', *Journal of Constructional Steel Research*. Elsevier Ltd, 139(February 2018), pp. 353–362. doi: 10.1016/j.jcsr.2017.09.033.

Giger Johansson, H. and Seebergs, E. (2018) *Buckling and post-buckling behaviours of fibre reinforced elements subjected to in-plane compression*. Chalmers University of Technology.

Håkansson, J. and Wallerman, H. (2015) *Finite Element Design of Orthotropic Steel Bridge Decks*. Chalmers University of Technology. Available at: http://publications.lib.chalmers.se/records/fulltext/219022/219022.pdf.

Hammond, G. and Jones, C. (2008) 'Inventory of Carbon & Energy (Ice)', *University of Bath*. Available at: http://www.organicexplorer.co.nz/site/organicexplore/files/ICE Version 1.6a.pdf.

Hollaway, L. C. and Head, P. R. (2001) *Advanced Polymer Composites and Polymers in the Civil Infrastructure*. Oxford: Elsevier Science Ltd.

I.E. Comittee (2006) *An Introduction to FRP Composites for Construction*.

Javier Veganzones Munoz, J. *et al.* (2016) 'Life-cycle cost analysis as a tool in the developing process for new bridge edge beam solution', *Structure ans Infrastructure Engineering*, 12:9, pp. 1185–1201. Available at: http://dx.doi.org/10.1080/15732479.2015.1095770.

Karlsson, A. and Wesley, C. (2015) *Fatigue Analysis for Orthotropic Steel Deck Bridges*. Chalmers University of Technology. Available at: http://publications.lib.chalmers.se/records/fulltext/217614/217614.pdf.

Kolstein, M. H. (2007) *Fatigue Classification of Welded Joints in Orthotropic Steel Bridge Decks*. Delft.

Kolstein, M. H. (2008) *Fibre Reinforced Polymer (FRP) Structures*. Delft.

Li, Y.-F. *et al.* (2013) 'The Carbon Footprint Calculation of the GFRP Pedestrian Bridge at Tai-Jiang National Park', *International Review for Spatial Planning and Sustainable Development*, 1(4), pp. 13–28. doi: 10.14246/irspsd.1.4_13.

Mara, V., Haghani, R. and Harryson, P. (2014) *Bridge decks of fibre reinforced polymer (FRP): A sustainable solution*. Gotheburg. Available at: http://publications.lib.chalmers.se/records/fulltext/185412/local_185412.pdf.

SBI (2008) *Stålbyggnad*. 6th edn. Stockholm: SBI.

SBI (2017) *Dimensionering av konstruktioner i rostfritt stål*. 4th edn. Stockholm: SBI.

Sétra (2006) *Technical Guide: Footbridges. Assesment of vibrational behaviour of footbridges under pedestrian loading*. Available at: http://www.projektering.nu/files/Footbridges.pdf.

SIS (2001) *Eurocode: Basis of structural design*. Brussels.

SIS (2003a) *Eurocode 1: Actions on structures - Part 1-3: General actions - Snow loads*. Brussels.

SIS (2003b) *Eurocode 1: Actions on structures - Part 2: Traffic loads on bridges*. Brussels.

SIS (2005a) *Eurocode 1: Actions on structures - Part 1-4: General actions - Wind actions*. Brussels.

SIS (2005b) *Eurocode 3: Design of steel structures - Part 1-1: General rules and rules for buildings*. Brussels.

SIS (2005c) *Eurocode 3: Design of steel structures - Part 1-8: Design of joints*. Brussels.

SIS (2006a) *Eurocode 3: Design of steel structures - Part 1-4: General rules - Supplementary rules for stainless steels*. Brussels.

SIS (2006b) *Eurocode 3: Design of steel structures - Part 2: Steel bridges*. Brussels.

StruSoft (2019) *FEM-Design*.

Trafikverket (2008) *Kodförteckning och beskrivning av Brotyper*. doi: 10.1007/s11947-009-0181-3.

Trafikverket (2011a) *TRVK Bro 11*. 2011:085.

Trafikverket (2011b) *TRVR Bro 11*. 2011:086.

Trafikverket (2019) 'Klimatkalkyl'. Available at: http://webapp.trafikverket.se/Klimatkalkyl/.

US Department of Transportation (2012) *Manual for Design, Construction and Maintenance of Orthotropic Steel Deck Bridges*. Pittsburgh. doi: FHWA-IF-12-027.

Zoghi, M. (2014) *The International Handbook of FRP Composites in Civil Engineering*. Boca Raton: Taylor & Francis Group, LLC.

Appendix A

Fi erline lan - product specification

Values for global analyses

Geometric Properties	**Unit**	**Value**
Moment of inertia, I_{yy}	mm^4/m	2.140.000
Shear area, A_{yshear}	mm^2/m	3.419
Total area, A_{ytotal}	mm^2/m	9.566
Material Properties (average)	**Unit**	**Value**
Elastic modulus, E_{ff}	N/mm^2	20.500
Poisson's ratio, axial, ν_{yx}	-	0,230
Poisson's ratio, transverse, ν_{xy}	-	0,090
Temperature expansion, axial, α_{tx}	1/K	$11 \cdot 10^6$
Temperature expansion, transverse, α_{ty}	1/K	$19 \cdot 10^6$

Classification	**Unit**	**Characteristic value**
Bending moment, between supports, $M_{R,k}$	kN·m	11,7
Bending moment, at the supports, $M_{R,k}$	kN·m	14,0
Upward vertical force at the supports, R_k	kN	3,53
Horizontal load, axial, R_k	kN	0,736
Horizontal load, transverse, R_k	kN	0,404
Stiffness, EI	$N \cdot mm^2$	$2{,}189 \cdot 10^{10}$

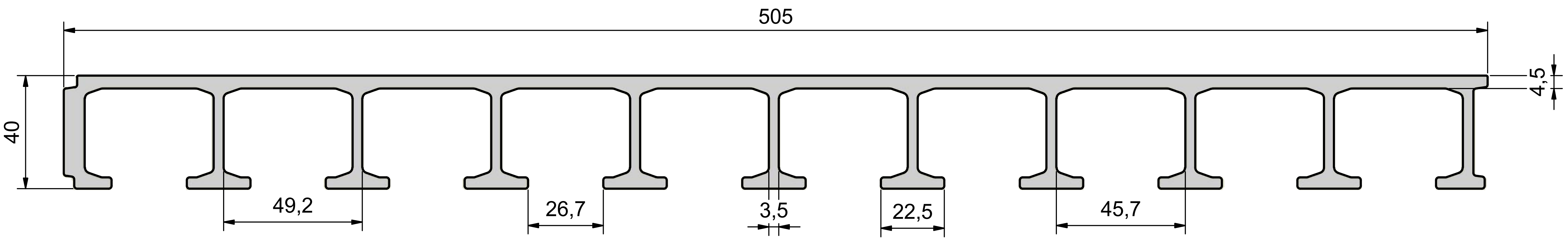

Date: 11/28/2016	Sign.: mma	FIBERLINE COMPOSITES www.fiberline.com	Tolerances acc. to:
Scale:			Material: Glasfiberarmeret polyester
			Replaces drawing No.:
Date of approval:	Approved by:	Subject:	Drawing No.: HD Plank
Revision:			

Appendix B

Calculation sheet for quantity estimations: weight, painted steel area and welding length

No.5 - FRP/VKR - Stainless - Optimized

Top Chords

Quantity estimation, Steel - for selected objects

Storey	Struct.	Identifier	Quality	Section/ Thickness	Unit weight [t/m, t/m2]	Total length[m]/ Total area[m2]	Total weight [t]	Painted area [m2]
-	Beam	B.23	1.4162	VKR 120x120x6.3	0,022	9,2	0,203	4,267
-	Beam	B.46	1.4162	VKR 120x120x8	0,027	12	0,329	5,513
-	Beam	B.47	1.4162	VKR 120x120x6.3	0,022	8,8	0,194	4,081
-	Beam	B.54	1.4162	VKR 120x120x6.3	0,022	9,2	0,203	4,267
-	Beam	B.55	1.4162	VKR 120x120x8	0,027	12	0,329	5,513
-	Beam	B.56	1.4162	VKR 120x120x6.3	0,022	8,8	0,194	4,081
TOTAL							1,451	27,721

Bottom Chords

Quantity estimation, Steel - for selected objects

Storey	Struct.	Identifier	Quality	Section/ Thickness	Unit weight [t/m, t/m2]	Total length[m]/ Total area[m2]	Total weight [t]	Painted area [m2]
-	Beam	B.48	1.4162	VKR 120x120x5	0,018	9,2	0,163	4,298
-	Beam	B.49	1.4162	VKR 120x120x5	0,018	12	0,213	5,605
-	Beam	B.50	1.4162	VKR 120x120x5	0,018	8,8	0,156	4,111
-	Beam	B.51	1.4162	VKR 120x120x5	0,018	9,2	0,163	4,298
-	Beam	B.52	1.4162	VKR 120x120x5	0,018	12	0,213	5,605
-	Beam	B.53	1.4162	VKR 120x120x5	0,018	8,8	0,156	4,111
TOTAL							1,064	28,027

Diagonals

Quantity estimation, Steel - for selected objects

Storey	Struct.	Identifier	Quality	Section/ Thickness	Unit weight [t/m, t/m2]	Total length[m]/ Total area[m2]	Total weight [t]	Painted area [m2]
-	Beam	B.1	1.4162	VKR 100x60x3.6	0,008	1,5	0,013	0,466
-	Beam	B.2	1.4162	VKR 100x60x3.6	0,008	1,5	0,013	0,466
-	Beam	B.3	1.4162	VKR 100x60x3.6	0,008	2,121	0,018	0,659
-	Beam	B.4	1.4162	VKR 100x60x3.6	0,008	2,121	0,018	0,659
-	Beam	B.5	1.4162	VKR 100x60x3.6	0,008	2,121	0,018	0,659
-	Beam	B.6	1.4162	VKR 100x60x3.6	0,008	2,121	0,018	0,659
-	Beam	B.7	1.4162	VKR 100x60x3.6	0,008	2,121	0,018	0,659
-	Beam	B.8	1.4162	VKR 100x60x3.6	0,008	2,121	0,018	0,659
-	Beam	B.9	1.4162	VKR 100x60x3.6	0,008	2,121	0,018	0,659
-	Beam	B.10	1.4162	VKR 100x60x3.6	0,008	2,121	0,018	0,659
-	Beam	B.11	1.4162	VKR 100x60x3.6	0,008	2,121	0,018	0,659
-	Beam	B.12	1.4162	VKR 100x60x3.6	0,008	2,121	0,018	0,659
-	Beam	B.13	1.4162	VKR 100x60x3.6	0,008	2,121	0,018	0,659
-	Beam	B.14	1.4162	VKR 100x60x3.6	0,008	2,121	0,018	0,659
-	Beam	B.15	1.4162	VKR 100x60x3.6	0,008	2,121	0,018	0,659
-	Beam	B.16	1.4162	VKR 100x60x3.6	0,008	2,121	0,018	0,659
-	Beam	B.17	1.4162	VKR 100x60x3.6	0,008	2,121	0,018	0,659
-	Beam	B.18	1.4162	VKR 100x60x3.6	0,008	2,121	0,018	0,659
-	Beam	B.19	1.4162	VKR 100x60x3.6	0,008	2,121	0,018	0,659
-	Beam	B.20	1.4162	VKR 100x60x3.6	0,008	2,121	0,018	0,659
-	Beam	B.21	1.4162	VKR 100x60x3.6	0,008	2,121	0,018	0,659
-	Beam	B.22	1.4162	VKR 100x60x3.6	0,008	2,121	0,018	0,659
-	Beam	B.24	1.4162	VKR 100x60x3.6	0,008	1,5	0,013	0,466
-	Beam	B.25	1.4162	VKR 100x60x3.6	0,008	1,5	0,013	0,466
-	Beam	B.26	1.4162	VKR 100x60x3.6	0,008	2,121	0,018	0,659
-	Beam	B.27	1.4162	VKR 100x60x3.6	0,008	2,121	0,018	0,659
-	Beam	B.28	1.4162	VKR 100x60x3.6	0,008	2,121	0,018	0,659
-	Beam	B.29	1.4162	VKR 100x60x3.6	0,008	2,121	0,018	0,659
-	Beam	B.30	1.4162	VKR 100x60x3.6	0,008	2,121	0,018	0,659
-	Beam	B.31	1.4162	VKR 100x60x3.6	0,008	2,121	0,018	0,659
-	Beam	B.32	1.4162	VKR 100x60x3.6	0,008	2,121	0,018	0,659
-	Beam	B.33	1.4162	VKR 100x60x3.6	0,008	2,121	0,018	0,659
-	Beam	B.34	1.4162	VKR 100x60x3.6	0,008	2,121	0,018	0,659
-	Beam	B.35	1.4162	VKR 100x60x3.6	0,008	2,121	0,018	0,659
-	Beam	B.36	1.4162	VKR 100x60x3.6	0,008	2,121	0,018	0,659
-	Beam	B.37	1.4162	VKR 100x60x3.6	0,008	2,121	0,018	0,659
-	Beam	B.38	1.4162	VKR 100x60x3.6	0,008	2,121	0,018	0,659
-	Beam	B.39	1.4162	VKR 100x60x3.6	0,008	2,121	0,018	0,659
-	Beam	B.40	1.4162	VKR 100x60x3.6	0,008	2,121	0,018	0,659
-	Beam	B.41	1.4162	VKR 100x60x3.6	0,008	2,121	0,018	0,659
-	Beam	B.42	1.4162	VKR 100x60x3.6	0,008	2,121	0,018	0,659
-	Beam	B.43	1.4162	VKR 100x60x3.6	0,008	2,121	0,018	0,659
-	Beam	B.44	1.4162	VKR 100x60x3.6	0,008	2,121	0,018	0,659
-	Beam	B.45	1.4162	VKR 100x60x3.6	0,008	2,121	0,018	0,659
TOTAL							0,77	28,231

TOTAL TRUSS (2 pieces)	**Total weight [t]**	**Painted area [m2]**
	3,285	**83,979**

Transversal beams

Quantity estimation, Steel - for selected objects

Storey	Struct.	Identifier	Quality	Section/ Thickness	Unit weight [t/m, t/m2]	Total length[m]/ Total area[m2]	Total weight [t]	Painted area [m2]
-	Beam	B.57	1.4162	VKR 120x120x5	0,018	3	0,053	1,401
-	Beam	B.58	1.4162	VKR 120x120x5	0,018	3	0,053	1,401
-	Beam	B.59	1.4162	VKR 120x120x5	0,018	3	0,053	1,401
-	Beam	B.60	1.4162	VKR 120x120x5	0,018	3	0,053	1,401
-	Beam	B.61	1.4162	VKR 120x120x5	0,018	3	0,053	1,401
-	Beam	B.62	1.4162	VKR 120x120x5	0,018	3	0,053	1,401
-	Beam	B.63	1.4162	VKR 120x120x5	0,018	3	0,053	1,401
-	Beam	B.64	1.4162	VKR 120x120x5	0,018	3	0,053	1,401
-	Beam	B.65	1.4162	VKR 120x120x5	0,018	3	0,053	1,401
-	Beam	B.66	1.4162	VKR 120x120x5	0,018	3	0,053	1,401
-	Beam	B.67	1.4162	VKR 120x120x5	0,018	3	0,053	1,401
-	Beam	B.68	1.4162	VKR 120x120x5	0,018	3	0,053	1,401
-	Beam	B.69	1.4162	VKR 120x120x5	0,018	3	0,053	1,401
-	Beam	B.70	1.4162	VKR 120x120x5	0,018	3	0,053	1,401
-	Beam	B.71	1.4162	VKR 120x120x5	0,018	3	0,053	1,401
-	Beam	B.72	1.4162	VKR 120x120x5	0,018	3	0,053	1,401
-	Beam	B.73	1.4162	VKR 120x120x5	0,018	3	0,053	1,401
-	Beam	B.74	1.4162	VKR 120x120x5	0,018	3	0,053	1,401
-	Beam	B.75	1.4162	VKR 120x120x5	0,018	3	0,053	1,401
-	Beam	B.76	1.4162	VKR 120x120x5	0,018	3	0,053	1,401
-	Beam	B.77	1.4162	VKR 120x120x5	0,018	3	0,053	1,401
TOTAL							1,117	29,429

FRP deck

Weight	17,06	kg/m2	Total weight [t]
Area	86,4	m2	
TOTAL			1,473984

TOTAL DECK	**Total weight [t]**	**Painted area [m2]**
	2,590984	**29,429**

TOTAL BRIDGE	**Total weight [t]**	**Painted area [m2]**
	5,875984	**113,408**

Welding Length

Transversal beams/Bottom Chord

42	st	Number of connections
480	mm	Circumference
20,16	m	

Transversal beams/FRP

Limmas

0 m

Diagonals/Chords

80	st	Number of connections
370	mm	Circumference
29,6	m	

Verticals/Chords

8	st	Number of connections
320	mm	Circumference
2,56	m	

Parts Top Chord

4	st	Number of connections
480	mm	Circumference
1,92	m	

Parts Bottom Chord

4	st	Number of connections
480	mm	Circumference
1,92	m	

TOTAL BRIDGE

56,16 m

Appendix

LCC-calculation sheet for ridge deisgn o

ETSI Bridge LCC

Optimal New Bridges - Life cycle cost analysis (LCCA)

Version 2.3 [2012-05-07], ETSI

This program was first developed by Raid Karoumi (Royal Institute of Technology, Structural Engineering & Bridges, raid.karoumi@byv.kth.se)
The work was funded by the Swedish Road Administration (SRA), and this is a prototype for testing. The program is intended only to compare the LCC of the alternative bridge solutions, which means that all factors that influence the LCC are not considered (e.g. costs of the design, land purchase and administration).
This version 2.3 in English has been developed in the ETSI project

NOTE

• Never feed a space in a non-current cell. Instead, please state 0 (i.e. zero).
• Repair interval entered will be adjusted depending on the chosen concrete quality, ADT, climate zone, salt quantity, placement on the bridge, and concrete cover.
• Repair intervals should be chosen to receive a maximum of about 3 - 4 major steps in the bridge lifetime and at least 10 years apart.
• Quantities specified for calculating the cost of repair need not to be equal to investment quantities. I.e. you can choose to repair some of the concrete in bridge deck rather than replace the whole.
• If no data is entered for the calculation of investment cost, the investment cost will be chosen as the cost given in the current tender (entered during the pre-subsidence) to allow the calculation of the total LCC.
• The program includes road user costs only in the form of restrictions on traffic benefits for the time work is underway on the bridge and restricts accessibility for road users.
• Many of the listed "default" values of the rates and intervals are guessed by the author of the program and could therefore be wrong.
• Always save the file xxx.xls under a new name before making changes / inputting of a new project.
• Boxes with a small red triangle in the upper right corner contain help text. The text is visible by setting the mouse pointer over the box

ETSI
BRIDGE LIFE CYCLE OPTIMISATION

OK

General conditions

Name of bridge:	Bridge No1: Warren truss with TRP deck
Project number:	No1
Administrator:	Josefin Tjernlund
Date:	2019-03-06

Climate zone:		Middle Sw eden
Road salting		Normal salt spreadin
Investment cost according to tender	CUR	0
Demolition cost in % of investment cost	%	10,0
Calculus period	years	50
Yearly real interest rent	%	3,0
Average daily traffic, ADT		5 000
Percentage of trucks	%	10,0
Allowed speed on the bridge	km/h	110
Reduced speed due to repair actions	km/h	50
Hourly cost, car	CUR/h	145
Hourly cost, truck	CUR/h	540
Total bridge length	m	30,0
Length of superstructure	m	30,0
Lengths of edge beams	m	60
Effective bridge width	m	2,9
Total bridge width	m	3,0
Bridge area	m^2	90
Area of surfacing	m^2	86
Painted area (steel beams etc)	m^2	365
Number of railings (parapets)	no.	0
Total length of railings(parapets)	m	0

	Weighting inputted default intervals factor	own factor
Climate zone	0,7	0,0
Average daily traffic, ADT	1,0	0,0
Saltning	1,0	0,0
Construction part subjected to salt action	1,0	0,0
Concrete quality > C30/C37	1,0	1,0
Concrete cover > Standard	1,0	0,0

Investment cost

	New construction costs	
	Unit price	
formwork	0	CUR/m^2
concrete	0	CUR/m^3
steel	25 000	CUR/ton
reinforcement	0	CUR/ton
cables	0	CUR/m
rammed piles	0	CUR/m
parapet	0	CUR/m
insulation	0	CUR/m^2
surfacing	0	CUR/m^2

Dotted fields contain the default values evaluated with the help of previously entered data. You have the possibility to input your own values in the fields.

	Quantities for calculation of investment cost							
	formwork [m^2]	concrete[m^3]	reinf. [ton]	steel [ton]	cables [m]	piles [m]	others, total cost	cost
SUBSTRUCTURE								
foundation slab								0
pier & column								0
front wall								0
wing wall								0
bridge seat								0
upper front wall								0
backfill								0
substructure others								0
SUPERSTRUCTURE								
main beams				5,777				144 425
deck				6,735				168 375
welding							90948	90 948
installation deck							0	0
painting							127610	127 610
								0
bridge deck	90							0
								0
superstructure others								0
BRIDGE DETAILS								
bearing								0
insulation							0	0
surfacing							0	0
railing or parapet							0	0
expansion joint								0
drainage system								0
bridge details others								0
OTHERS								
aesthetics								0
other construction costs								0
							Σ Investment cost/CUR	531 358

Operation and Maintenance cost

dotted fields contain the default values evaluated with the help of previously entered data. You have the possibility to input your own values in the fields.

	MR&R unit cost & quantities			MR&R interval alt. Single year				Traffic disturbance		MR&R cost		User cost	
	unit costs		quantities	interval, year	action year	action year	action year	days	length	cost each time	tot cost	cost each time	tot cost
yearly surveillance		CUR		0	0	0	0	0,0	0,0	0	0	0	0
superficial inspection	3 240	CUR		1	0	0	0	0,5	0,0	3 240	83 364	0	0
main inspection	18 900	CUR		6	0	0	0	0,5	0,5	18 900	73 827	2 516	9 828
cleaning (removal of salt etc.)	0	CUR/m^2	90					0,5	0,2	0	0	1 006	0
rodding of drainage system		CUR						0,0	0,0	0	0	0	0
impregnation of edge beams	300	CUR/m	60					5,0	0,0	18 000	0	1 510	0
maintenance of parapets, patch painting	1 100	CUR/m	0					3,0	0,0	0	0	906	0
maintenance of bridge seat	5 000	CUR						10,0	1,0	5 000	0	100 636	0
maintenance of expansion joints	3 000	CUR/m	6					4,0	0,0	18 000	0	1 208	0
backfilling and restoration of erosion protection	12 000	CUR						0,0	0,0	12 000	0	0	0
painting patching	2 100	CUR/m^2	365					5,0	0,5	765 660	0	25 159	0
dehumidification device, el + maintenance	25 000	CUR/a						0,0	0,0	25 000	0	0	0
edge beam rep 0 - 30 mm/m^2	3 000	CUR	418					20,0	0,8	1 254 000	0	161 018	0
change of rubber in expansion joint	3 000	CUR	6					5,0	0,1	18 000	0	5 032	0
adjustment of wearing course	400	CUR	86					0,0	0,0	34 320	0	0	0
bearings minor repair + painting	7 000	CUR	8					0,0	0,0	56 000	0	0	0
										Σ present cost	157 191 kr	Σ present cost	9 828 kr

BaTMan-account		Repair quantities and unit costs			MR&R interval alt. Single year				Traffic disturbance		Input for weighting of time interval		
		unit cost		quantities	interval, year	action year	action year	action year	days	length	salt exposure	Concrete quality CX/37	cover qoutient
	SUBSTRUCTURE												
	bottom slab intermediate piers	1 000	CUR/m^2										
0340.x	piers	4 000	CUR/m^2										
	intermediate support cross beams		CUR/m^2										
	Other		CUR										
	bottom slab abutments		CUR/m^2										
0310.x	front wall	4 000	CUR/m^2										
0410.x	wing wall	2 800	CUR/m^2										
0320.x	bearing seat	2 000	CUR/m^2										
0330.x	upper front wall	2 800	CUR/m^2										
0190.x ; 210.x ...	backfilling	900	CUR/m^3										
	SUPERSTRUCTURE												
0630.x	main beams re-painting	2 100	CUR/m^2	365		25			5,0	0,5		60	1
0730.x	cross beams, re-painting	2 100	CUR/m^2										
	main beams patch painting	2 100	CUR/m^2										
0900.x	edge beam partial repair	3 000	CUR/m										
	Bridge deck partial repair		CUR/m^2										
0660.x	truss	2 100	CUR/m^2										
0650.x	arch	1 300	CUR/m^2										
	pylons	1 300	CUR/m^2										
	cables	4 000	CUR/m										
0800.x; 0610.x	bridge deck	2 100	CUR/m^2										
0900.x	edge beam replacement	9 000	CUR/m										
	BRIDGE DETAILS												
500.x	bearings	7 000	CUR/item							0,0			
1000.x	insulation	1 800	CUR/m^2	86						0,0			
1100.x	surfacing	600	CUR/m^2	86						0,0			
1200.x	parapets and noise barriars, partial painting	1 100	CUR/m	0						0,0			
1300.x	expansion joints	30 000	CUR/m	6						0,0			
	parapets replacement	5 000	CUR/m	0									
	surfacing, partial repair	400	CUR/m^2	86						0,0			
	expansion joints, change of rubber sealing	3 000	CUR/m	6						0,0			
1400.x	drainage system	2 500	CUR/item										
	MISCELLANEOUS												
	aesthetics	0	CUR										
	other repair actions (total cost)	0	CUR										
	other repair actions (total cost)	10 000	CUR										

ETSI, Bridge Stand alone LCC
Optimal new bridges - Life cycle analysis

Life cycle cost
Bridge No1: Warren truss with TRP deck

INVESTMENT COST	531 358
REPAIR COSTS	365 683
OPERATION AND MAINTENANCE	157 191
USER COSTS	21 844
DEMOLITION COST	12 121
SUM NET PRESENT VALUE	**1 088 197**
SUM NET PRESENT VALUE / BRIDGE AREA [CUR/m^2]	**12 091**

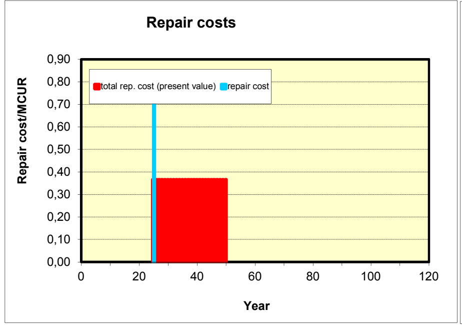

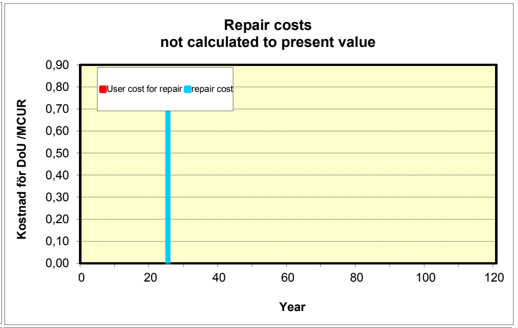

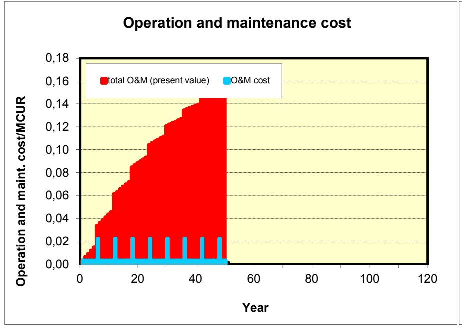

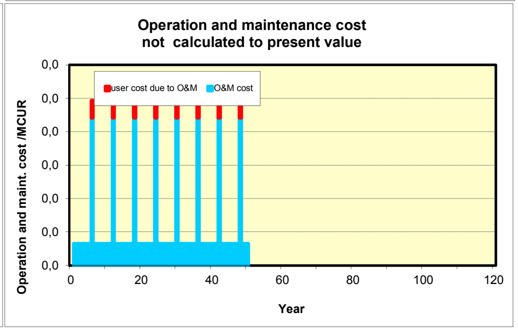

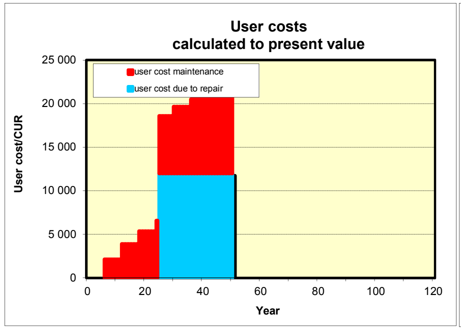

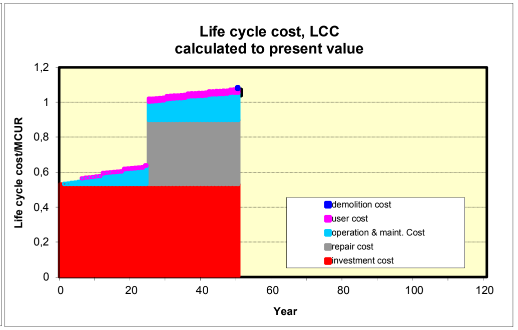

Appendix

Life cycle cost analysis:
- Values for total- and in estment costs
- ensiti ity analaysis for total cost
- ensiti ity analaysis interest rate for total cost

LIFE CYCLE COST ANALYSIS (LCC)

TOTAL COST

	Investment	Maintenance	Repair	User	Demolition	Total
TRP	531 358	157 191	365 683	21 844	12 121	1 088 197
Plate + I-beam	457 481	157 191	317 641	21 844	10 435	964 592
FRP + VKR	317 802	157 191	113 436	21 844	7 249	617 522
FRP + I-beam	353 631	157 191	123 265	21 844	8 067	663 998
Stainless: FRP + VKR	449 392	73 827	0	9 828	10 251	543 298

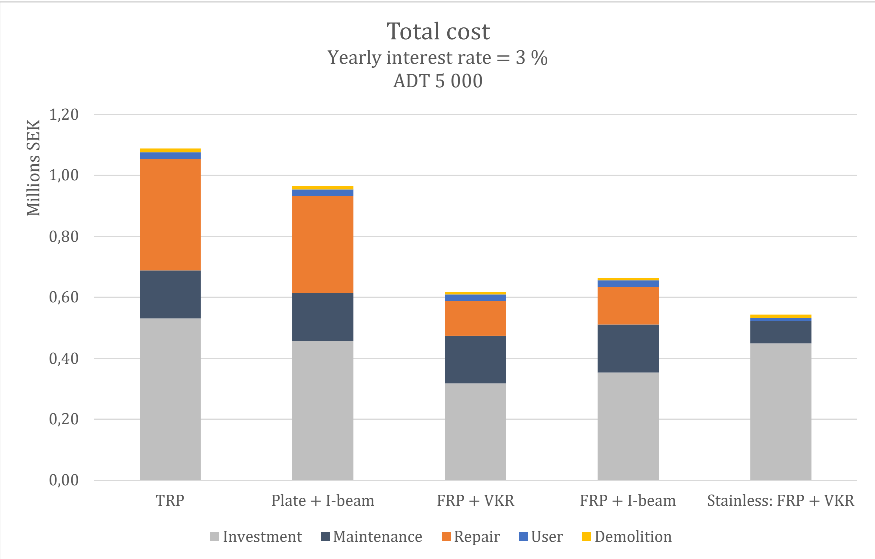

INVESTMENT COST

	Main beams	Deck	Welding	tion deck	Painting	Total
TRP	144 425	168 375	90 948	0	127 610	531 358
Plate + I-beam	141 575	168 375	15 686	21 000	110 845	457 481
FRP + VKR	120 125	129 600	12 364	16 128	39 585	317 802
FRP + I-beam	151 050	129 600	13 838	16 128	43 015	353 631
Stainless: FRP + VKR	286 130	129 600	17 534	16 128	0	449 392

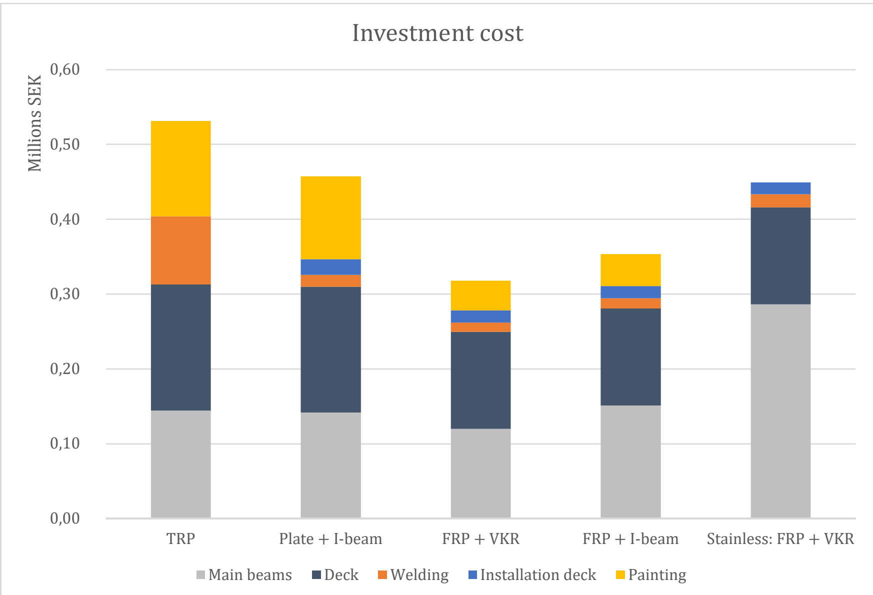

LIFE CYCLE COST ANALYSIS (LCC)
Sensitivity analysis - ADT

TOTAL COST

	Investment	Maintenance	Repair	User	Demolition	Total [SEK]
	531 358	157 191	365 683	21 844	12 121	1 088 197
TRP	531 358	157 191	365 683	43 687	12 121	1 110 040
	531 358	157 191	365 683	87 375	12 121	1 153 728
	457 481	157 191	317 641	21 844	10 435	964 592
Plate + I-beam	457 481	157 191	317 641	43 687	10 435	986 435
	457 481	157 191	317 641	87 375	10 435	1 030 123
	317 802	157 191	113 436	21 844	7 249	617 522
FRP + VKR	317 802	157 191	113 436	43 687	7 249	639 365
	317 802	157 191	113 436	87 375	7 249	683 053
	353 631	157 191	123 265	21 844	8 067	663 998
FRP + I-beam	353 631	157 191	123 265	43 687	8 067	685 841
	353 631	157 191	123 265	87 375	8 067	729 529
	449 392	73 827	0	9 828	10 251	543 298
Stainless: FRP + VKR	449 392	73 827	0	19 655	10 251	553 125
	449 392	73 827	0	39 310	10 251	572 780

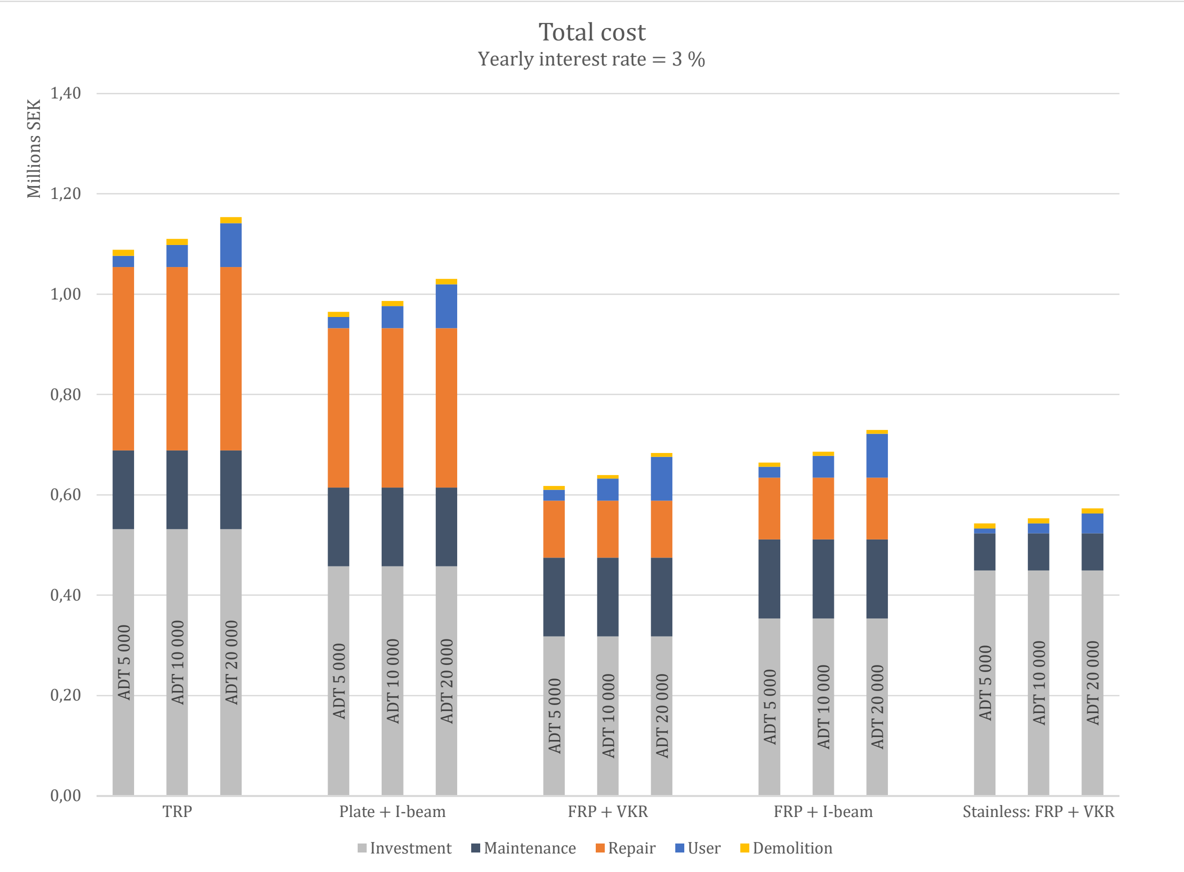

LIFE CYCLE COST ANALYSIS (LCC)

Sensitivity analysis - Interest rate

TOTAL COST

	0%	1%	2%	3%	4%	5%	6%	7%
TRP	1 708 640	1 439 510	1 239 075	1 088 197	973 519	885 588	817 620	764 691
Plate + I-beam	1 526 785	1 282 704	1 101 141	964 592	860 870	781 362	719 905	672 030
FRP + VKR	945 579	801 134	695 661	617 522	558 841	514 206	479 847	453 099
FRP + I-beam	1 005 570	855 189	745 365	663 998	602 894	556 424	520 665	492 841
Stainless: FRP + VKR	665 659	608 909	570 223	543 298	524 149	510 227	499 881	492 025

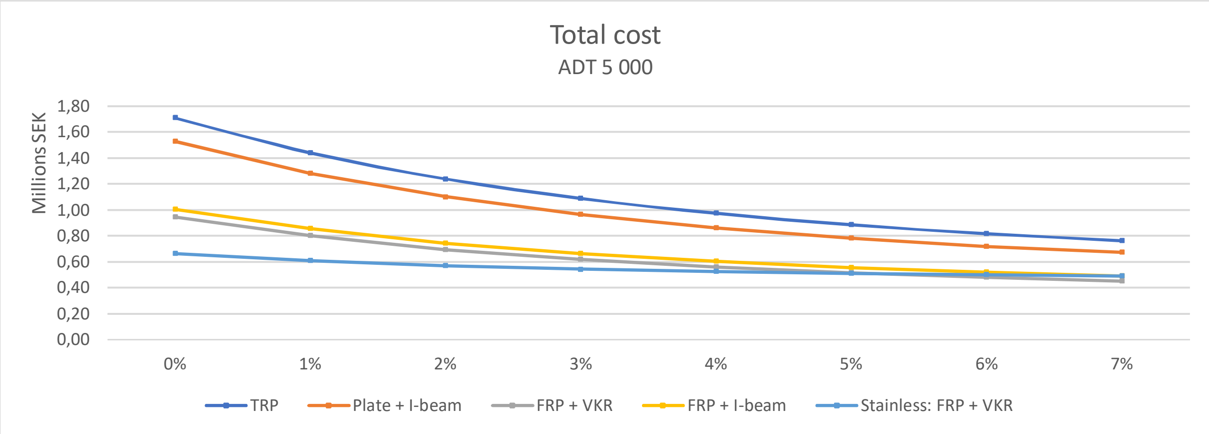

Appendix E

Life cycle assessment:
- Values for total emissions

LIFE CYCLE ASSESSMENT (LCA)

EMISSIONS

CO2-emissions	Carbon steel	Stainless steel	FRP	Paint
Unit	*kg CO2 / kg*	-	-	*kg CO2 / m2*
	1,5	4,5	5	1,6

TOTAL EMISSIONS [kg]

	Carbon steel	Stainless steel	FRP	Paint	Total [kg]
TRP	18 750,00	0,00	0,00	1 166,72	19 916,72
Plate + I-beam	18 600,00	0,00	0,00	1 013,44	19 613,44
FRP + VKR	7 207,50	0,00	7 370,00	361,92	14 939,42
FRP + I-beam	9 063,00	0,00	7 370,00	393,28	16 826,28
Stainless: FRP + VKR	0,00	19 809,00	7 370,00	0,00	27 179,00